To the Graduate Council:

I am submitting herewith a thesis written by Jupiter Sitorus Pane entitled " Analysis of Coolant Pressure Dynamics in the Primary System of Pressurized Water Reactors." I have examined the final copy of this thesis for form and content and recommend that it be accepted in partial fulfillment of the requirements for the degree of Master of Science, with a major in Nuclear Engineering.

Belle R Upadhyaya

Belle R. Upadhyaya, Major Professor

We have read this thesis
and recommend its acceptance:

Laurence F. Miller

[signature]

Accepted for the Council:

[signature]

Associate Vice Chancellor
and Dean of The Graduate School

STATEMENT OF PERMISSION TO USE

In presenting this thesis in partial fulfillment of the requirements for a Master's degree at The University of Tennessee, Knoxville, I agree that the Library shall make it available to borrowers under rules of the Library. Brief quotations from this thesis are allowable without special permission, provided that accurate acknowledgment of the source is made.

Permission for extensive quotation from or reproduction of this thesis may be granted by my major professor, or in his absence, by the Head of Interlibrary Services when, in the opinion of either, the proposed used of the material is for scholarly purposes. Any copying or use of the material in this thesis for financial gain shall not be allowed without my written permission.

Signature ____________________

Date 4/29/1993

ANALYSIS OF COOLANT PRESSURE DYNAMICS IN THE PRIMARY SYSTEM OF PRESSURIZED WATER REACTORS

A Thesis

Presented for the

Master of Science

Degree

The University of Tennessee, Knoxville

Jupiter Sitorus Pane

May 1993

DEDICATION

This thesis is dedicated to my parents

Mr. Stephanus Sitorus Pane and Mrs. Kristiana br. Siregar Pane

who have dedicated their lives to make me what I am now,

and

to my lovely wife

Norma br. Purba Pane

who always gives me encouragement and love.

ACKNOWLEDGMENTS

This research work could not have been completed successfully without the invaluable supervision and support of my advisor, Dr. Belle R. Upadhyaya. I would like to express my deepest gratitude to him.

I would like also to extend my gratitude to the other committee members Dr. Laurence F. Miller and Dr. Rafael B. Perez for their suggestions and for serving on my committee.

I would like to thank Dr. Erdinc Turkcan (ECN, Netherlands), Mr. Ray Fain (Analysis & Measurement Services Corp.), and Dr. J.A. Thie for providing me with data and giving me some technical advice.

I would like to thank my friend Greg Swaggerty for helping me in data analysis and for his friendship.

My special thanks to Dr. Thomas W. Kerlin for his priceless advice and support during my study at the University of Tennessee in the Nuclear Engineering department.

I would like to thank all my fellow colleagues, the academic and technical staff in the Department of Nuclear Engineering, especially, Wu Yan, Masoud Naghedolfeizi, Benan Basoglu, Evren Eryurek and Kadir Kavaklioglu.

To my wife, Norma, I thank her for her understanding and patience while taking care of our two sons Josua Sloane and Javier Augustson alone in Indonesia while I am studying in the USA.

Finally, I thank The Lord for all His guidance and blessing, and for the great people that He let me have contact with. Glory to Him forever and ever.

ABSTRACT

The purpose of the present research is to study the dynamic behavior of coolant pressure in the primary loop of a pressurized water reactor (PWR). One of the objectives is to determine the important parameters that influence the standing wave behavior of the pressure noise process. As a consequence of this analysis, certain frequency range of the pressure noise spectrum may be related to coolant temperature in a PWR.

Previous studies of pressure noise behavior were able to identify the standing wave frequency for a given operating condition. This frequency varies in the range 6 - 8 Hz, depending on the system dimensions and operating characteristics. This frequency shifts with changes in coolant temperature. The present research is motivated by these experimental observations. One of the objectives is to perform a detailed theoretical analysis of the relationship between pressure noise signature and primary coolant temperature in a PWR. As a consequence of this, it is possible to develop a technique for estimating average hot leg temperature. This approach, when properly implemented, could be used as an alternative estimator of average hot leg temperature.

Because pressure noise dynamics, driven by the compressibility behavior of water, is proportional to sound velocity in water, the pressure noise characteristics can be studied through an acoustical phenomenon in water. It is hypothesized that if the temperature of water is greater than 300 °F (150 °C), sound velocity in the water decreases, with increasing temperature. As a result, the frequency of the pressure noise standing wave would also decrease. Therefore, the changes in pressure noise spectra may be related to changes in hot leg temperature. The analytical calculations are applied to operating PWRs and compared with measured pressure noise data. The limited

availability of the data is a drawback in performing detailed comparison of analytical and experimental results. Typical four-loop Westinghouse PWRs have wide-range pressure transmitters in their hot leg piping. The actual implementation of the technique for estimating hot leg temperature can be enhanced by the use of narrow-range pressure transmitters.

Detailed modeling of pressure fluctuations in the primary coolant systems of a two-loop (470 MWe) PWR and a four-loop (1140 MWe) PWR clearly showed the standing wave frequencies in the range 6 - 8 Hz at full power conditions. These frequencies were also seen in the power spectral densities of pressure noise signals. It was observed that the standing wave frequency changes as a function of average hot leg temperature, decreasing with increasing temperature. Eventhough the magnitude of the frequency is influenced by temperatures in the components of the primary coolant system, the dominant effect is due to the compressibility changes in the vessel upper plenum and temperature in the hot leg.

For a typical four-loop Westinghouse PWR, the measured pressure noise frequency was 7.27 Hz at an average hot leg temperature of 618.3 °F (325.7 °C). The theoretical (model-based) natural frequency for this condition was 7.34 Hz. This result establishes the direct relationship between coolant temperature and pressure noise frequency.

When primary coolant temperature and pressure are measured accurately in a PWR, a calibration-type curve may be generated and used for estimation of hot leg temperature. Further study is necessary to prove that the frequencies in the range 6 - 8 Hz are affected dominantly by the hot leg temperature.

TABLE OF CONTENTS

LIST OF TABLES

TABLE **PAGE**

LIST OF FIGURES

FIGURE PAGE

CHAPTER 1

INTRODUCTION

1.1 Statement of the Problem

One aspect of the dynamic behavior of the Primary Coolant System (PCS) of a Pressurized Water Reactor (PWR) involves coolant pressure fluctuations along the PCS loop. The pressure is modulated by several parameters in the system, such as coolant flow oscillation in the piping connected between the pressurizer and the hot leg, coolant flow oscillation in the primary loop, neutron noise perturbations, pump rotation, and others. In a compressible fluid, the pressure variations may cause density variations. Such a medium can give rise to pressure waves that propagate with the velocity of sound [23,24]. Therefore, one of the pressure fluctuations in the primary coolant system involves the resonance frequency of pressure signal that is proportional to sound velocity.

An observation of this *pressure noise* signal shows that there is a direct relationship between the average *hot leg* temperature and certain characteristics of pressure noise signals such as the *power spectral density* of the pressure noise [1,2,3]. The peaks in the power spectral density shift with changes in coolant temperature. However, the shift in the peak whose frequency is proportional to the sound velocity is more sensitive to coolant temperature than to other peaks. This fact provides the motivation to perform a more detailed study of the relationship between pressure noise and coolant temperature in PWRs. In addition, this frequency also depends on the physical dimensions of the primary loop.

The objectives of this study are

(a) to develop a dynamic model of the coolant flow system in a PWR,

(b) to study the relationship between primary pressure fluctuations to coolant temperature,

(c) to study the characteristics of primary pressure noise signal using available power plant data for various coolant temperature conditions,

(d) to perform a sensitivity analysis of the pressure noise as a function of other parameters that may influence its characteristics (primarily spectral features), and

(e) to provide guidelines for estimating coolant temperature using spectral features of the primary pressure signal.

Since the standing wave frequency is proportional to the sound velocity in water, a theoretical model was developed using two differential equations for acoustic fields in a liquid flow in a pipe. After linearization, these equations were shown to be similar to a two-port network in an electrical circuit. Therefore, the entire flow in the piping and vessel in the system will be treated using a two-port electrical network analogy.

The analytical model was applied to the Borssele PWR in the Netherlands and to a typical four-loop PWR. The Borssele PWR has narrow-range pressure transmitters installed in the hot leg pipings, whereas typical PWRs in the United Stated have wide-range pressure transmitters. Thus, implementation of this technique for coolant temperature estimation is possible in these systems. However, the accuracy of the approach could be enhanced by the addition of at least one narrow-range pressure transmitter in the hot leg piping.

1.2 Hypothesis

Based on the observations cited above, the displacement of frequency in the pressure noise spectrum may be described as follows: the pressure noise wave in the PCS propagates through the coolant with a velocity equal to the velocity of sound in the medium. The velocity of these waves is determined by the compressible characteristics of the medium; in this case the medium is water. Because the compressibility of water is affected strongly by temperature [24], the changes in coolant temperature causes changes in compressibility of the coolant. As a result, the pressure fluctuation velocity changes with changes in coolant temperature.

In an acoustic field, the frequency of the sound wave is equal to the sound velocity, c, divided by the wavelength, λ, or $f = c/\lambda$. At temperatures above 300 °F (150 °C), the velocity of sound decreases with increasing temperature. Therefore, it is hypothesized that the frequency of the pressure noise wave would decrease with increasing temperature in the primary coolant system of a PWR, and conversely. Physically, this frequency shift may be seen as a shift of the peaks of the pressure noise power spectral density. In other words, a shift in the peak of the pressure noise spectrum may correlate with a change in the coolant's average temperature. In order to prove this hypothesis, it is necessary to have pressure noise data for several temperature levels and to study the spectral pattern.

1.3 Conditions and Assumptions

The theoretical model deals with lumped parameters; therefore, it is necessary to treat the coolant as a single phase so that a mixture between gas and liquid in the coolant may be avoided. The presence of gas in the coolant would give another effect to the model that is not related to average temperature. Therefore, for this study, the coolant condition was chosen to be in the *subcooled phase*.

Because the information about liquid density at high temperatures that match with reactor operating conditions is not available, the coolant density has to be approximated by empirical equations. Then, it is assumed that within a certain range of temperature, the density of coolant decreases linearly with increasing temperature. A similar assumption is made for sound velocity; the sound velocity changes linearly with temperature, but with a negative slope.

1.4 Contributions of the Thesis

The previous studies dealt with establishing a model and measurement of pressure noise in a primary coolant system. The results indicated a relationship between pressure noise and temperature in primary coolant systems of PWRs. The present research studies analytically that coolant temperature affects the pressure noise in the primary coolant system. Furthermore, this study is helpful in developing guidelines for estimating primary coolant temperature using spectral features of primary pressure signals. This research has also established the spectral characteristics of pressure noise in a typical four-loop PWR (both analytically and experimentally).

1.5 Organization of the Thesis

This thesis consists of eight chapters. Chapter 1 provides the introduction and includes a statement of the problem, hypotheses, conditions and assumptions, contributions of the thesis, and the definition of terms commonly used in this thesis. The review of previous work related to this subject and the fundamental background on pressure noise and acoustic noise in a fluid flow are given in Chapter 2. Chapter 3 describes the theoretical model design for pressure noise in the primary coolant system. The model was developed using a two-port electrical network method. Chapter 4 presents parameter information for the Borssele Nuclear Power Plant (the Netherlands) and the theoretical model calculation results of the pressure noise frequency. Similar calculations are also presented for a typical four-loop Westinghouse PWR. Chapter 5 provides the basic theory of the signal analysis method that was used in this study. The data acquisition performed in the Borssele Nuclear Power Plant and in the four-loop Westinghouse PWR are presented in Chapter 6, along with the results of data analysis. The discussion of results of application to pressurized water reactors are given in Chapter 7. Chapter 8 presents a summary, conclusions, and recommendations for future research.

1.6 Definition of Terms

1. *Pressure noise* is the pressure fluctuation of fluid flow in a closed-loop pipe in the primary coolant system of a PWR due to noise sources such as flow and vibration.
2. *Standing wave* is the pressure fluctuation wave that resonates due to interference of the incident and reflected pressure waves. Mathematically, the frequency of the standing wave of the closed-loop is the eigenfrequency of the closed-loop system.
3. *Compressibility* is change in density per unit change in pressure.

4. *Subcooled liquid* is the liquid at a temperature below the saturation temperature for the pressure that exists.
5. *Two-port network* is an electrical network which consists of four terminals arranged in two pairs. A port is a pair of network terminals in which the current entering one terminal is equal to the current leaving the other terminal.
6. *Branch line* is the branch scheme of flow in a complex pipe system.
7. *Acoustical impedance* is the acoustic pressure noise divided by volumetric flow rate.
8. *Hot leg* is the segment of the primary coolant piping in a PWR that carries the outlet coolant from the reactor vessel to the steam generator.
9. *Pressure Transmitter* is a device that converts the fluid pressure into an electrical parameter.

CHAPTER 2

REVIEW OF PREVIOUS STUDIES AND THEORETICAL BACKGROUND

2.1 Pressure Noise Sources in The Primary Coolant Systems of Pressurized Water Reactors (PWRs)

The primary coolant system of a PWR is equipped with a pressurizer that is connected to the hot leg piping through a surge line. The pressurizer is designed to control the primary pressure and maintain it at a large enough value so that the coolant temperature is below the saturation condition. About forty percent of the pressurizer tank is occupied by steam vapor during full power operation, and the rest is filled with liquid water. The water in the pressurizer is connected to the PCS. Because of the fluid motion in the PCS and temperature fluctuations, the water from the PCS moves in and out of the pressurizer, and thus, the pressurizer water level is very dynamic. This condition causes the vapor volume of the pressurizer to fluctuate and in turn causes the pressure to fluctuate. For the sake of spectral analysis, every fluctuation in the static value is referred to as noise. Hence, the fluctuation of the pressure in the pressurizer is recognized as one of the pressure noise sources in the PCS.

When the water moves in and out of the pressurizer, the water volume in the pipe between the pressurizer and the PCS oscillates. This oscillatory motion causes a momentum transfer to the PCS. In liquid flow, the momentum perturbation transfer is known as the pressure perturbation. The study of this motion proved that this oscillation is an universal phenomenon because (1) the frequency of oscillation appears in all loops of the PCS, and (2) the frequency does not change even though the reactor is operated with a different number of pumps. Generally, in commercial power reactor plants, the frequency of this oscillation is about 0.65 Hz [3,4,5].

Another universal phenomenon of pressure noise in PWRs involves the pressure noise originated by a hydraulic displacement caused by the compressible behavior of the PCS. An increase of pressure in the coolant forces a volume of water to move forward, but since the geometry of PCS is almost constant, the displacement of water is converted to a compression of the water volume. Under this condition, density of coolant changes accordingly. The fluctuation of pressure in the PCS transfers a perturbation momentum to the pressure. This perturbation is recognized as one of the pressure noise sources that propagates in the PCS. Similar to all other waves that propagate in pipes, some of the incident waves are transmitted and some are reflected. If the waves propagate from a bigger diameter pipe to a smaller one, some of the waves will be reflected along the pipe. At certain positions along the PCS closed loop, these waves will resonate and establish a standing wave. This frequency is also recognized as a natural frequency of the system. Because this standing wave will appear in all loops, it is also categorized as a universal phenomenon. The dependence of this pressure noise on the compressible behavior of the coolant causes the pressure noise waves to propagate with frequency proportional to the velocity of sound [2,4,24].

Another recognized pressure noise source in the PCS is the primary pumps. The pumps force the coolant through all the primary loops with a certain flow rate. Because the rotational speed itself fluctuates according to mechanical restrictions and because of imbalance, the force or the pressure generated by pumps will also fluctuate. This fluctuation propagates through the coolant as a wave propagation with a certain frequency. A study of the pump pressure noise showed that the frequency of pressure noise caused by the pump oscillation is in the 20 - 24 Hz range and depends on the pump speed itself [6].

The pump mechanism that creates noises is categorized as a mechanical vibration process. In a similar way, every mechanical vibration process in the PCS, such as core barrel motion inside the reactor vessel, also generates pressure noise in the PCS, but with different frequencies depending on the system.

Several authors have performed pressure noise data analysis of the PCS in order to have a complete record of the noise pattern for their specific reactors, but some also sought to study the possibility of using the pressure noise signal for monitoring the thermal-hydraulic performance of the coolant in a PCS. However, none studied the use of this pressure noise to determine the coolant temperature and parameters affecting it. The present study focuses on the study of pressure noise dynamics and its application to monitor the temperature of the coolant in the PCS. Because the pressure noise driven by hydraulic displacement is affected by temperature most dominantly, this noise will be investigated in this study.

Previous work on pressure noise proved that the frequency of the standing wave is strongly influenced by the temperature condition [1,2,4]. The influence can be explained by the following example. The specific volume of water at a temperature of 100 °C and at a pressure of 1 atmosphere is 1.0435e-3 m^3/kg. Because of pressure fluctuation, the magnitude of this specific volume will fluctuate around this value. In this condition, the sound velocity will fluctuate around 1544 m/sec. However, at a temperature of 150 °C and its saturation pressure, the specific volume is 1.0906e-3 m^3/kg. Therefore, the specific volume will fluctuate around 1.0906e-3 m^3/kg. Then, the sound velocity will fluctuate around 1465 m/sec[19]. These examples illustrate that the pressure noise has a distinct spectral characteristic at each temperature condition.

Nagy and Katona [1] calculated an eigenfrequency of a theoretical two-loop commercial reactor using two partial differential equations of mass continuity and a momentum conservation model. The differential equations were converted into two linear equations and were treated as a two-port network. They found that the model provides results that agree approximately with the experimental data analysis. A similar model was also used by Grunwald [6,7] to analyze the pressure noise frequency spectrum of the WWER-440 reactor, but with a different approach. He also proved that the model results are close to the results from experimental data analysis. It was also mentioned that from several eigenfrequencies calculated from the model, the frequency of 6.3 Hz was influenced by the compressibility in the upper plenum of reactor vessel. The upper plenum temperature was assumed equal to the temperature of coolant in hot leg pipings. However, the effect of temperature on this frequency was still left unexamined in their studies. Turkcan [2,3] experimentally found that the frequency of 6.5 Hz of the BNPP shifted as the temperature increased or decreased. He also added that this frequency is related to the core-exit temperature. In this study, the pressure noise signal acquisition was made at temperatures above 200 °C. At these temperatures, the absolute pressure may be assumed to be almost constant. This observation is additional motivation to study the use of the pressure noise feature as an alternative technique for monitoring hot leg coolant temperatures in PWRs. The fluid motion was studied in order to understand the relationship between pressure noise and temperature in a liquid flow.

2.2 Fluid Motion

By simplifying the liquid as an ideal liquid, we can divide the fluid motion into two categories: (1) internal motion or molecular motion, and (2) macroscopic motion, commonly called fluid flow.

2.2.1 Internal Motion

The internal motion involves an enormous number of particles or molecules that move randomly. The motion of the particles or molecules are driven by an internal energy that every particle or molecule has. Therefore, this motion is also called thermal motion. Adding heat or energy to the material can cause more distance among particles or molecules, as a result, the particles become less dense in a volume and vice versa. A similar condition also happens in a compressible medium. A pressure variation may cause considerable density variation, which is represented using a compressibility value, κ. Such a medium can give rise to pressure waves that propagate with the velocity of sound [24]:

$$c = \sqrt{\frac{dp}{d\rho}}. \tag{2.1}$$

The relationship among pressure P, temperature T and density ρ cannot be exactly formulated because P and T are two independent state variables. Their relationship can only be determined by an empirical equation based on experiment. The most recent experimental research on the relationship between density and temperature is published in the CRC Handbook of Chemistry and Physics, Edition 70 (1981) [19]. The data showed that the density decreases with increasing temperature.

2.2.2 Macroscopic Motion

A volumetric fluid flow in a three-dimensional space is usually categorized as macroscopic motion. This motion can be described in two different ways: (1) Lagrangian, and (2) Eulerian. The Lagrangian description involves the motion of a collection of macroscopic elements that move as a function of time, whereas the Euler description involves the motion of particles in a fixed coordinate system x,y,z and of time. In this case the velocity will be expanded in x,y,z directions. The Euler description was used in this study because with this description it is easy to understand the effect of momentum of internal motion on one of the macroscopic motions.

Consider the flow motion in the control volume as shown in Figure 2.1. The control volume is subjected to one-dimensional flow. There are three conservation laws involved in this volume: (1) conservation of mass, (2) conservation of momentum, and (3) conservation of energy.

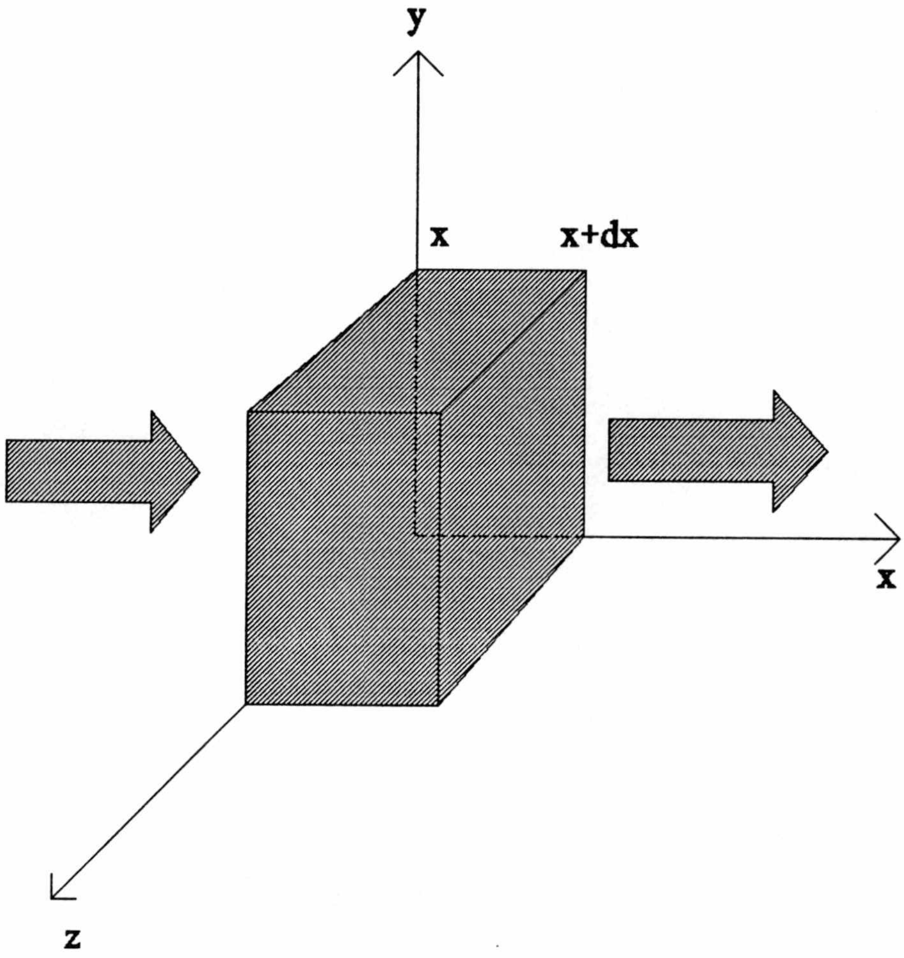

Figure 2.1: Control volume.

The difference in mass between x and $x+dx$ at time t is defined as

$$M(x+dx,t) - M(x,t) = (\frac{\partial M}{\partial x})dx \tag{2.2}$$

where $M(x,t) = \rho(x,t)\ U(x,t)$,

$\partial M/\partial x$ = net mass influx,

$\rho(x,t)$ = liquid density, and

$U(x,t)$ = fluid velocity.

The total mass inside the control volume can be approximated as $1/2[\rho(x,t) + \rho(x+dx,t)]$. Since dx is small, the total mass of fluid inside the control volume becomes $\rho(x,t)$. The amount of net mass influx entering the control volume increases the total mass inside the control volume. In other words, the time rate of density change is equal to the net mass influx. Mathematically, this relationship is

$$\frac{\partial \rho}{\partial t} + \frac{\partial M}{\partial x} = 0. \tag{2.3}$$

This equation is known as the mass conservation law or the continuity equation. At this point, thermal motion does not contribute to the mass flux, but it will appear in the momentum transfer law.

The momentum transferred to the control volume consists of two components: (1) the momentum of flow, MU, through the left side of the control volume, and (2) the momentum due to the collisions between particles coming from the left and those inside the control volume (as a thermal motion). The second momentum component involves the liquid pressure, P, per unit length. Thus the total momentum transfer, G, through the surface of control volume at x equals $P + MU$ or $P + \rho U^2$. Therefore, the time rate of momentum density equals the increase of momentum flux:

$$\frac{\partial M}{\partial t} + \frac{\partial G}{\partial x} = 0. \tag{2.4}$$

This equation is called the momentum conservation law.

The total energy in a control volume also consists of two energy sources: (1) the kinetic energy of volumetric flow, $1/2\ \rho U^2$, and (2) the sum of internal energy of each particle, ρE. Hence, the total energy density coming to the control volume is

$$W = \frac{1}{2}\rho U^2 + \rho E. \tag{2.5}$$

If we define an energy flux as S, the time rate of energy density equals the energy flux entering the control volume. The conservation of energy equation is

$$\frac{\partial W}{\partial t} + \frac{\partial S}{\partial x} = 0. \tag{2.6}$$

2.3 Acoustic Waves in Fluid Flow

In an ideal condition, the change of pressure and density at steady-state conditions is so rapid [23,24] that practically no transient heat transfer occurs, and therefore, it is not necessary to include heat conduction in the fluid pressure model [1,11]. As a result, pressure now becomes a function of density only. However, the density of liquid is different at different temperatures, therefore the pressure noise characteristics of the primary coolant are also different at different coolant temperatures. In order to differentiate the static and the perturbation terms, the static term is written in upper case and the perturbation terms in lower case. Also it is assumed that $\delta\rho << \rho_o$.

Mathematically, the perturbation equation of the pressure can be derived as a Taylor expansion of $P(\rho+\delta\rho)$.

$$P(\rho+\delta\rho) \approx P_o + (\frac{\partial P}{\partial \rho})\delta\rho + \frac{1}{2}(\frac{\partial^2 P}{\partial \rho^2})\delta\rho^2 + ... \tag{2.7}$$

If $P_o = P_o(\rho_o)$ is the static value, then the perturbation value of P is

$$\approx P_o + (\frac{\partial P}{\partial \rho})\delta\rho. \tag{2.8}$$

$$p = (\frac{\partial P}{\partial \rho})\delta\rho. \tag{2.9}$$

By definition, the compressibility is

$$\kappa = \frac{1}{\rho}\frac{\partial \rho}{\partial P}. \tag{2.10}$$

Therefore, from Equation (2.9)

$$p = \frac{1}{\kappa\rho_o}\delta\rho, \tag{2.11}$$

where p and $\delta\rho$ are perturbations of pressure and density.

Analogous to the mass flow equation, the mass perturbation equation is written as

$$m = (\rho_o + \delta\rho)(U_o + u) - \rho_o U_o, \tag{2.12}$$

where m and u are perturbations with respect to the nominal values.

Because this study involves random perturbations, we assume that the unperturbed fluid to be at rest, so that $m = \rho_o u + \delta\rho u$. Because $\delta\rho u$ is ignored compared to $\rho_o u$, the mass flux perturbation approximately equals $m = \rho_o u$.

The total momentum flux of flow, G, is $\rho U^2 + P$. Analogous to this equation, the momentum perturbation equation is written as

$$g = (\rho_o + \delta\rho)\,(U_o + u)^2 + (P_o + p) - (\rho_o U_o^2 + P_o), \tag{2.13}$$

where g, $\delta\rho$, u, and p are perturbations of momentum, density, velocity, and pressure. Similarly, P_o and U_o are assumed equal to zero, so that $g = \rho_o u^2 + \delta\rho u + p$. Approximately $\rho_o u^2$ is negligible compared to p. As a result, the momentum perturbation approximately equals p. The last assumption is valid if flow velocity, U_o, is much smaller than the wave speed.

Under these conditions Equation (2.11) can be derived as

$$\frac{\partial p}{\partial t} = \frac{1}{\kappa\rho_o}\frac{\partial\delta\rho}{\partial t}, \tag{2.14}$$

where p and $\delta\rho$ are perturbations of pressure and density.

From Equations (2.3) and (2.4) it follows that

$$\frac{\partial\delta\rho}{\partial t} + \frac{\rho_0\partial u}{\partial x} = 0 \tag{2.15}$$

and

$$\frac{\rho_o\partial u}{\partial t} + \frac{\partial p}{\partial x} = 0, \tag{2.16}$$

where $\delta\rho$, p, and u are perturbations of density, pressure, and velocity.

By combining Equations (2.14) and (2.15),

$$\kappa \frac{\partial p}{\partial t} = - \frac{\partial u}{\partial x}. \tag{2.17}$$

From Equations (2.1) and (2.10) the compressibility is given by $\kappa = (\rho c^2)^{-1}$. Therefore,

$$\frac{\partial p}{\partial t} + c^2 \rho_o \frac{\partial u}{\partial x} = 0, \tag{2.18}$$

where p, u are perturbations of pressure and velocity and c is sound velocity.

Finally, Equations (2.16) and (2.18) are called the acoustic wave field equations in fluid flow. These two basic equations are used to model the acoustic wave propagation in the primary coolant system of a PWR.

CHAPTER 3

THEORETICAL MODEL

3.1 Pressure Noise Model in a System Segment

Compared to all pressure noise components that propagate in a PCS, the pressure noise driven by the compressible behavior of the coolant depends most dominantly on coolant temperature. This is because the compressibility (κ) of the coolant is strongly affected by temperature. Physically, this condition appears as the shift of frequency of peak of the pressure noise power spectral density in the PCS when coolant temperature changes. Therefore, this pressure noise source meets a physical condition required for studying the relationship between coolant temperature and pressure noise spectral characteristics. This chapter deals with the aspect of the theoretical frequency shift of pressure noise in the primary coolant system of the PWRs.

The equations for acoustic fields in liquid flow are used here as basic equations to model the pressure noise of the primary coolant system. According to the previous chapter, the acoustic field equations in one-dimensional flow are

$$\frac{\partial p}{\partial t} + c^2 \rho_o \frac{\partial u}{\partial x} = 0 \qquad (3.1)$$

and

$$\frac{\partial p}{\partial x} + \rho_o \frac{\partial u}{\partial t} = 0, \tag{3.2}$$

where p and u are perturbations with respect to nominal values, and ρ_0 and c are average density of the coolant and sound velocity in coolant.

For future discussion, the flow velocity, u, is converted to a volume flow rate, q (where $q = u.S$, S is surface area of the piping) in order to match the equations to an electrical network. Every part of the PCS (for example, the pressure vessel, the hot leg piping) is named a segment. Equations (3.1) and (3.2) are applied to each segment.

Because these two partial differential equations are linear, they can be separated into two second order partial differential equations: pressure perturbation and volume flow rate equations. These equations can then be solved separately for space and time domain solutions by using a separation of variables method. The general solution of these equations is given as [13]

$$\begin{aligned} p(x) &= Ae^{-\Gamma x} + Be^{\Gamma x} \\ q(x) &= \frac{S}{\rho_o c}\left[Ae^{-\Gamma x} - Be^{\Gamma x}\right], \end{aligned} \tag{3.3}$$

where

$q(x)$	$= u(x).S$	
A, B	= constants of solution,	
S	= surface area,	
Γ	$= i\ \omega/c$, and	
Z_c	$= S/\rho_o c$.	

These equations are also well known as general solutions of the Helmholtz equations.

Because the flow enters and leaves the various segments at certain initial and final values, the boundary conditions of the flow in each segment are

$$\text{at } x = 0, \;\; p = p(0), \; q = q(0)$$

$$x = x, \;\; p = p(x), \; q = q(x)$$

By considering that $\cosh(x) = (e^x + e^{-x})/2$ and $\sinh(x) = (e^x - e^{-x})/2$, the hyperbolic solution of the Helmholtz equations is

$$\begin{aligned} p(x) &= A \cosh(\Gamma x) + B \sinh(\Gamma x) \\ q(x) &= C \cosh(\Gamma x) - D \sinh(\Gamma x). \end{aligned} \tag{3.4}$$

By applying the boundary conditions to the equations, we can set up two simultaneous linear equations that represent the solution of these two partial differential equations as

$$\begin{aligned} p(0) &= p(x) \cosh(\Gamma x) + q(x)\, Z_c \sinh(\Gamma x) \\ q(0) &= \frac{p(x)}{Z_c} \sinh(\Gamma x) + q(x) \cosh(\Gamma x) \end{aligned} \tag{3.5}$$

where $Z_c = S/\rho_o c$.

These equations are represented in the matrix notation as

$$\begin{bmatrix} p(0) \\ q(0) \end{bmatrix} = \begin{bmatrix} \cosh(\Gamma x) & Z_c \sinh(\Gamma x) \\ Z_c^{-1} \sinh(\Gamma x) & \cosh(\Gamma x) \end{bmatrix} \begin{bmatrix} p(x) \\ q(x) \end{bmatrix}. \tag{3.6}$$

The matrix that relates *p(0), q(0)* and *p(x), q(x)* is called the A-parameter matrix and is defined below.

$$A(\omega) = \begin{bmatrix} \cosh(\Gamma x) & Z_c \sinh(\Gamma x) \\ Z_c^{-1} \sinh(\Gamma x) & \cosh(\Gamma x) \end{bmatrix} \tag{3.7}$$

Equations (3.6) can also be expressed as

$$\begin{bmatrix} q(x) \\ \\ q(0) \end{bmatrix} = \begin{bmatrix} -\dfrac{\coth(\Gamma x)}{Z_c} & \dfrac{1}{Z_c \sinh(\Gamma x)} \\ \\ \dfrac{1}{Z_c \sinh(\Gamma x)} & \dfrac{\coth(\Gamma x)}{Z_c} \end{bmatrix} \begin{bmatrix} p(x) \\ \\ p(0) \end{bmatrix}. \tag{3.8}$$

The matrix that relates *p(x),p(0)* and *q(x),q(0)* is called the Y-parameter matrix and is defined below.

$$Y(\omega) = \begin{bmatrix} -\dfrac{\coth(\Gamma x)}{Z_c} & \dfrac{1}{Z_c \sinh(\Gamma x)} \\ \\ \dfrac{1}{Z_c \sinh(\Gamma x)} & \dfrac{\coth(\Gamma x)}{Z_c} \end{bmatrix} \tag{3.9}$$

The above equations are valid if the diameters of pipings are much smaller than the lengths of pipings.

For a coolant flow in a tube, these equations are not valid. Instead, an acoustic compliance due to compressibility of the liquid in a cavity or a tank is used. The compliance C is written as [13]

$$C = \frac{V}{\rho_o c_o^2}$$

where V = volume of cavity or tank,
ρ_o = density of water,
c_o = sound velocity .

For a liquid flow in tank, inlet and outlet pressures are assumed equal, so that

$$p(0) = p(x),$$

and the coupling between piping and tank is considered as a Helmholtz resonator.

Therefore the acoustic impedance of the Helmholtz resonator can be modeled as a series inertance of the liquid in a pipe and an acoustic compliance. Therefore, the matrix coefficient of the fluid flow in the tank is written as

$$A(\omega) = \begin{bmatrix} 1 & 0 \\ i\dfrac{\omega V}{\rho_o c^2} & 1 \end{bmatrix}. \tag{3.10}$$

Compared to current and voltage in a two-port network circuit, the coefficient matrix of the fluid flow in a segment is similar to the A-parameter of the two-port network. Therefore, a pressure noise model for the primary coolant system can be developed using the two-port network analogy. Indeed, the pressure noise, $p(x)$, is analogous to voltage (V) and the flow rate, $q(x)$, is analogous to current (I). A brief review of the nature of the two-port network of an electrical circuit is presented.

3.2 Two-Port Electrical Networks

A two-port network, shown in Figure 3.1, is an electrical network that consists of four terminals arranged in two pairs. In each pair, called a port, the current entering one terminal equals the current leaving the other terminal [14]. The open-circuit impedance parameters of the two-port network are given as

$$\begin{aligned} V_1 &= Z_{11} I_1 + Z_{12} I_2 \\ V_2 &= Z_{21} I_1 + Z_{22} I_2 \end{aligned} \tag{3.11}$$

$$[V] = [Z].[I]. \tag{3.12}$$

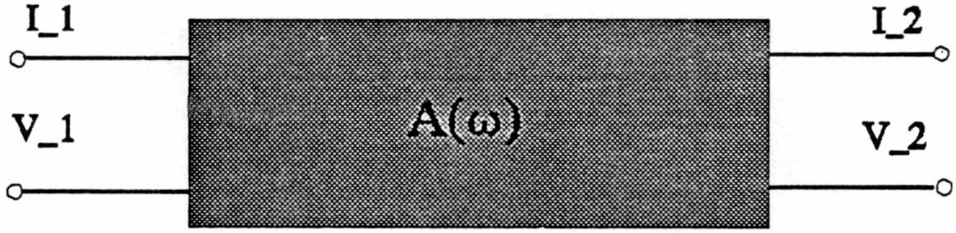

Figure 3.1: The two-port network.

[Z] is called the impedance characteristic of the network. Equation (3.12) can also be expressed as

$$[Z]^{-1}.V = I \tag{3.13}$$

and $[Z]^{-1}$ = Y, which is called the conductance characteristic of the network or the Y-parameter of the network.

Because voltage (*V*) and current (*I*) are independent variables, the linear simultaneous equations are expressed in the form shown in Equation (3.14).

$$\begin{bmatrix} V_1 \\ I_1 \end{bmatrix} = \begin{bmatrix} a_{11} & a_{12} \\ a_{21} & a_{22} \end{bmatrix} * \begin{bmatrix} V_2 \\ I_2 \end{bmatrix}. \tag{3.14}$$

The matrix coefficient of the linear equation is called an A-parameter of the two-port network. The components of the A-parameter of the two-port network are similar to the components of pressure noise and fluid flow equations (acoustic field equations). Therefore, electrical properties of the two-port network may be applied to the acoustic field equations for system components.

3.2.1 Interconnected Two-Port Network

If two two-port networks are connected in cascade, as shown in Figure 3.2, the A-parameter equivalent of the connection is calculated as [15]

$$A(eq) = A_1 \,.\, A_2, \tag{3.15}$$

where A_1 is the A-parameter of network 1 and A_2 is the A-parameter of the network 2.

In a parallel network connection, as shown in Figure 3.3, the A-parameter

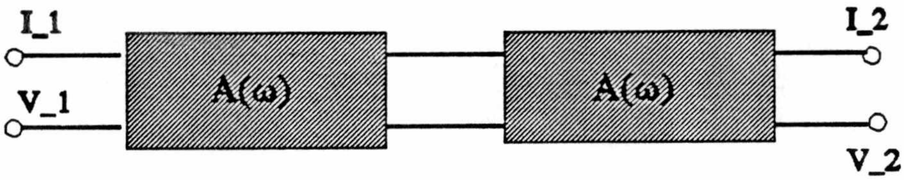

Figure 3.2: Two-port network in cascade connection.

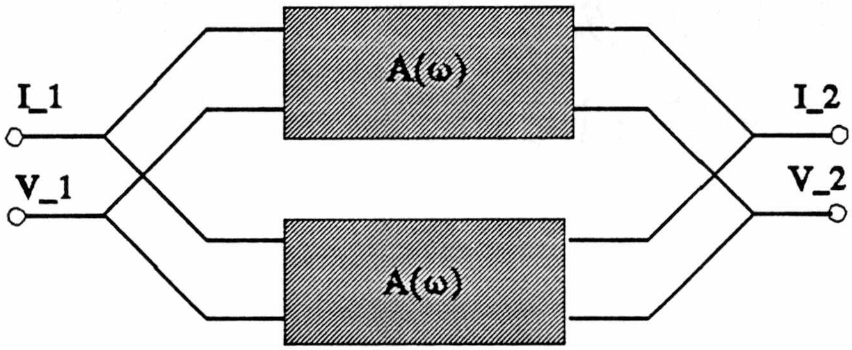

Figure 3.3: Two-port network in parallel connection.

equivalent of the connection is easier to determine through the conductance characteristic (Y-parameter) of the two networks rather than through the inverse of the A-parameter. The Y-parameter equivalent of two parallel network is calculated as [15]

$$Y(eq) = Y_1 + Y_2 \tag{3.16}$$

where Y_1 is the Y-parameter of network 1 and Y_2 is the Y-parameter of network 2. The Y(eq) is then converted to the A-parameter. This parameter is the A-parameter equivalent of the parallel networks. An example for calculating the A-parameter of a closed-loop system is provided in Appendix A.

For a closed-loop system, the input and output of the segment are equal. In other words

$$\begin{bmatrix} V_1 \\ I_1 \end{bmatrix} = \begin{bmatrix} V_2 \\ I_2 \end{bmatrix}. \tag{3.17}$$

Therefore,

$$\mathrm{Det}[A(\omega)-I] = 0. \tag{3.18}$$

The value of ω that fulfills this equation provides the eigenfrequency of the system. This frequency is also called the natural frequency of the system. The solution to Equation (3.18) was obtained by a sequential approximation approach.

3.3 The Pressure Noise Model of the Borssele Nuclear Power Plant Primary Coolant System

In this study, the model was applied to the two-loop Borssele Nuclear Power Plant (BNPP). This reactor has an on-line measurement system that includes pressure noise measurements in the hot legs. Figure 3.4 provides a schematic representation of the

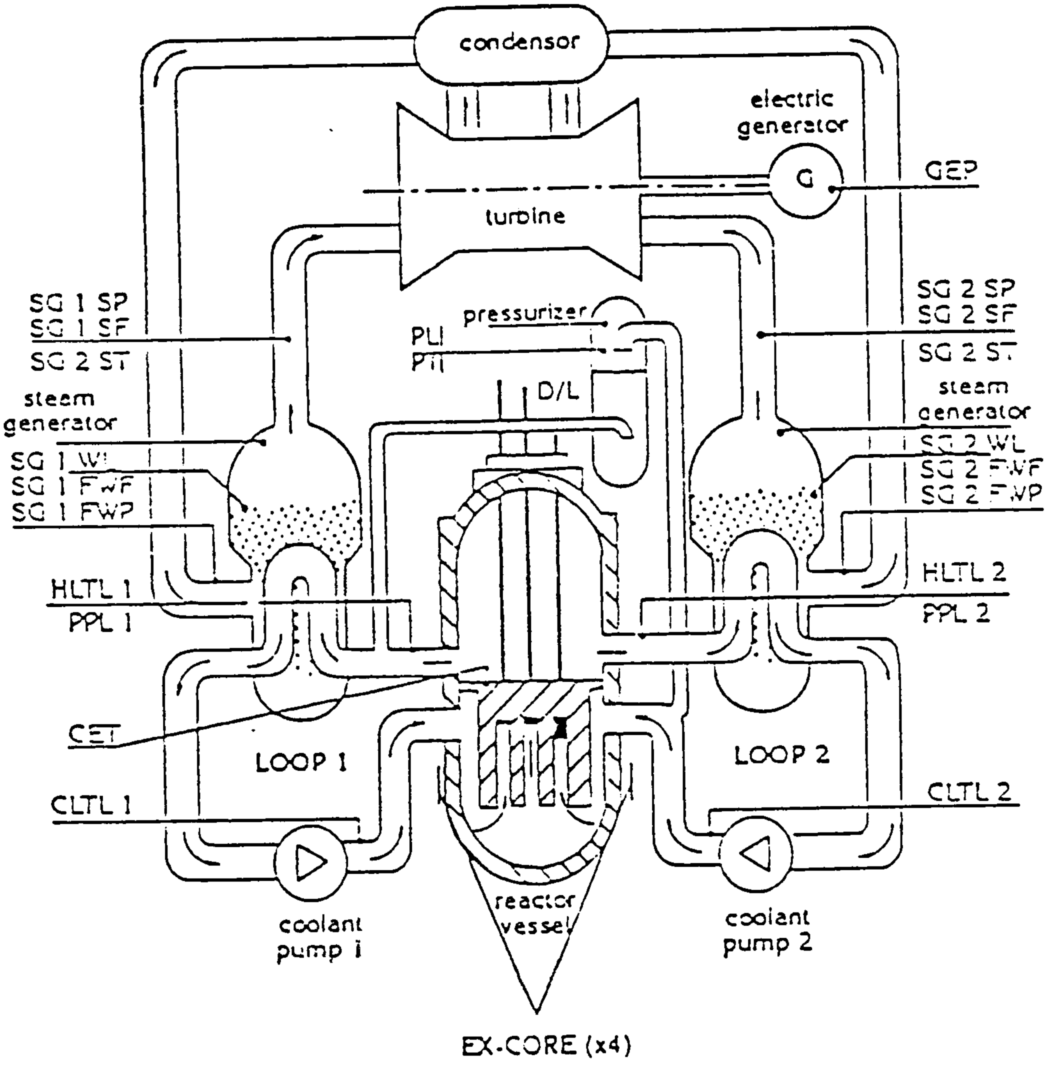

Figure 3.4 : Schematic representation of the Borssele Nuclear Power Plant (BNPP) primary coolant system [2].

BNPP and the position of the various sensors. The PCS consists of two loops, where each loop includes reactor outlet piping (hot leg, PP1), a steam generator (SG), pump suction piping(PP2), a pump, and pump outlet piping (PP3). One of the loops consists of a pressurizer in addition to those components. The liquid from the pressure vessel is first distributed to loop 1 and loop 2 of the PCS, and then it flows back to the pressure vessel. After converting the PCS into the branch pipe scheme, the fluid flow direction is shown in Figure 3.5. This conversion allows us to treat the fluid flow as an electrical current network.

The objective of this chapter is to determine the matrix coefficient equivalent of the pressure noise in the whole system by using a two-port network approach for a complex system. Figure 3.5 shows that the system network involves connections of the PCS components. The hot leg (PP1), pressurizer (PP), steam generator (SG), pump suction piping (PP2), pump (Pump), and pump outlet piping (PP3) are in cascade in loop 1. The hot leg, steam generator, pump suction piping, pump and pump outlet piping are in cascade in loop 2. The *A*-parameter matrices for loop 1 and loop 2 are determined by the dot-product multiplication of the *A*-parameters of their components.

$$A_{loop1}(\omega) = A_{PP1}(\omega).A_{PP}(\omega).A_{SG}(\omega).A_{PP2}(\omega).A_{Pump}(\omega).A_{PP3}(\omega). \tag{3.20}$$

$$A_{loop2}(\omega) = A_{PP1}(\omega).A_{SG}(\omega).A_{PP2}(\omega).A_{Pump}(\omega).A_{PP3}(\omega). \tag{3.21}$$

These matrix equivalents are converted to their *Y*-parameter matrices and then both *Y*-parameters are added in order to get the Y-parameter equivalent of parallel-parallel combination of the loops.

$$Y_{Loop(eq)}(\omega) = Y_{Loop1}(\omega) + Y_{Loop2}(\omega). \tag{3.22}$$

This $Y_{Loop(eq)}$-parameter is converted to $A_{Loop(eq)}$-parameter. This parallel connection is in

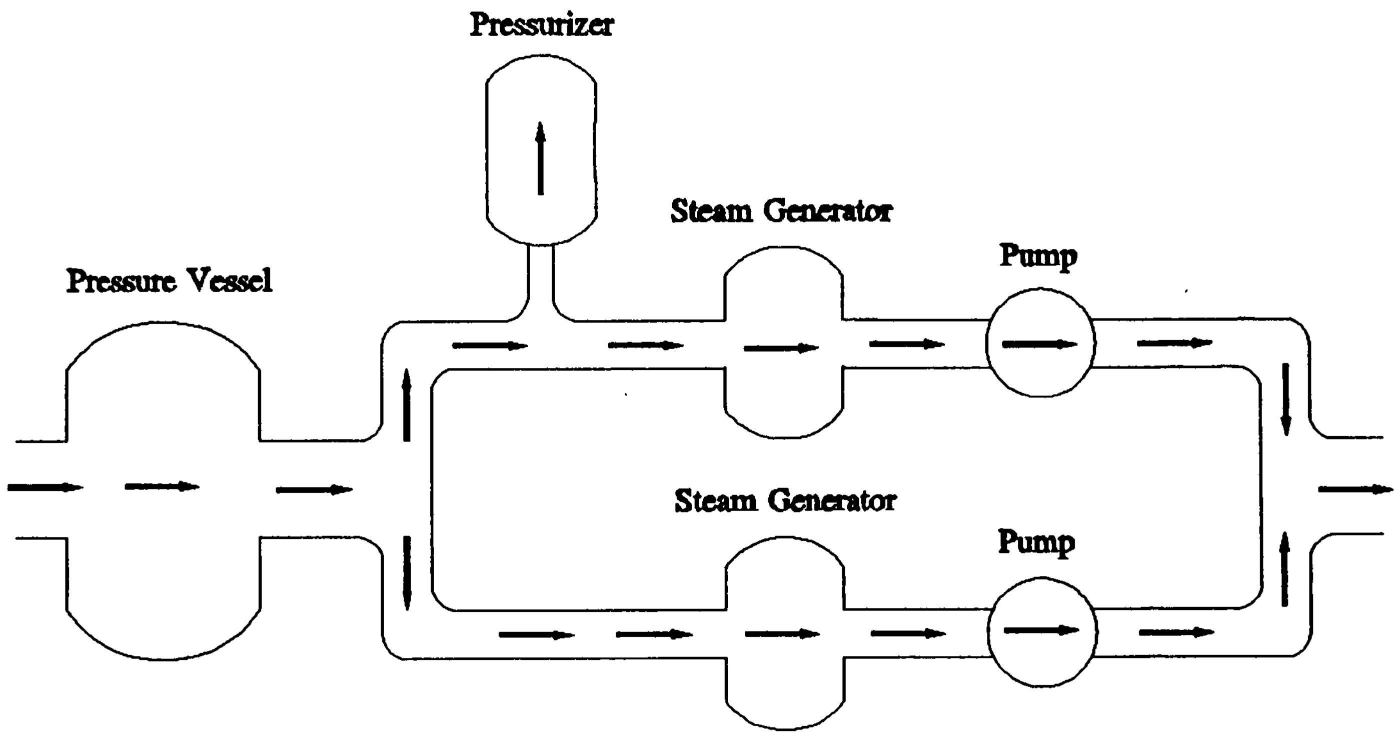

Figure 3.5: Borssele primary coolant flow branch lines.

cascade with the pressure vessel; therefore the matrix coefficient of this connection is calculated by dot-product multiplication of the A-parameter of the pressure vessel and of the combined loops.

$$A_{System}(\omega) = A_{PV}(\omega).A_{Loop(eq)}. \tag{3.23}$$

This final matrix coefficient represents a matrix equivalent of the pressure noise and flow rate in the whole PCS.

For four-loop PWRs, a similar procedure also applied for eigenfrequency calculations. Indeed, the number of parallel loops are four instead of two and one of these loops consists of a pressurizer.

In Chapter 4, this model was applied to calculate the eigenfrequencies of the pressure dynamics of Borssele PWR and a four-loop Westinghouse PWR.

CHAPTER 4

EIGENFREQUENCY CALCULATION OF PRESSURE NOISE DYNAMICS

4.1 Description of the Primary Coolant System of Borssele PWR

The Borssele reactor is a two-loop pressurized water reactor with a rated electrical output of 477 MW. The reactor core is composed of 121 fuel assemblies and is divided into three fuel enrichment groups. The first group consists of 41 assemblies with an enrichment of 2.5%; the second consists of 40 assemblies with an enrichment of 2.8 %; and the third group consists of 40 assemblies with an enrichment of 3.1%. The rated core thermal power is 1370 MW. Table 4.1 provides information about the primary coolant system of the Borssele PWR at full power operation. Plant information and calculations are also presented for a typical four-loop Westinghouse PWR.

4.2. Approximation of Water Density and Sound Velocity at High Pressures and Temperatures

The water density and sound velocity in water at high pressures and temperatures (such as during power operation) can only be approximated because there is no exact state equation that can represent the two independent variables, pressure (P) and temperature (T). It is extremely difficult to find a source where these data may be

Table 4.1 : Primary coolant system information for Borssele PWR [20]

Components	Value	Unit
Pressure Vessel		
Coolant Inlet Temperature	295.4	°C
Coolant Outlet Temperature	319.4	°C
Water Volume	97.0	m^3
Core Coolant Flow Rate	9.2	Kg/sec
Average Core Coolant Velocity	4.3	m/sec
Specific Gravity of Water	795.0	Kg/m^3
Steam Generator		
Type	KWU	
Volume of Primary Side	27.2	m^3
Total Heat Transfer Area	3600.0	m^2
Mass of Water per SG	26289.0	Kg
Mass of Steam per SG	2663	Kg
Primary Coolant Pump		
Type	Sulzer	
Total Volume	4.974	m^3
Speed of Pump	1490	
Pressurizer		
Volume	40	m^3
Inner Diameter	2.24	m
Connection to the primary loop		
Volume	0.87	m^3
Internal Diameter	0.315	m
Equivalent Length	53	m

available. Nonetheless, Wilson (1991) has developed empirical equations that approximate density at high pressures and temperatures by interpolating saturation data as shown in the following equation [18]:

$$DFSUB = DF(PS) + \left(\frac{170}{375.00-TT} - 0.2 \right) * (PP-PS), \tag{4.1}$$

where

$DF(sub)$	=	density of water at subcooled phase,
DF	=	density of water at saturation,
PS	=	pressure at saturation,
TT	=	temperature of water, and
PP	=	pressure of water.

In order to avoid too much deviation in the approximation (because of two independent variables involved in the state equation), the measurements were assumed to be performed at constant pressure conditions. In other words, the density almost depends only on temperature. In the Borssele reactor, if the reactor coolant temperature is above 200 °C, the pressure of 15.4 MPa (or 2235 psia) can be assumed to be constant. For a certain temperature range, the density can also be assumed to change linearly with the temperature. Therefore, the density of water may be approximated by

$$\rho(T) = \rho_o \left[1 + \beta(T - T_o) \right], \tag{4.2}$$

where

$$\beta = \frac{1}{\rho} \frac{\partial \rho}{\partial T}, \tag{4.3}$$

ρ_o	=	density at T_o,
T_o	=	initial temperature, and
β	=	density gradient

A computer subroutine to calculate density approximation for this study was developed and is called DENSITY.

Likewise, the sound velocity data for high temperatures and pressures also must be approximated. The information about velocity was based on the information available in the CRC Handbook of Chemistry and Physics, and Handbook of the Acoustical Engineering[19]. The basic computer routine for the interpolation used in subroutine VELOCITY is given as [21]

```
      FUNCTION SNTEMP(SVEL,PRESS)
      DIMENSION A(4)
      DATA A / 5281.56, -3.21547, 7.71407E-04, -6.26228E-08/
      SV = SVEL+.0404*(725.-PRESS)
      SUM = 0
      DO 10 I=1,4
   10 SUM=SUM+A(I)*SV**(I-1)
      SNTEMP = SUM
      END,
```

where PRESS involves a pressure (in psia) in the primary coolant system and SVEL involves an initial value of sound velocity at a certain temperature.

During full power operation and normal conditions, the reactor is operated at 15.4 MPa with an average temperature of 307.4 °C. Therefore, the density and sound velocity data were interpolated at a temperature of about 310 °C and a pressure of 15.4 MPa, where it is assumed that the equation is still valid for this approximation.

4.3. Eigenfrequency Calculation for Borssele PWR

The branch line flow scheme in Figure 3.5 was translated into an electrical network as shown in Figure 4.1. Every component of PCS is considered a two-port network and is connected to other components as cascade-cascade connections and parallel-parallel connections.

The various circuit components are pressure vessel (PV), reactor outlet piping (PP1), pressurizer (PP), steam generator (SG), pump suction piping (PP2), pump, and pump outlet piping (PP3). The pressure vessel, pressurizer, steam generator, and pump were categorized as tanks, and their A-parameters were calculated using Equation (3.10). Others are treated as pipes, and their A-parameters were calculated using Equation (3.7). In addition, it is assumed that temperatures and sound velocities in PP2, Pump, and PP3 are the same. They are called temperature and sound velocity of the cold leg. Following the procedure mentioned in Chapter 3 (Equations (3.20) - (3.23)), the equivalent A-parameter matrix of the pressure noise dynamics for the whole system was established. The eigenfrequency of the system was then determined by using a sequential approximation approach in Equation (3.14). In brief, the algorithm of the calculation are shown in Figure 4.2, and this calculation was performed in a computer code called PCSPRES. This code was developed specifically for eigenfrequency calculations. A complete computer program code PCSPRES is given in Appendix B. The input of this program includes the average water density, average coolant temperature, coolant pressure, length and cross-section area of the pipings in the primary coolant system, and water volume of the pressure vessel, pressurizer, steam generator and pump.

Tables 4.2 - 4.5 provide the output of PCSPRES at power levels of 0%, 10%, 30%, and 100%. Figure 4.3 shows the plot of theoretical pressure noise calculations as a function of temperature. Several frequencies were seen in the result.

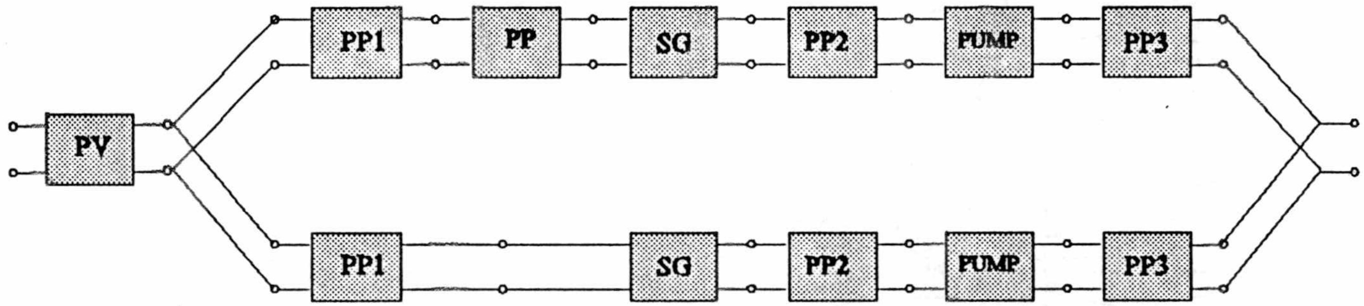

Figure 4.1: The Borssele primary coolant system electrical analogy network.

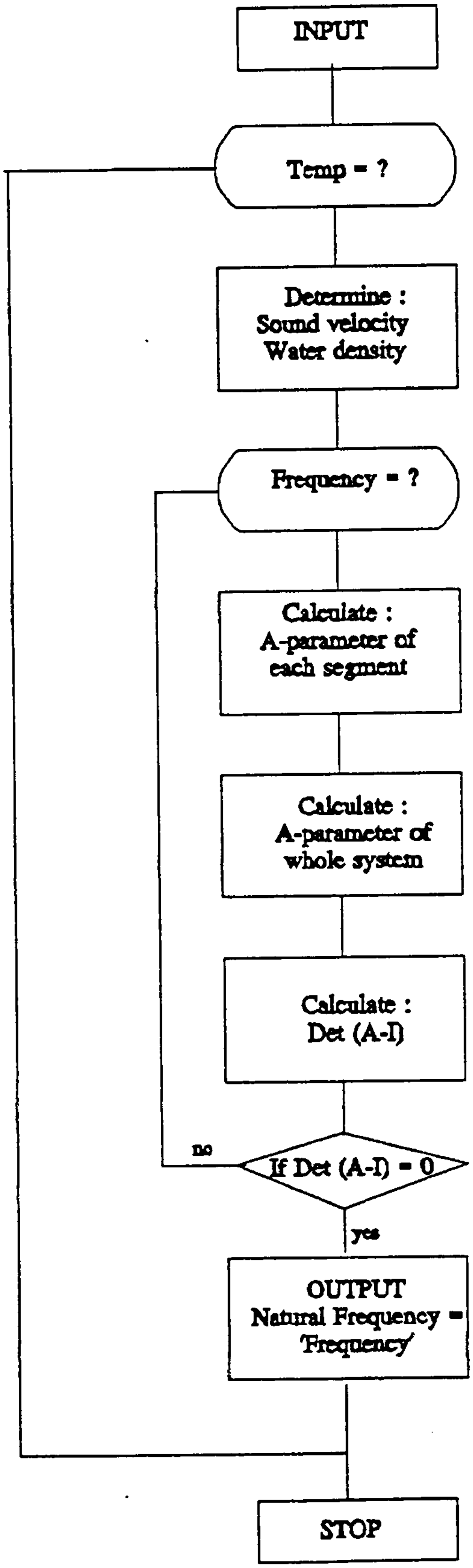

Figure 4.2: The flow scheme of the algortihm in PCSPRES

Table 4.2 : Data output program PCSPRES for 0% power level of cycle 17 (BNPP)

Condition	Value	Unit
File	B17001AF9	
System Pressure	2190.11	psia
Hot Leg Temperature	269.5	°C
Cold Leg Temperature	269.5	°C
Water Density	854.9	Kg/m^3
Sound Velocity in Water	1122.8	m/sec.
Natural Frequency	7.73	Hz.

Table 4.3 : Data output program PCSPRES for 10% power level of cycle 17 (BNPP)

Condition	Value	Unit
File	B17003F2	
System Pressure	2219.11	psia
Hot Leg Temperature	290	°C
Cold Leg Temperature	287	°C
Water Density	829.9	Kg/m^3
Sound Velocity in Water	1069.3	m/sec.
Natural Frequency	7.37	Hz

Table 4.4 : Data output program PCSPRES for 30% power of cycle 17 (BNPP)

Condition	Value	Unit
File	B17002F3	
System Pressure	2240.87	psia
Hot Leg Temperature	297.5	°C
Cold Leg Temperature	290.5	°C
Water Density	816.2	Kg/m^3
Sound Velocity in Water	1052.3	m/sec.
Natural Frequency	7.26	Hz.

Table 4.5 : Data output program PCSPRES for 100% power of cycle 17 (BNPP)

Condition	Value	Unit
File	B17012	
System Pressure	2303.2	psia
Hot Leg Temperature	315	°C
Cold Leg Temperature	292	°C
Water Density	772.8	Kg/m^3
Sound Velocity in Water	1016.4	m/sec.
Natural Frequency	7.02	Hz.

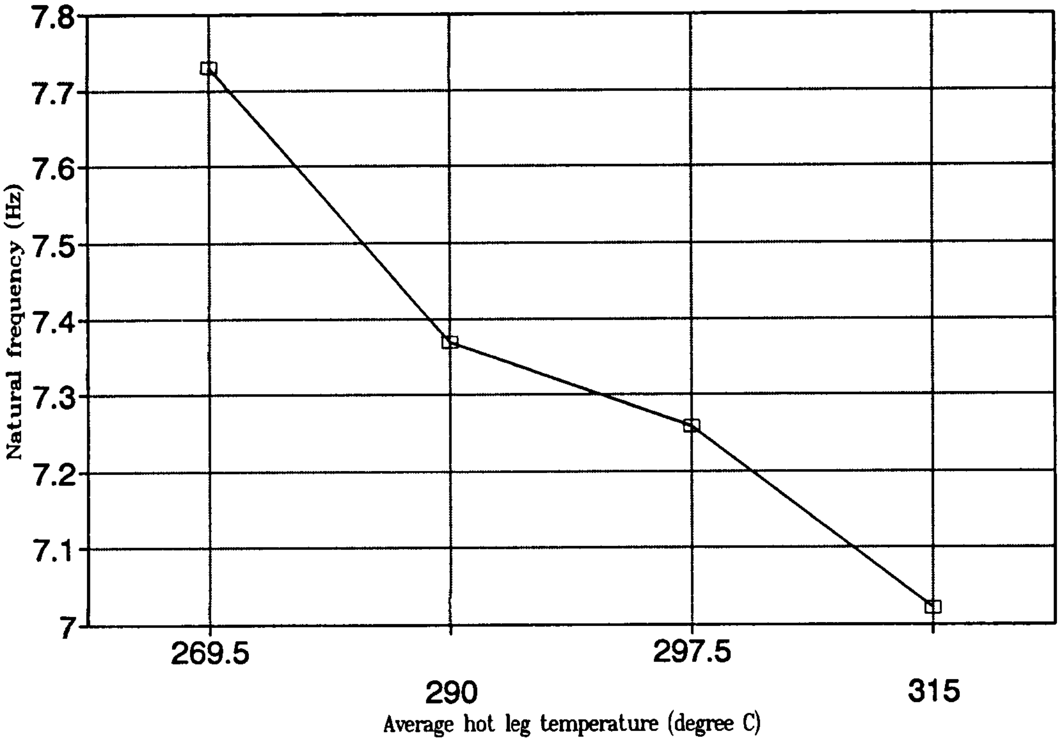

Figure 4.3 : Theoretical natural frequency as a function of temperature for Borssele PWR.

The correct eigenfrequency related to the standing wave must match the corresponding frequency in the pressure noise measurements. For the Borssele PWR, this is in the region of 7 Hz.

4.4. Eigenfrequency Calculation for a Typical Four-Loop PWR

An 1140 MWe four-loop Westinghouse-type PWR was considered in this analysis. Principally, the computations for two-loop and four-loop systems are similar; only the number of parallel loops is changed from two loops to four loops. Figures 4.4 and 4.5 show the primary coolant system of a typical four-loop PWR and the primary coolant flow branch lines. The dimensions for four-loop PWR were not completely available. Therefore, some of the data must be approximated. The information pertaining to the primary coolant system of the four-loop reactor is given in Table 4.6. The eigenfrequencies of the four-loop PWR were calculated using a procedure similar to the Borssele calculations, and the results are shown in Table 4.7. The frequency of interest, which was calculated with the conditions mentioned in Table 4.6, is about 7.5 Hz.

There is a possibility that the total water volume in the primary system is more than that shown in Table 4.6. Therefore, calculations were also made with various pipe lengths and the results are shown in Table 4.8 or Figure 4.6. The table shows that the eigenfrequency is sensitive to the physical dimensions. Therefore, the accuracy of the result of model analysis depends on the accuracy of design data available.

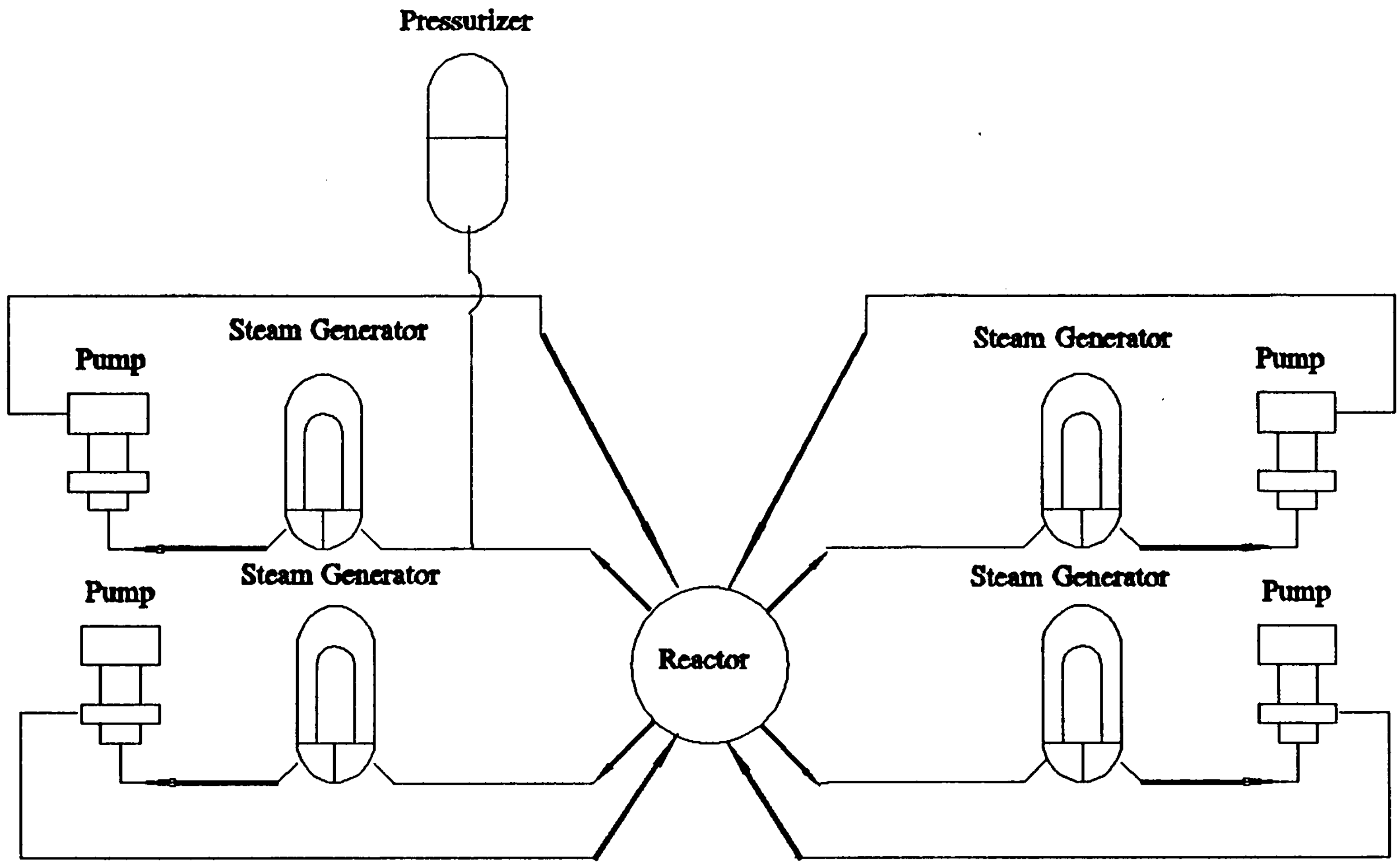

Figure 4.4: The primary coolant system of the four-loop PWR.

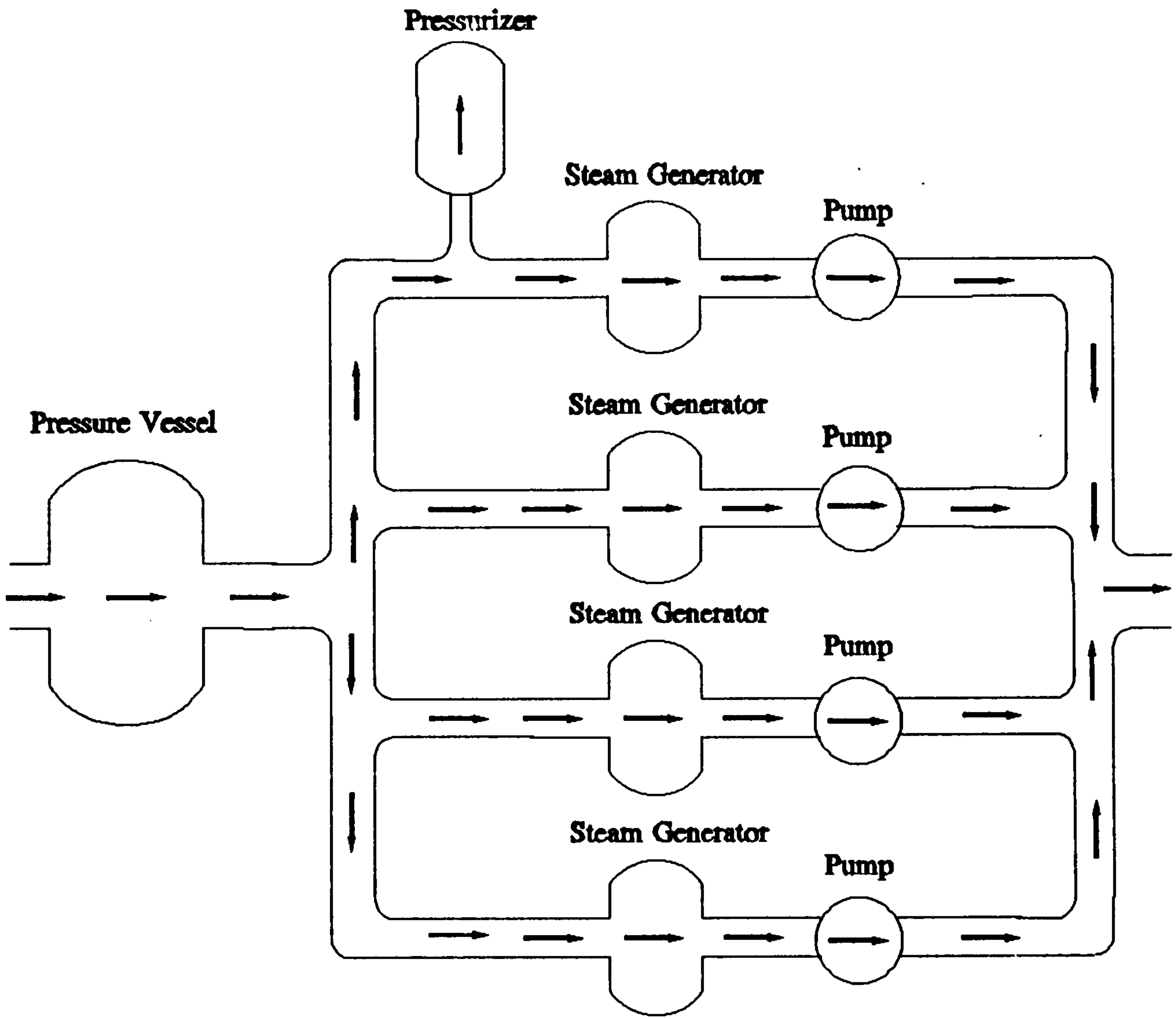

Figure 4.5: Primary coolant flow branch line of the four-loop PWR.

Table 4.6 : Primary coolant system information for a typical four-loop PWR [25]

Component	Value	Unit
Pressure Vessel		
Core Diameter (*119.7 inches*)	3.04	m
Core Height (*144 inches*)	3.66	m
Nominal Power Output	3436	MWt
Reactor Coolant Inlet Temperature (*530.2 °F*)	276.7	°C
Reactor Coolant Outlet Temperature (*594.2°F*)	312.3	°C
Total Water Volume Below Core (*1050 ft^3*)	29.74	m^3
Water Volume in Active Core Region (*665 ft^3*)	18.83	m^3
Total water Volume on Top of Core (*2164 ft^3*)	61.24	m^3
Total Reactor Vessel Volume (*4945 ft^3*)	140.04	m^3
Pressurizer		
Water Volume, Full Power (*1080 ft^3*)	30.59	m^3
Steam Volume, Full Power (*720 ft^3*)	20.4	m^3
Operating Pressure (*2235 psia*)	15.21	MPa
Steam Generator		
Number of Steam Generator	4	
Reactor Coolant Flow (*33.8 10^6 lb/hr*)	4258.8	Kg/sec
Reactor Coolant Water Volume (*1080 ft^3*)	30.58	m^3
Pumps		
Number of Pumps	4	
Pump Discharge Nozzle (*27.5 inches*)	0.6985	m
Pump Suction Nozzle (*31 inches*)	0.7874	m
Water Volume (*56 ft^3*)	1.59	m^3
Piping		
Reactor Inlet Piping Diameter (*27.5 inches*)	0.6985	m
Reactor Outlet Piping Diameter (*29 inches*)	0.7344	m
Coolant Pump Suction Piping Diameter (*31 inches*)	0.7874	m
Pressurizer Surge Line Piping Diameter (*11.118 inches*)	0.2824	m
Water Volume (all 4 loops including surge line)(*1545ft^3*)	43.75	m^3

Table 4.7 : Data output program PCSPRES for a full power level typical four-loop PWR

Conditions	Value	Unit
System Pressure	2235	psia
Hot Leg Temperature	312.3	°C
Cold Leg Temperature	276.7	°C
Water Density	684.3	Kg/m^3
Sound Velocity	1020	m/sec
Natural Frequency	7.51	Hz

Table 4.8 : **The pressure noise natural frequency of a typical four-loop PWR for different primary loop lengths ($T_{hot\ leg}$ = 312.3°C)**

Pipe 1 length (m)	Pipe2 length (m)	Pipe 3 length (m)	Natural frequency (Hz)
12.62	5.49	6.97	7.51
13.62	5.99	7.47	7.20
14.62	6.49	7.97	6.93
15.62	6.99	8.47	6.69
16.62	7.49	8.97	6.47
17.62	7.99	9.47	6.26
18.62	9.49	10.97	5.89

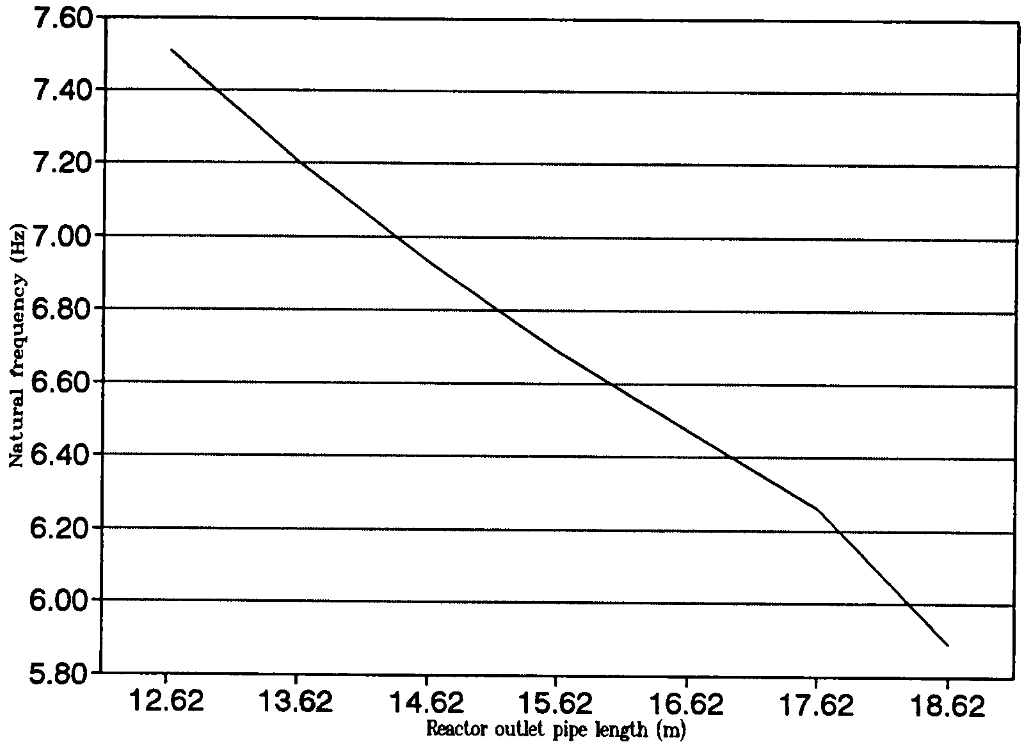

Figure 4.6: Theoretical natural frequency of pressure noise for different lengths of hot leg piping for a hot leg temperature of 312.3°C.

The calculations of natural frequencies were also made at different temperatures as shown in Table 4.9 and Figure 4.7. In this calculation, it is assumed that temperature differences between hot leg and cold leg are almost the same for a slight change in hot leg temperature. The calculations show that the natural frequency decreases with increasing temperature. At a temperature of around 618.3 °F or 325.7 °C, the natural frequency is 7.34 Hz. The detailed discussion of results are presented in Chapter 7. These include both the two-loop and the four-loop PWRs.

Table 4.9 : The pressure noise natural frequency of a typical four-loop PWR for different temperatures

Temperature (°C)	Natural frequency (Hz)
302	7.64
308	7.57
312	7.51
319	7.41
325.7	7.34

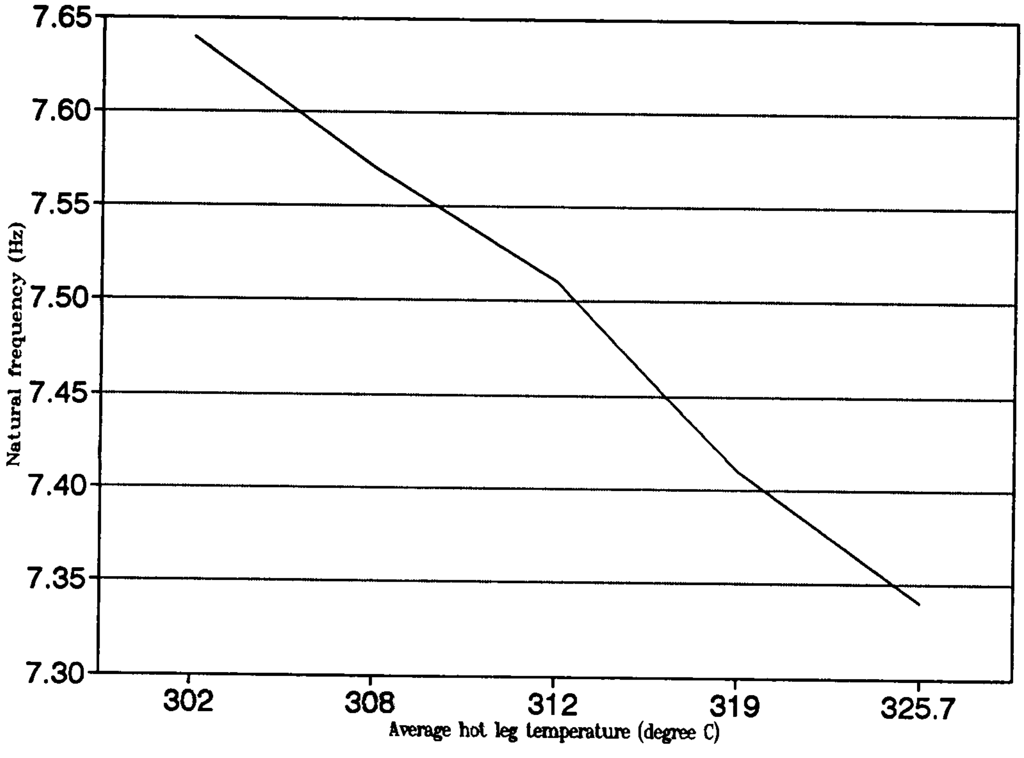

Figure 4.7 : **Theoretical natural frequency as a function of temperature for a typical four-loop PWR.**

CHAPTER 5

SIGNAL ANALYSIS METHODS

As described in Chapter 2, the pressure noise in a primary coolant system provides important information of some of the physical aspects that occurr along the primary loop, including temperature changes. The data are acquired from pressure transmitters installed in the primary loop. Because the level of pressure noise signal is generally small, it is recommended that a narrow range pressure sensor be used for this type of measurement.

In noise analysis, the mean value of presssure signal is assumed to be either zero or constant. There are three categories of random signal representation: (1) amplitude, (2) time, and (3) frequency. This study evaluates the changes in these signatures due to temperature changes in the primary coolant system of PWRs. Only the univariate analysis of signals is considered in this work.

5.1 Amplitude Probability Density Function

The mean value and the variance of a random process are calculated as

$$x_{mean} = \frac{1}{N} \sum_{i=1}^{N} x_i \tag{5.1}$$

$$\sigma_x^2 = C_x(O) = = \frac{1}{N} \sum_{i=1}^{N} (x_i - x_{mean})^2, \tag{5.2}$$

where $\{x_i\}$ are the samples of the continuous stationary signal $x(t)$. By definition, the probability function is the fraction of time $x(t)$ spends between x and $x+dx$. Computationally, this is called the amplitude probability density (APD) function. Generally, the random process in a nuclear power plant follows Gaussian distribution. The Gaussian probability density function is defined as

$$APD(x_i) = \frac{1}{\sqrt{2\pi C_x(0)}} \exp\{-\frac{(x_i - x_{mean})^2}{2C_x(0)}\} \tag{5.3}$$

where $C_x(0)$ is defined in Equation (5.2).

In order to verify the extent of deviation of the actual APD from the Gaussian distribution, we need to calculate the skewness (G_{skew}) and flatness (G_{flat}) of the APD. For a random process, the formulas are defined as

$$G_{skew} = \frac{1}{N * C_x(0)^{3/2}} \sum_{i=1}^{N} (x_i - x_{mean})^3 \tag{5.4}$$

$$G_{flat} = \frac{1}{3N * C_x(0)^2} \sum_{i=1}^{N} (x_i - x_{mean})^4, \tag{5.5}$$

where x_{mean} is the mean value of signal x.

In practice, the measured data may not exactly have a Gaussian distribution. Therefore, it is necessary to measure the deviation of the measured data from the Gaussian distribution. One approach to measure this deviation is to calculate a modified

APD (MPAD) function. The MAPD is defined as the logarithm of the previously calculated APD values and is expressed as a function of the square deviation of the signal from its mean value. Theoretically, the Gaussian APD function, as given in Equation (5.3), has the form where the two parameters, x_{mean} and $C_x(0)$, determine the distribution uniquely. By taking the natural logarithm of both sides and rearranging them, we will get the equation

$$2C_x(0)\ \ln\ (\sqrt{2\pi C_x(0)}\ APD(x_i)) = -\ (x_i - x_{mean})^2. \tag{5.6}$$

The left-hand side of this equation is called the modified amplitude probability density function ($MAPD(x_i)$). Therefore

$$MAPD(x_i)\ =\ -\ (x_i\ -\ x_{mean}\ )^2. \tag{5.7}$$

For a stationary random process, the mean and variance do not change with time. For a signal with Gaussian distribution, the skewness is approximately zero and the flatness is approximately unity.

5.2 Time-Domain Analysis

To analyze the correlation among signals, the time-domain analysis is generally used. For a single signal and a pair of signals, the auto correlation and cross correlation functions are defined as follows:

$$R_{xx}(\tau)\ =\ \lim_{T\to\infty}\frac{1}{T}\int_0^T x(t)\ x(t+\tau)dt \tag{5.8}$$

$$R_{xy}(\tau) = \lim_{T \to \infty} \frac{1}{T} \int_0^T x(t)\, y(t+\tau)dt \tag{5.9}$$

The auto correlation represents the dependence of the data values separated by a lag τ. The existence of periodic components in the signal and its bandwidth characteristics can be observed in $R_{xx}(\tau)$. $R_{xy}(\tau)$ is the cross correlation between two jointly stationary signals *x(t)* and *y(t)*.

5.3 Power Spectral Density Function

The data acquired at a power plant are digitized at an appropriate sampling rate and are converted to discrete values. The fast Fourier transform (FFT) technique is generally used to convert the time-domain information to frequency-domain information and to calculate auto power spectral density (APSD) of signal *x(t)*, and cross power spectral density (CPSD) between two signals *x(t)* and *y(t)*.

The APSD function $S_{xx}(f)$ and the CPSD function $S_{xy}(f)$ are related to the corresponding correlation functions.

$$S_{xx}(f) = \int_{\infty}^{\infty} R_{xx}(\tau) e^{-j2\pi f\tau} d\tau \tag{5.10}$$

$$S_{xy}(f) = \int_{-\infty}^{\infty} R_{xy}(\tau) e^{-j2\pi f\tau} d\tau. \tag{5.11}$$

S_{xy} is a complex function of frequency f.

The magnitude and phase of CPSD are

$$|S_{xx}| = \{ReS_{xy}(f)^2 + ImS_{xy}(f)^2\}^{\frac{1}{2}} \tag{5.12}$$

$$\phi_{xy}(f) = \tan^{-1}\left\{\frac{ImS_{xy}(f)}{ReS_{xy}(f)}\right\}. \tag{5.13}$$

In practice the above equations are computed from finite Fourier transform. The finite Fourier transform of $x(t)$ and $y(t)$ are given by

$$x(f,T) = \int_0^T x(t)e^{-jn2\pi t}dt \tag{5.14}$$

$$y(f,T) = \int_0^T y(t)e^{-jn2\pi ft}dt. \tag{5.15}$$

These are converted to discrete Fourier transforms (DFTs). The APSD and CPSD functions are estimated at integer frequency points. A fast algorithm, called the fast Fourier transform (FFT), is generally used for this computation. This is performed for a number of blocks of data N, and the average is taken over the N blocks. The spectrum between two signals x_i and x_j is

$$S_{ij}(k) = \frac{\Delta t}{M*N}\sum_{1}^{N}\left\{\sum x_i^{(1)}\exp(-\frac{j2pimk}{M})\sum x_j^{(1)}\exp(+\frac{j2\pi nk}{M})\right\}$$

$$i=1,2,...,m \tag{5.16}$$

where m = number of signals for processing,

M = number of data points per block,

N = number of blocks of data,

k = discrete frequency point

= 0,1,2,..., M/2.

The frequency resolution of the power spectrum is $\Delta f = 1/(M\Delta t)$, where Δt = sampling interval (second). A digital signal processing (DSP) software system was used in all the calculations presented in this thesis.

CHAPTER 6

PRIMARY COOLANT PRESSURE SIGNAL ANALYSIS

6.1 Noise Measurement System at Borssele PWR

The Borssele Nuclear Power Plant (BNPP) in the Netherlands is a 470 MWe pressurized water reactor (PWR) supplied by KWU. Operational data were acquired from BNPP since 1974 by the Netherlands Energy Research Foundation (ECN), Petten. ECN has been instrumental in performing continuous monitoring of the BNPP, and in some cases, diagnostics of incipient problems.

The purpose of the measurements is (1) to determine the noise pattern of the reactor as completely as possible, (2) to follow the pattern in time, and (3) to try to anticipate the changes in the signal and relate them to physical phenomena [3]. The data acquisition and analysis system performs multi-processing, multi-tasking, real-time monitoring, on-line calculation of reactor parameters, and database preparation for expert systems. It also provides early information on possible malfunctions. In addition, an expert system operating on the VAX station has been added for surveillance and diagnostics task and for database management.

Figure 6.1 shows a detailed scheme of the Borssele Nuclear Power Plant data acquisition and monitoring system. Signals from the plant are sent to a patch-panel, which can accept 90 sensory signals simultaneously. The signals are then conveyed to the microcomputer-based signal conditioning unit in order to precondition the signal for telephone transmission. The signal conditioning unit itself can process 32 signals at a

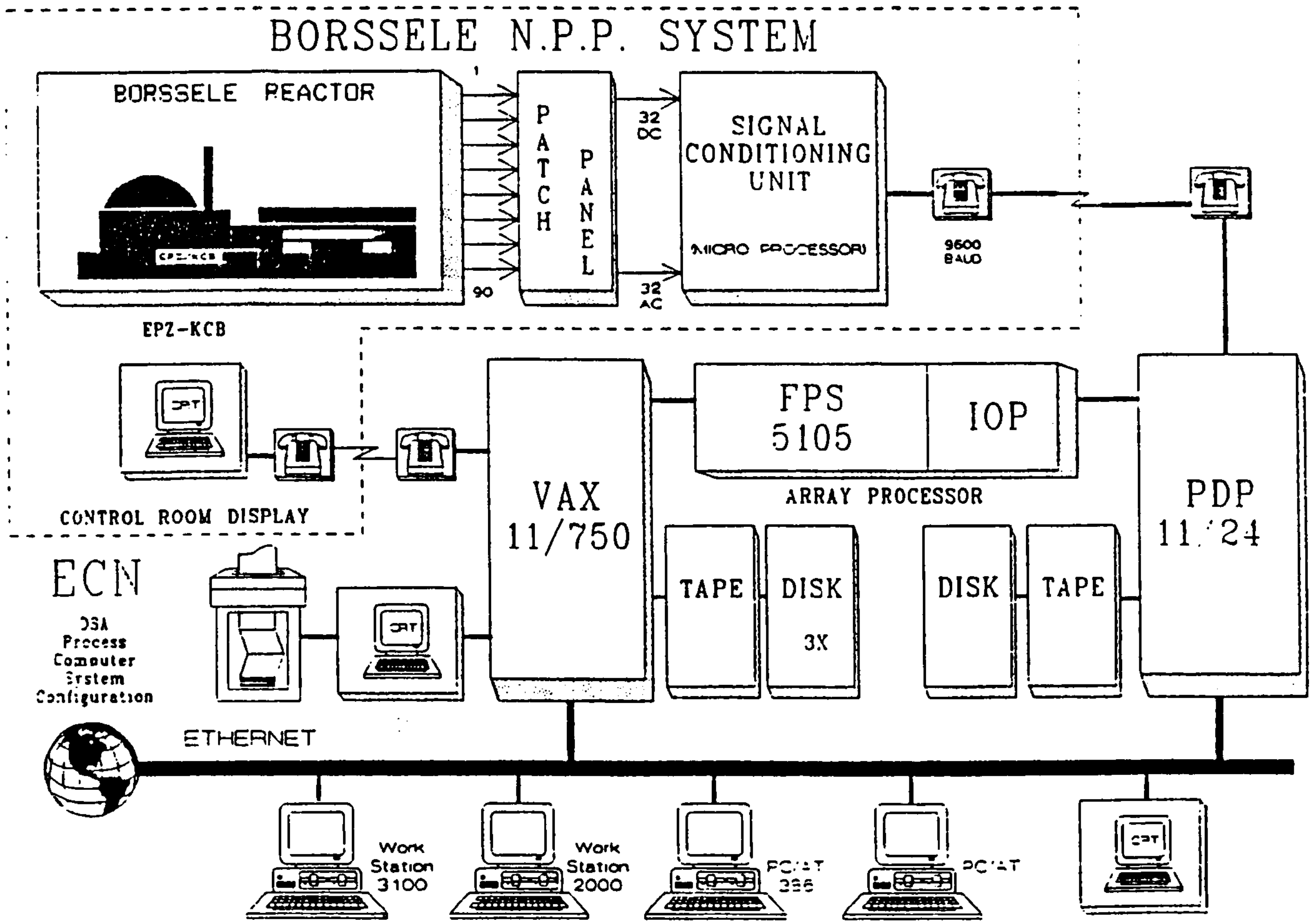

Figure 6.1 : Detailed Schematic of the BNPP signal acquisition system [2].

time in both DC and AC modes. For processing, the system uses a VAX 11/750 computer, equipped with an array processor (Floating Point System 5105), along with a PDP 11/24 front-end processor. Presently, the front-end processor is also used as a redundant device for data storage and as a direct monitor of the signals transmitted through the telephone lines. Two additional workstations are connected to the main processor through the universal communication net, Ethernet, so that the system forms a distributed real-time computer system.

Briefly, the data are processed as follows: The data received in multichannel form from the plant are introduced to the array processor. The data are then stored as a block for FFT processing. This process is performed for a pre-selected number of channels and cross combinations. For each block consisting of N samples, together with the preceding data block, N/2-point Fourier transform is performed for each channel. For all desired pairs of channels, the transforms are complex conjugated and multiplied.

This kind of system is not fully available at other reactors. It was specifically designed for BNPP for noise monitoring and diagnostics purposes. Therefore, this reactor was used for modeling and analysis in this study. Other reactors, for example a typical four-loop Westinghouse reactor, are equipped with wide-range pressure transmitters. The disadvantage of using this sensor is the reduced resolution in the fluctuating component of the signal. Nevertheless, the signal analysis is useful for studying the pressure noise behavior in the primary coolant system.

6.2 Pressure Noise Measurement at Borssele PWR

Figure 6.2 shows the schematic of the Borssele reactor and the position of the sensors. YA01 and YAO2 represent loop 1 and loop 2. There are five pressure transmitters in each loop: three at the same position (P001, P002, P011) but in different continuous tubes, one transmitter 1.5m from these (P063), and one differential transmitter across the main pump (P003).

The Borssele pressure noise data used for analysis were acquired during cycle 17 at power levels of 0%, 10%, 30% and 100%. Table 6.1 gives information about the pressure noise and sampling condition of each file taken in loop 1 and loop 2 (YA01-P002 and YA02-P002).

In fact, not all data were found to be stationary or valid. This is because the pressure noise data were acquired during the start-up period. Most of the pressure noise was recorded when either temperature or pressure was changing. In other words, the statistical characteristics of the data were changing. The noise analysis can still be performed by selecting portions of the data during which the process is stationary. After analyzing all files in Table 6.1, only 6 files fulfill the criteria of stationary signals as shown in Table 6.2. These data correspond to 0%, 10%, 30% and 100% power levels during cycle 17, and two records at 100% power level during cycle 18. Each file consists of two pressure noise signals (i.e. pressure signals from loop 1 and loop 2). Figures 6.3 - 6.12 show the amplitude probability density and power spectral densities of the pressure noise listed in Table 6.2.

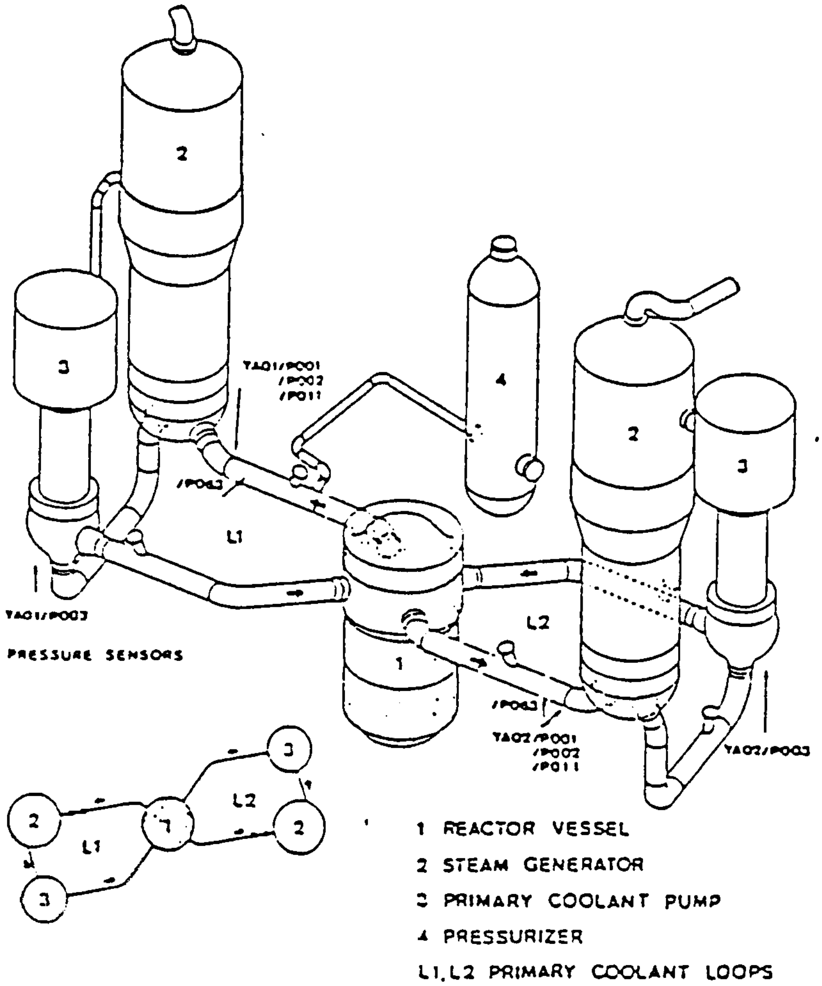

Figure 6.2: Schematic of the Borssele reactor showing the position of sensors [2].

Table 6.1: Data acquisition information for Borssele PWR during cycles 17 and 18

File name	Reactor power (in %)	Temperature (°C)	Number of data blocks	Gain
B17001AF2	0	40	1003	200
B17001AF3	0	*	1003	200
B17001AF4	0	*	1003	200
B17001AF5	0	*	1003	200
B17001AF6	0	*	1003	200
B17001AF8	0	*	1003	200
B17001AF9	0	267	2003	200
B17002F3	0	*	2003	200
B17002F4	0	*	3003	200
B17002F5	0	*	3003	200
B17002F6	0	*	2003	200
B17002F7	0	*	2003	200
B17002F9	0	*	2003	200
B17003F2	10	287	1003	500
B17003F3	30	292	2003	500
B17012	100	315	3003	500
B18141A	100	317	3003	500
B18143A	100	318	3003	500

* Temperatures are not constant.
Low-pass filter setting = 40 Hz.
Sampling frequency = 64 Hz.

Table 6.2 : Results of analysis of Borssele reactor pressure noise data

File name	Power (in %)	Temperature (°C)	RMS value	Skewness	Flatness	Natural Frequency (Hz)
B17001AF9	0	267	4.76E-3	-6.26E-3	1.004	7.07
			2.06E-3	1.13E-3	1.012	7.07
B17003F2	10	287	2.20E-3	7.32E-3	1.002	6.59
			2.07E-3	1.13E-3	1.012	6.59
B17003F3	30	292	2.33E-3	1.08E-3	1.008	6.41
			2.54E-3	1.91E-3	1.002	6.41
B17012	100	315	1.94E-3	3.78E-3	1.006	6.53
			1.85E-3	1.19E-3	1.010	6.57
B18141A	100	317	1.99E-3	-9.41E-4	0.988	6.53
B18143A	100	318	2.00E-3	5.89E-4	0.978	6.57

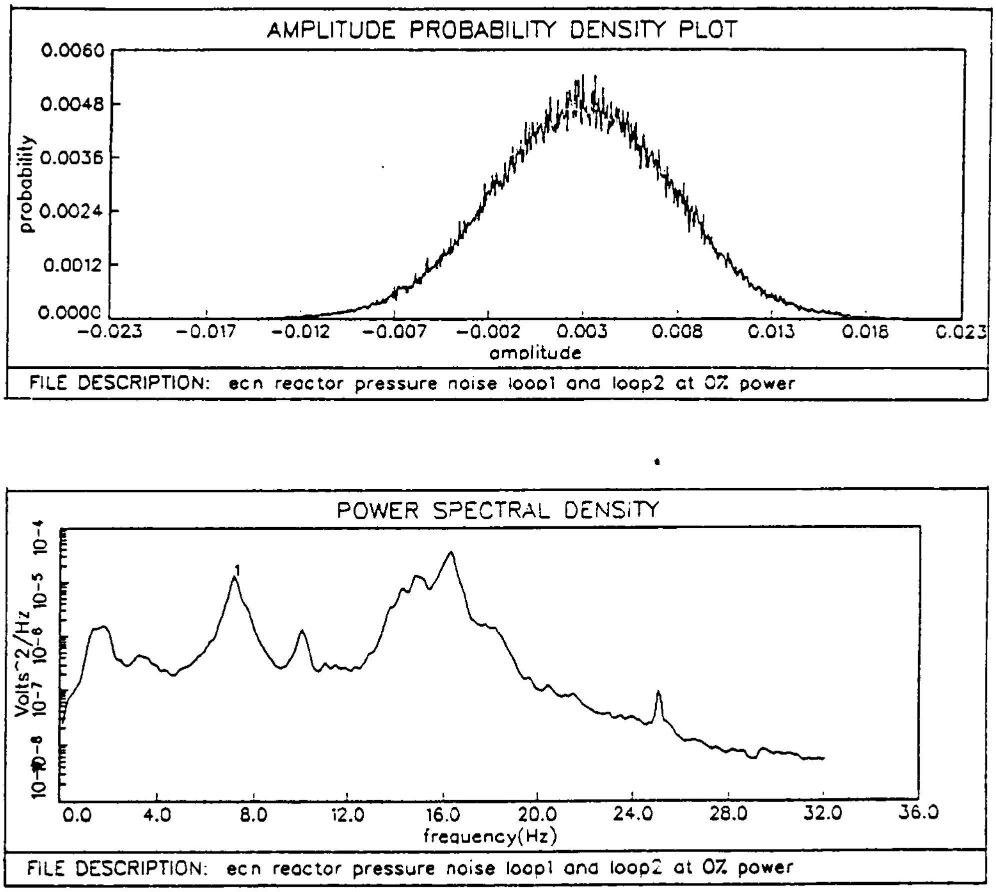

Figure 6.3 : Pressure noise amplitude probability density and power spectral density of BNPP primary coolant system loop 1 during cycle 17 at 0% power level.

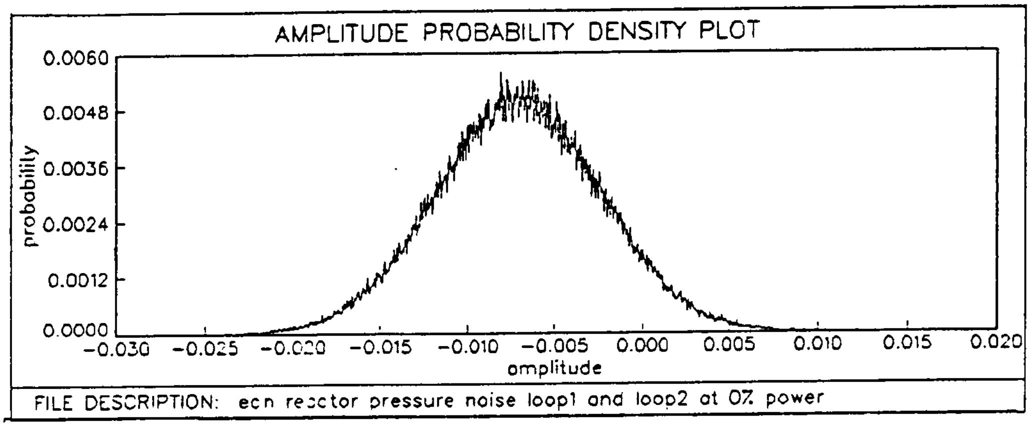

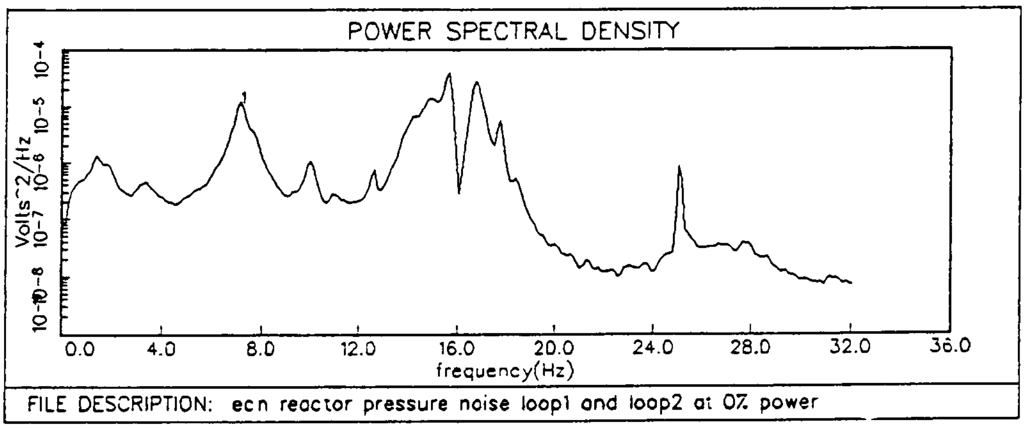

Figure 6.4 : Pressure noise amplitude probability density and power spectral density of BNPP primary coolant system loop 2 during cycle 17 at 0% power level

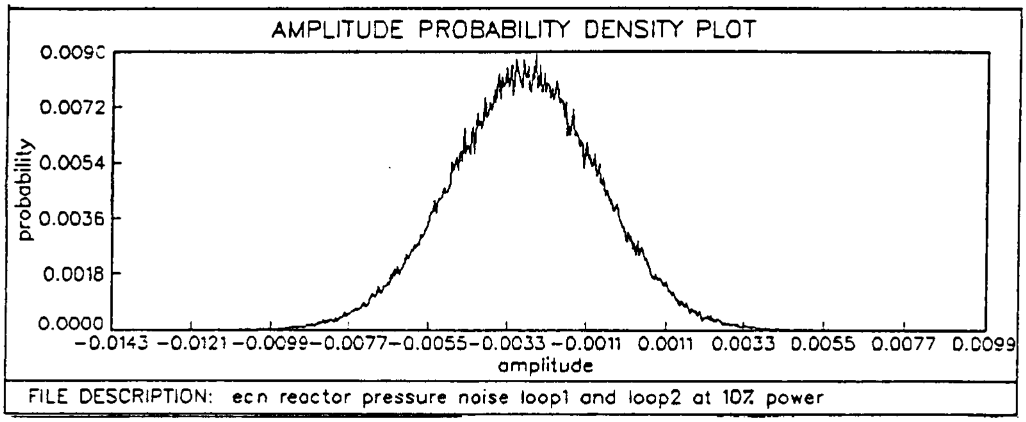

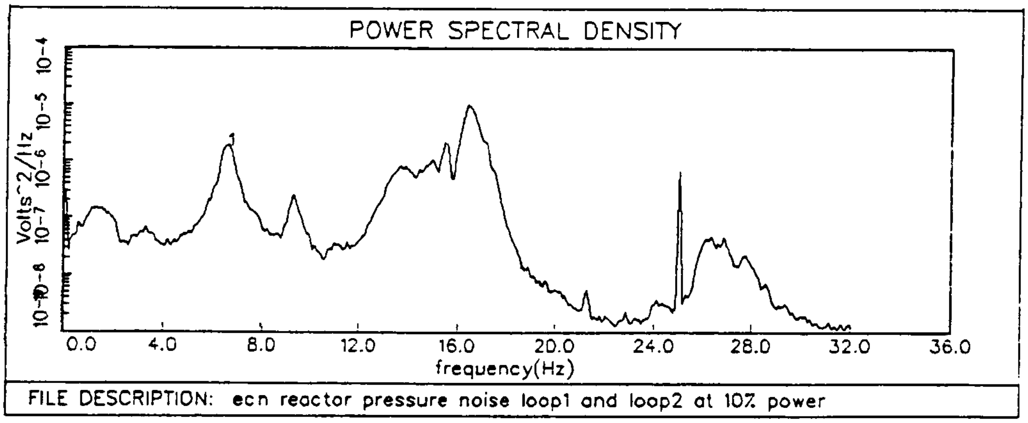

Figure 6.5 : Pressure noise amplitude probability density and power spectral density of BNPP primary coolant system loop 1 during cycle 17 at 10% power level.

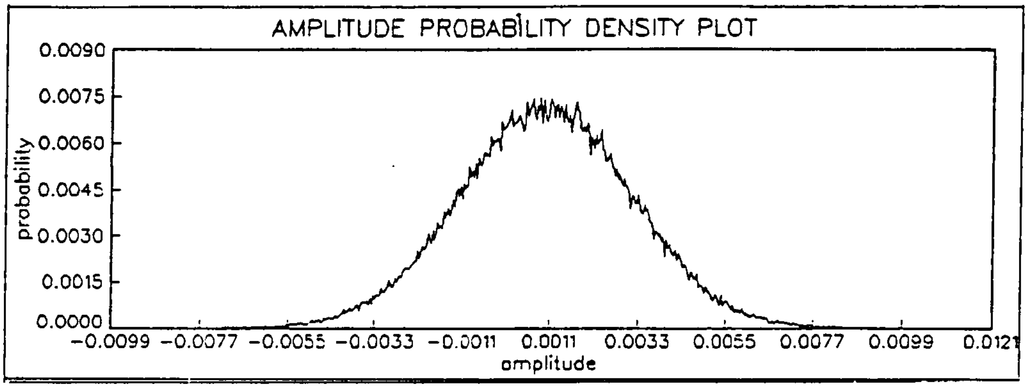

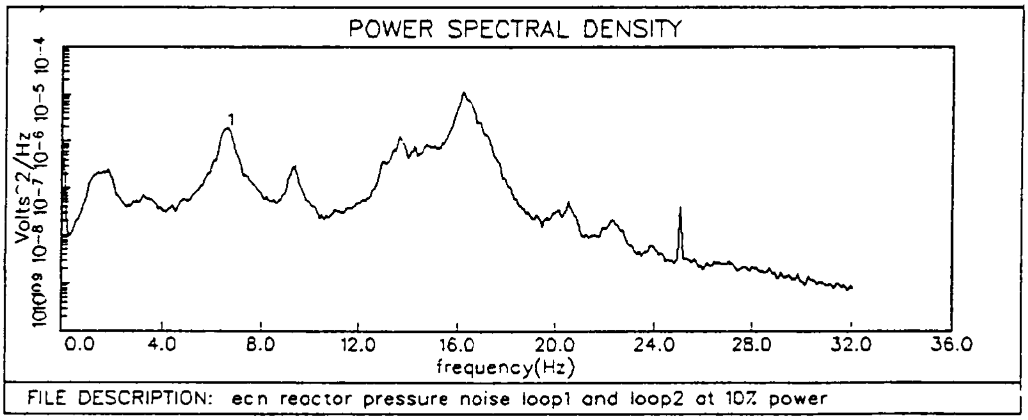

Figure 6.6 : Pressure noise amplitude probability density and power spectral density of BNPP primary coolant system loop 2 during cycle 17 at 10% power level.

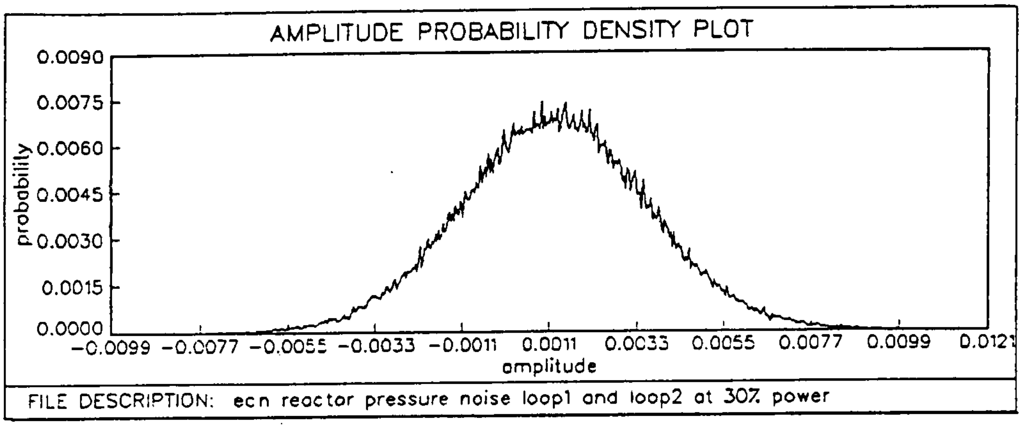

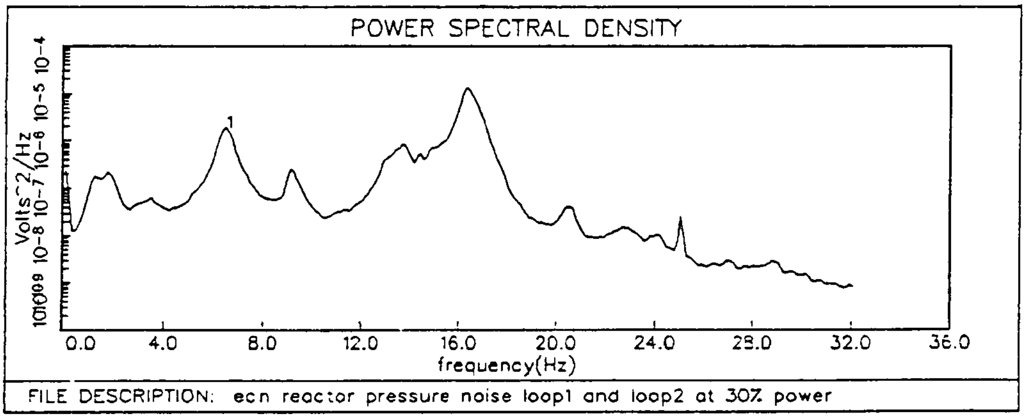

Figure 6.7 : Pressure noise amplitude probability density and power spectral density of BNPP primary coolant system loop 1 during cycle 17 at 30% power level.

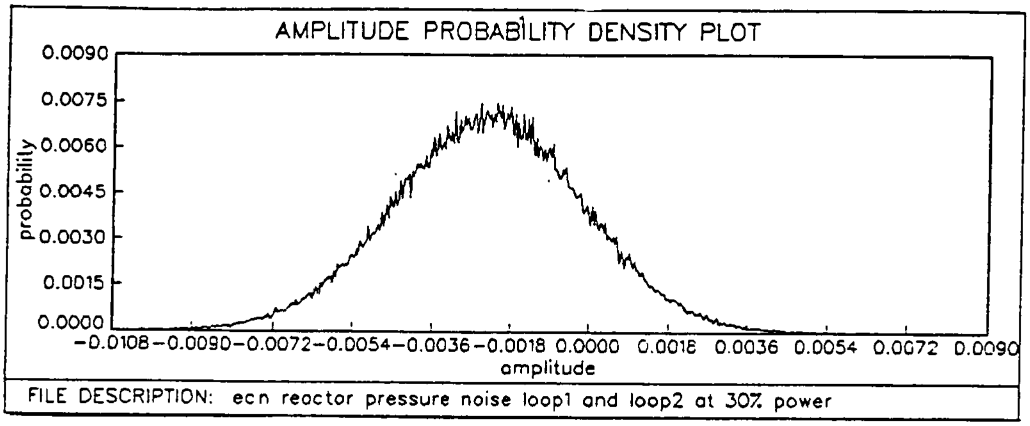

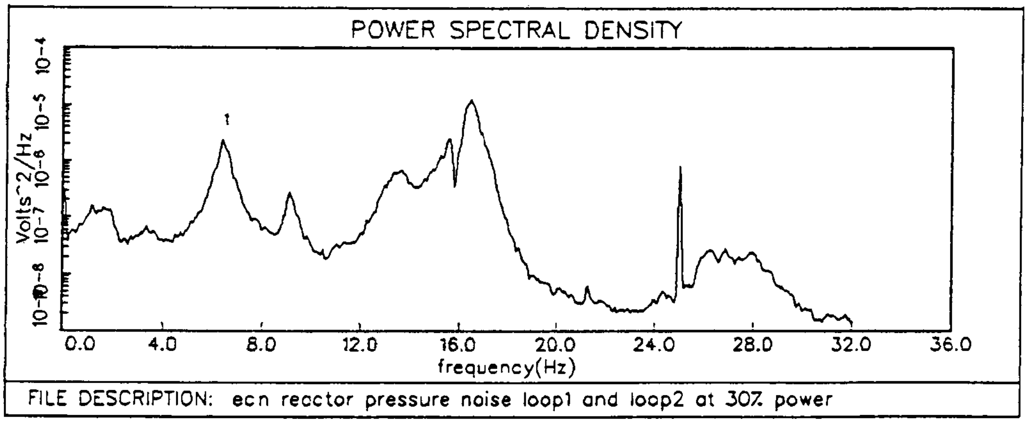

Figure 6.8 : Pressure noise amplitude probability density and power spectral density of BNPP primary coolant system loop 2 during cycle 17 at 30% power level.

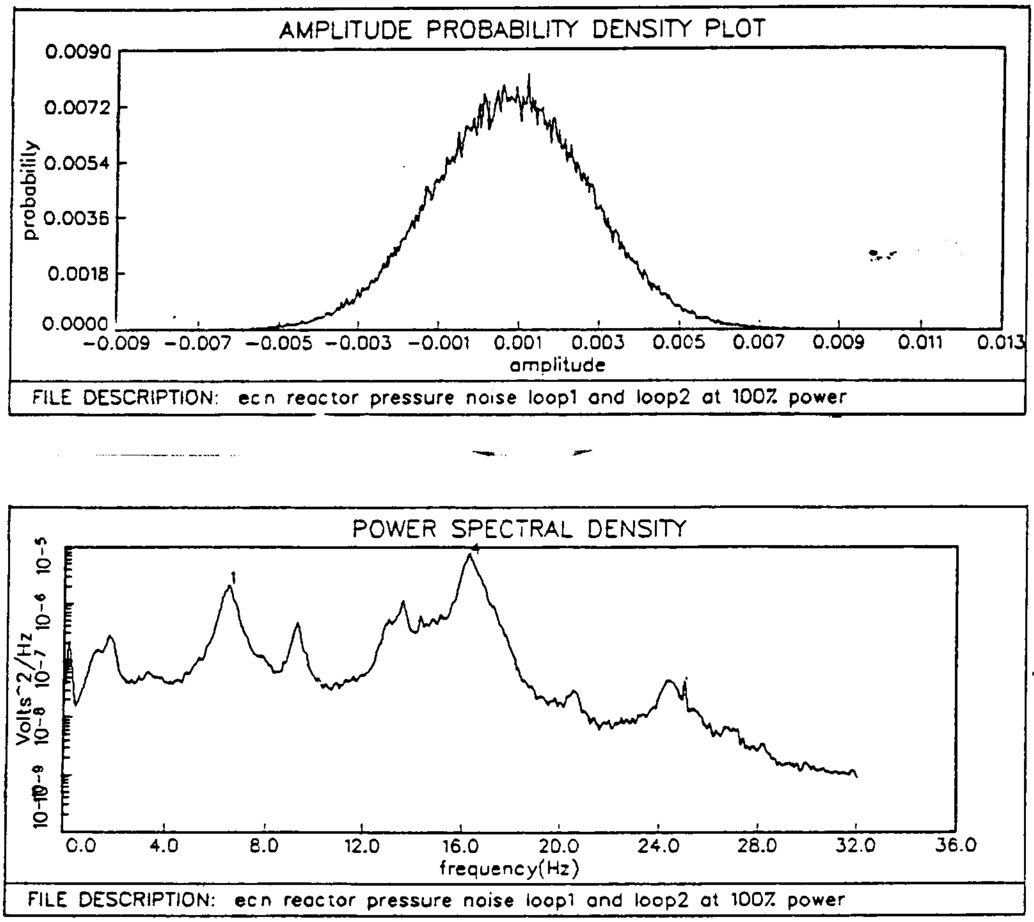

Figure 6.9 : Pressure noise amplitude probability density and power spectral density of BNPP primary coolant system loop 1 during cycle 17 at 100% power level.

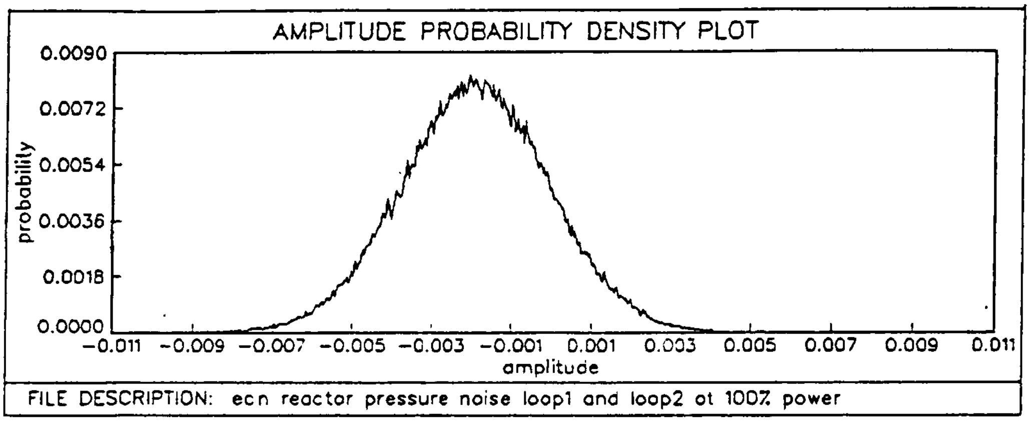

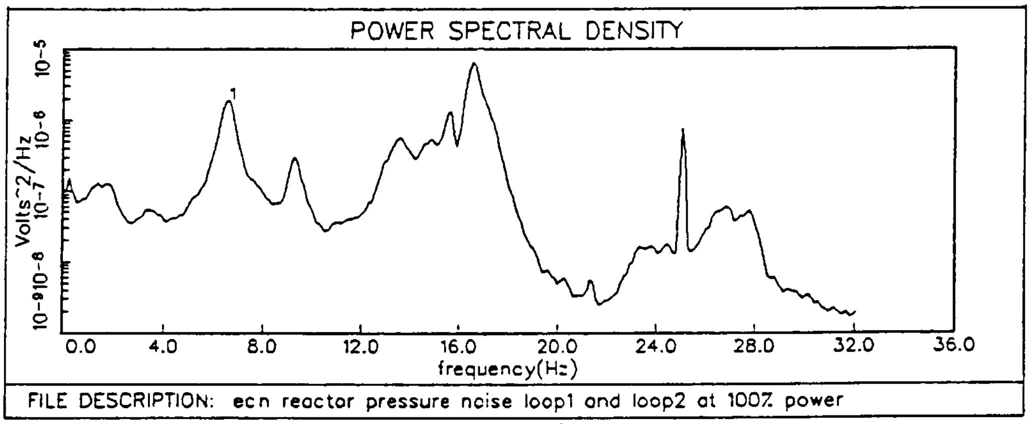

Figure 6.10 : Pressure noise amplitude probability density and power spectral density of BNPP primary coolant system loop 2 during cycle 17 at 100% power level.

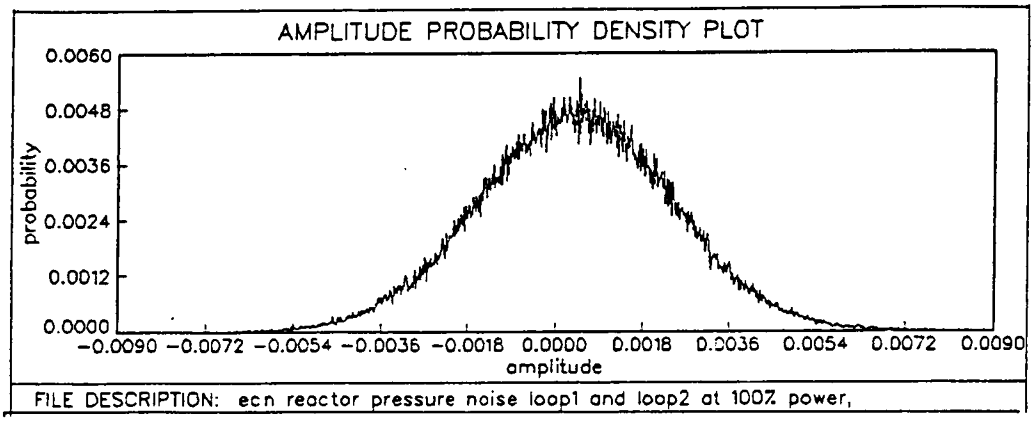

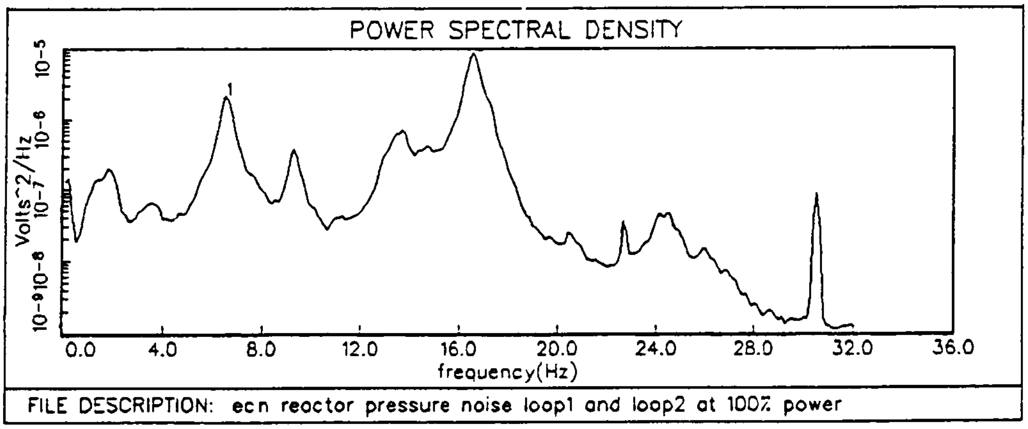

Figure 6.11 : Pressure noise amplitude probability density and power spectral density of BNPP primary coolant system loop 1 during cycle 18 at 100% power level.

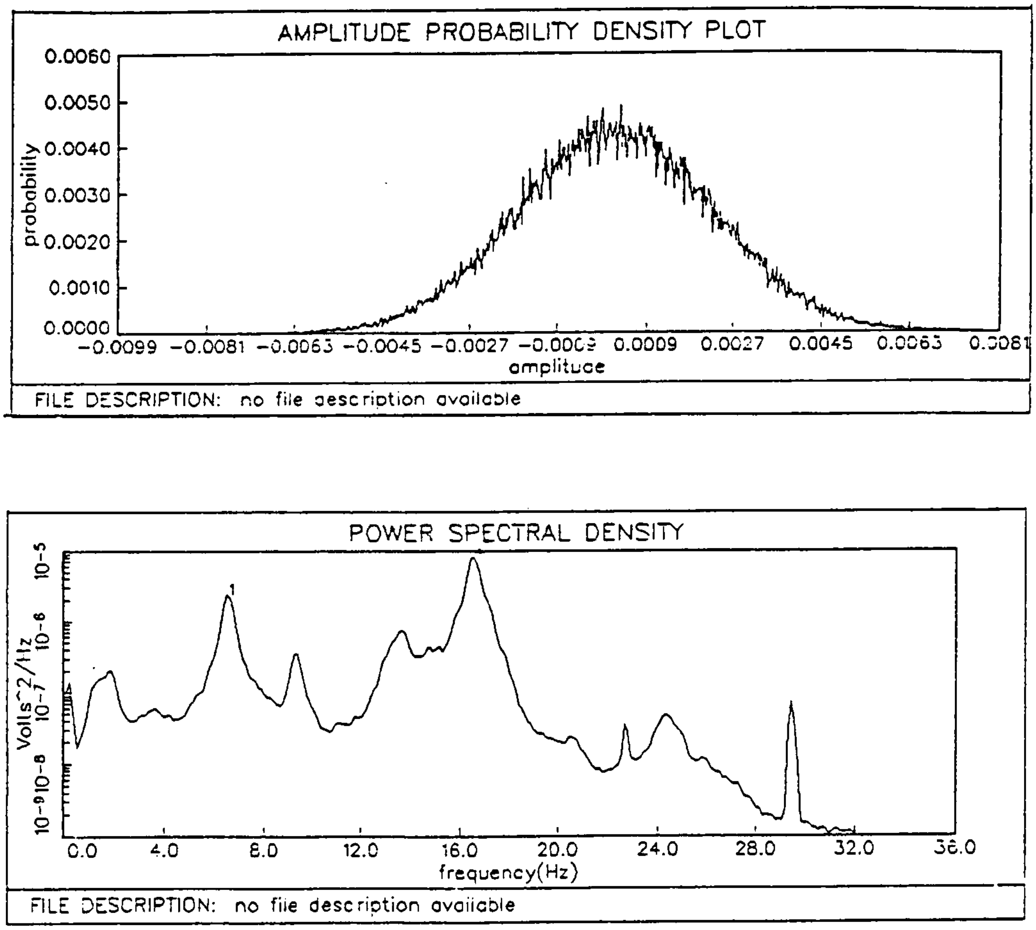

Figure 6.12 : Pressure noise amplitude probability density and power spectral density of BNPP primary coolant system loop 1 during cycle 18 at 100% power level.

Several peaks appear in the power spectral density. For example, in file B17012, there are peaks around 6.5 Hz, 9.2 Hz, 13.6 Hz, 16.3 Hz, and 25 Hz. Previous study [2,3] of pressure noise indicated that the peak frequency at 6.5 Hz is due to the natural frequency of the pressure noise (standing wave frequency) in the primary coolant system [2,4], whereas the frequency of 9.2 Hz is due to the pressure oscillation in the primary coolant system correlated with neutron noise [2]. Grunwald et al [6,7] showed that the reactor pump can cause the pressure noise frequency to be around 24 Hz. Pump frequency varies from 20 to 25 Hz.

As described in the previous study [2.3], the most sensitive frequency to the temperature change is the pressure noise frequency caused by hydraulic displacement and is around 6.5 Hz. This is also seen in the power spectral density function where this frequency shifts from 7.07 Hz to 6.57 Hz.

6.3. Pressure Noise Measurement at a Typical Four-Loop Westinghouse PWR

The four-loop PWR that was considered in this study is equipped with wide-range pressure transmitters in its primary loop. The main purpose of these transmitters is to keep track of the primary pressure of the coolant from its start-up until it achieves full power. For pressure noise measurements, narrow-range transmitters should be used because the measurements involve small changes of pressure. However, the wide-range transmitter signal is still useful in establishing the characteristic frequencies of primary pressure noise, and it relates to the present study. The data clearly show the presence of a standing wave in the pressure noise at a frequency close to the theoretical calculation.

The data acquisition used a sampling frequency of 20 Hz with a low-pass filter setting at 8 Hz. Each signal consists of 10,240 points. Table 6.3 shows detailed information about the pressure noise data files. Table 6.4 shows the summary of results of statistical analysis and the peak frequency value for each case. Figures 6.13 - 6.25 show the amplitude probability density and power spectral density for each of the signals listed in Table 6.3.

The statistical analysis of the signals showed that the skewness value of all signals are close to zero, and the flatness values are approximately unity. Therefore the signals follow the Gaussian distribution. The power spectral densities of all files show two peaks around 0.7 Hz and 7.2 Hz. It is clear that the low frequency peak at 0.7 Hz is due to the pressurizer dynamics. The resolution of the spectrum is not sensitive enough to identify a small change in the peak frequency due to a small change in coolant temperature. An average frequency value of the peak frequency corresponding to the standing wave frequency was calculated and is equal to 7.27 Hz.

Table 6.3: Data acquisition information for the four-loop PWR

File name	Power (%)	Temperature (°F)
NEM1031	98.9	618.3
NEM1033	99.3	618.5
NEM1034	99.7	618.4
NEM1035	100.3	618.5
NEM1036	100.6	618.3
NEM1037	97.2	618.2
NEM1038	97.7	618.2
NEM1039	97.7	618.2
NEM1040	97.8	618.3
NEM1041	98.3	618.4
NEM1042	98.2	618.3
NEM1043	98.9	618.3
NEM1044	99.2	618.3

Low-pass filter setting = 8 Hz.
Sampling frequency = 20 Hz.
Number of data blocks = 512

Table 6.4: Statistical analysis and peak frequency values of pressure noise for the four-loop PWR.

Data File	Power (%)	Temperature (°C)	RMS value	Skewness	Flatness	Peak Frequency (Hz)
NEM1031	98.9	618.3	3.09E-4	6.37E-3	0.900	7.19
NEM1033	99.3	618.5	3.08E-4	9.67E-3	1.080	7.21
NEM1034	99.7	618.4	3.14E-4	8.05E-3	1.047	7.22
NEM1035	100.3	618.4	3.09E-4	1.05E-2	0.960	7.29
NEM1036	100.6	618.2	3.16E-4	1.31E-2	0.987	7.26
NEM1037	97.2	618.2	3.23E-2	3.34E-2	1.015	7.33
NEM1038	97.7	618.2	3.24E-2	4.87E-3	1.016	7.31
NEM1039	97.7	618.2	3.20E-2	4.36E-3	0.919	7.26
NEM1040	97.8	618.3	3.22E-2	1.02E-3	0.969	7.26
NEM1041	98.3	618.4	3.28E-2	4.43E-3	0.965	7.23
NEM1042	98.2	618.3	3.26E-2	2.52E-2	0.988	7.28
NEM1043	98.9	618.3	3.23E-2	1.75E-2	1.018	7.31
NEM1044	99.2	618.3	3.30E-2	4.28E-2	1.006	7.25

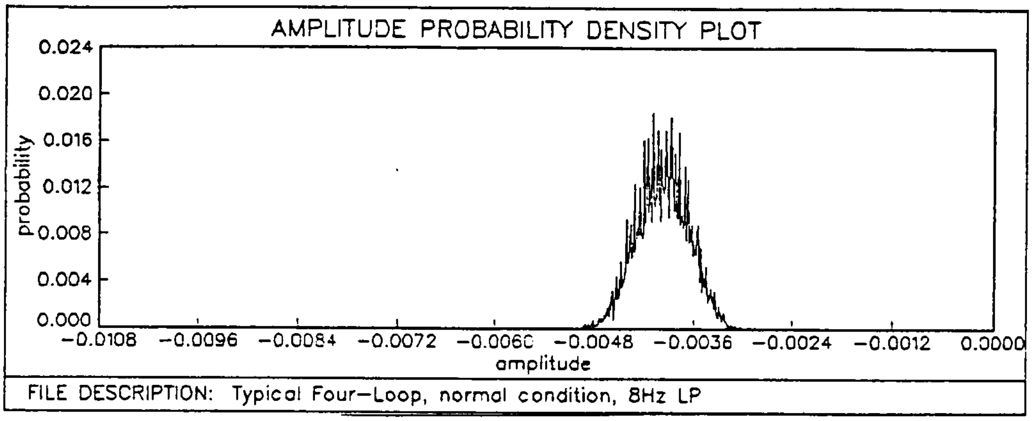

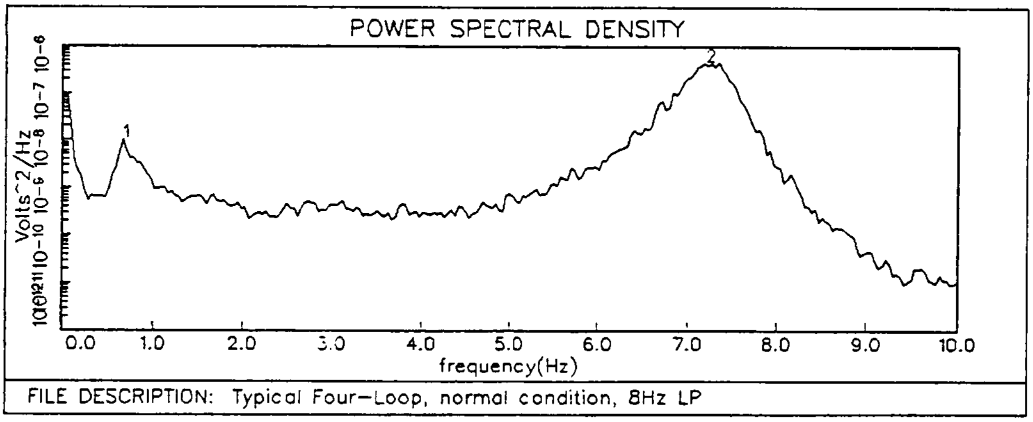

Figure 6.13 : Pressure noise amplitude probability density and power spectral density of typical four-loop PWR primary coolant loop-C at 98.9% power level.

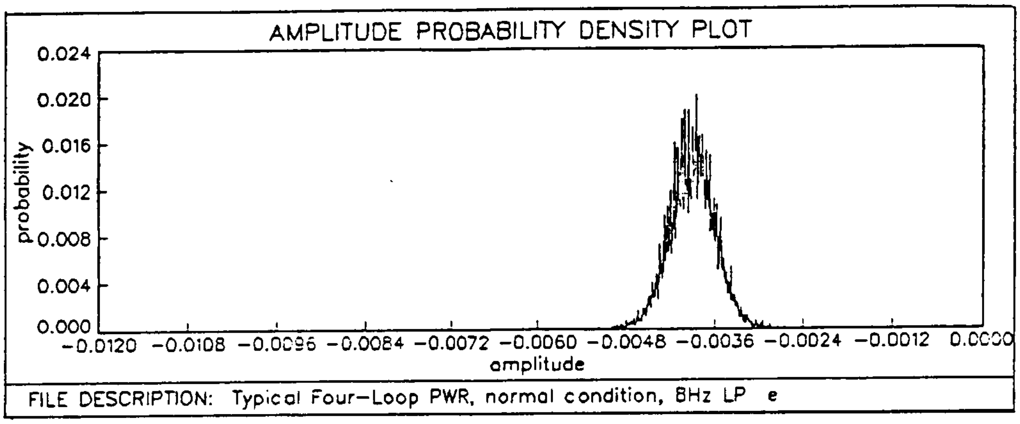

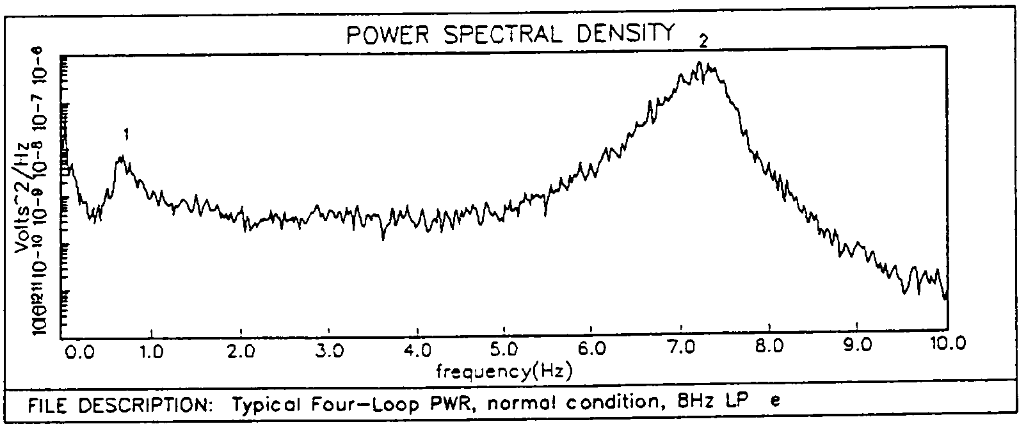

Figure 6.14 : Pressure noise amplitude probability density and power spectral density of typical four-loop PWR primary coolant loop-C at 99.3% power level.

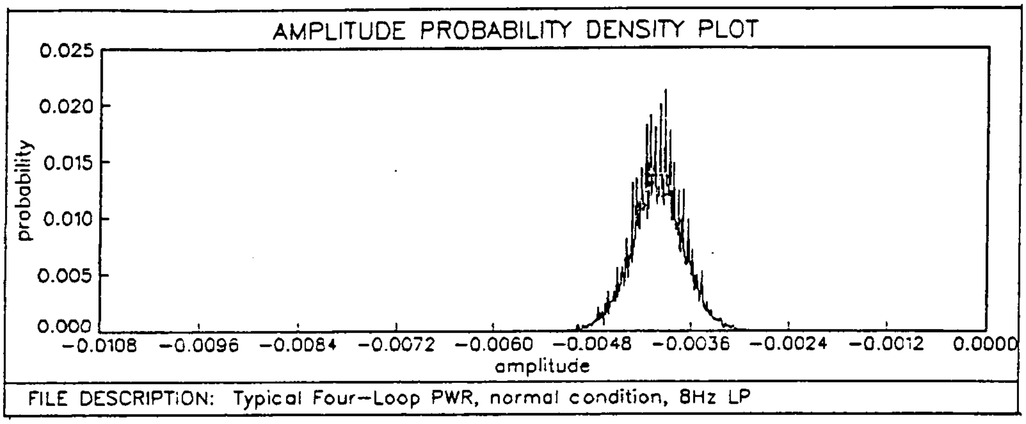

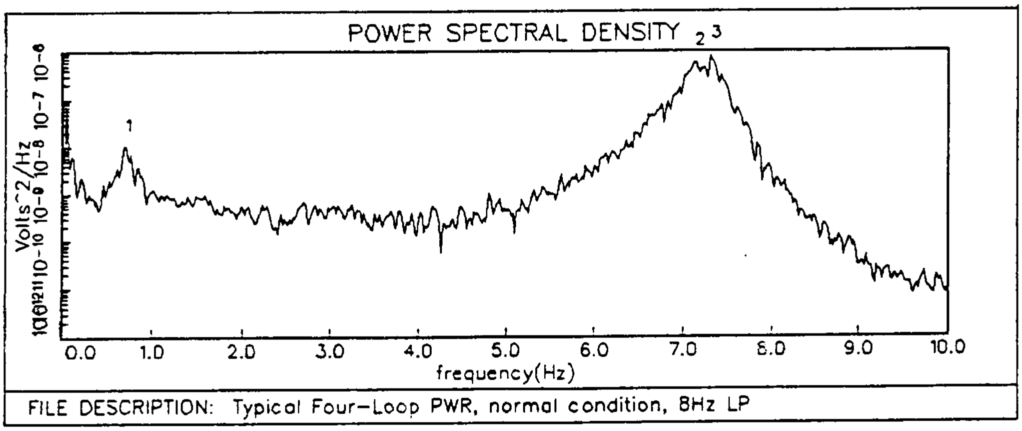

Figure 6.15 : Pressure noise amplitude probability density and power spectral density of typical four-loop PWR primary coolant loop-C at 99.7% power level.

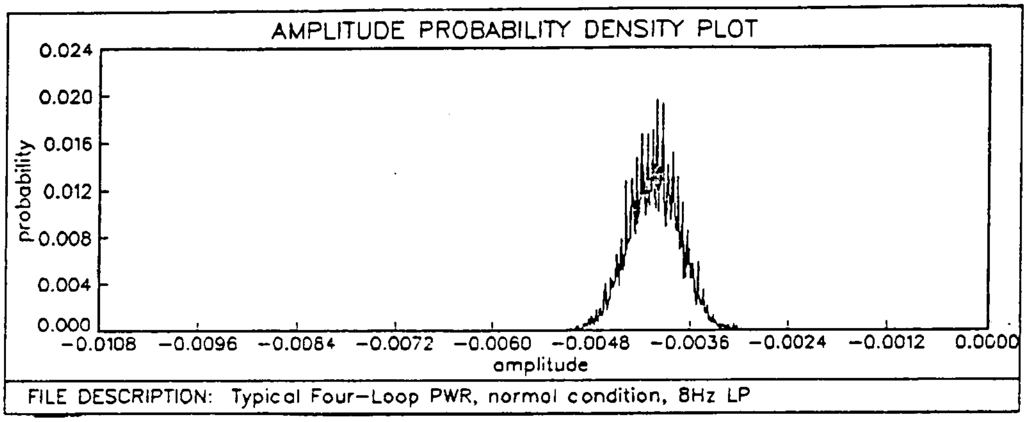

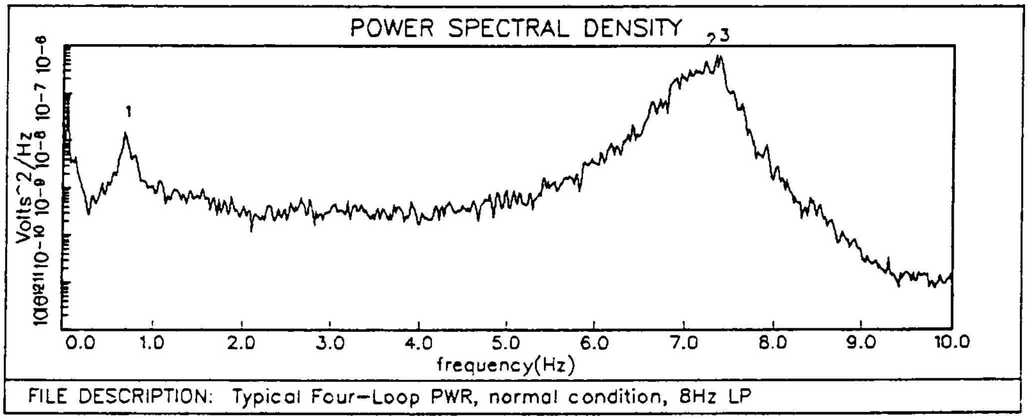

Figure 6.16 : Pressure noise amplitude probability density and power spectral density of typical four-loop PWR primary coolant loop-C at 100.3% power level.

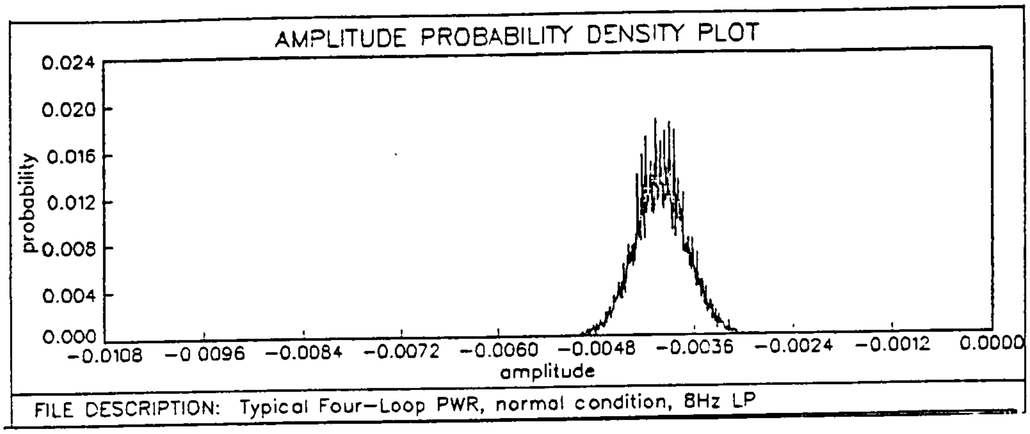

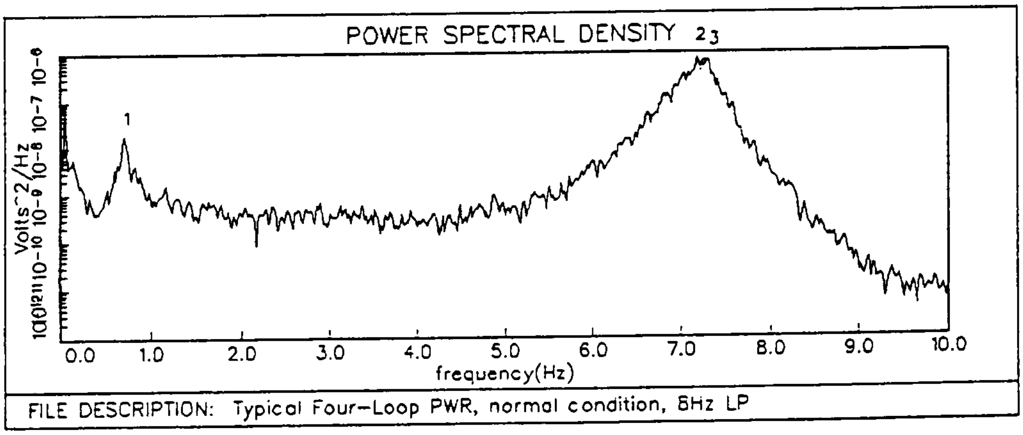

Figure 6.17 : Pressure noise amplitude probability density and power spectral density of typical four-loop PWR primary coolant loop-C at 100.6% power level.

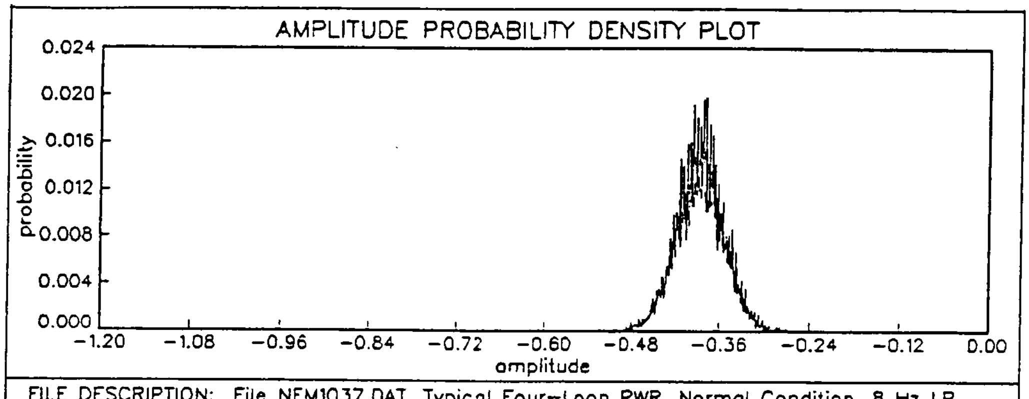

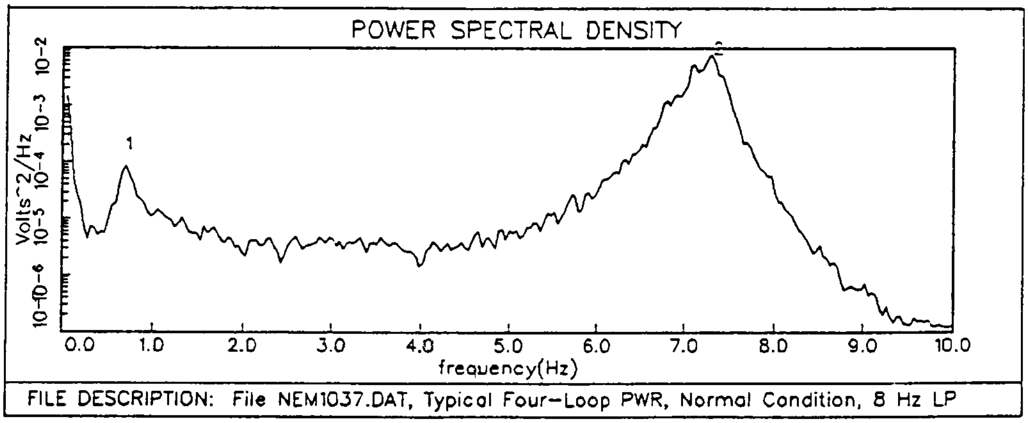

Figure 6.18 : Pressure noise amplitude probability density and power spectral density of typical four-loop PWR primary coolant loop-C at 97.2% power level.

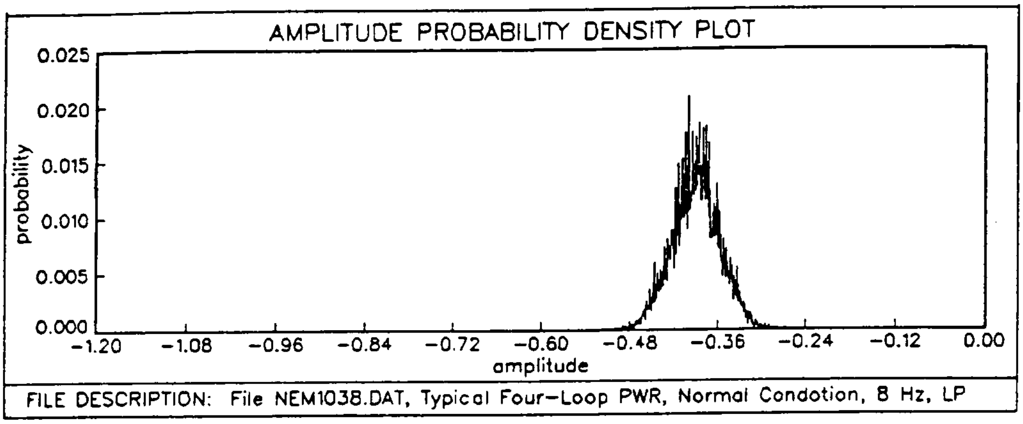

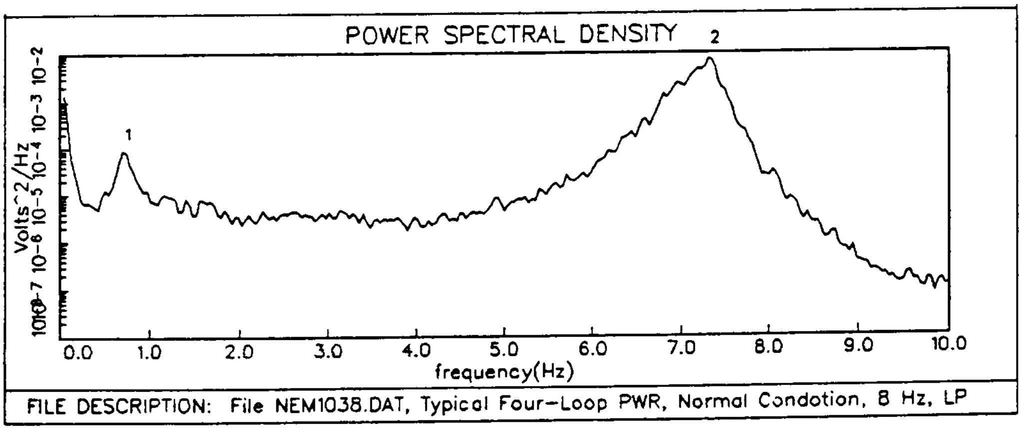

Figure 6.19 : Pressure noise amplitude probability density and power spectral density of typical four-loop PWR primary coolant loop-C at 97.7% power level.

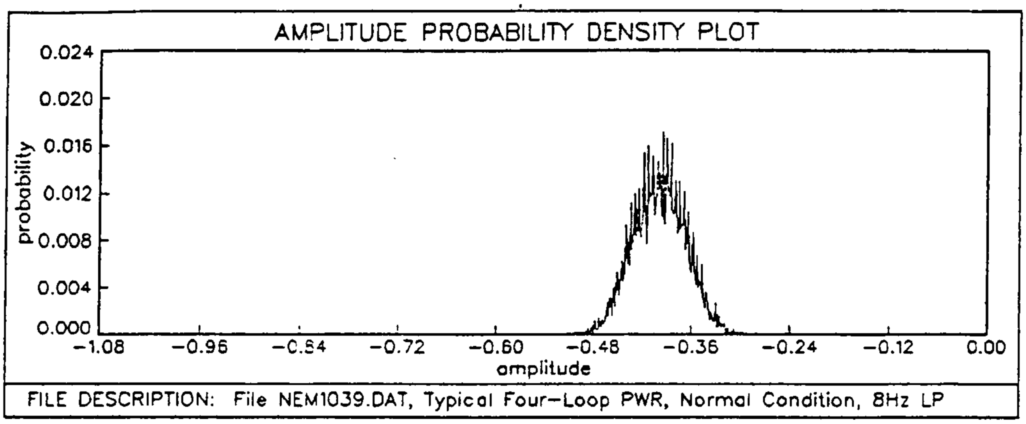

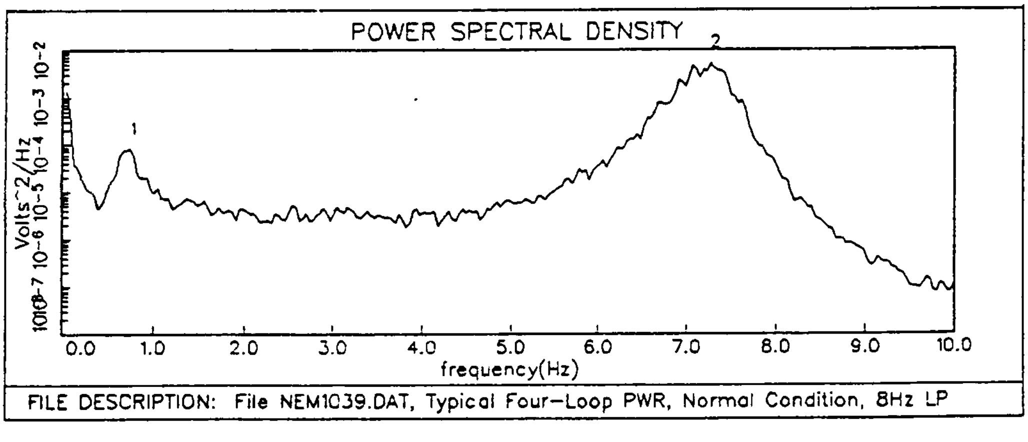

Figure 6.20 : Pressure noise amplitude probability density and power spectral density of typical four-loop PWR primary coolant loop-C at 97.7% power level.

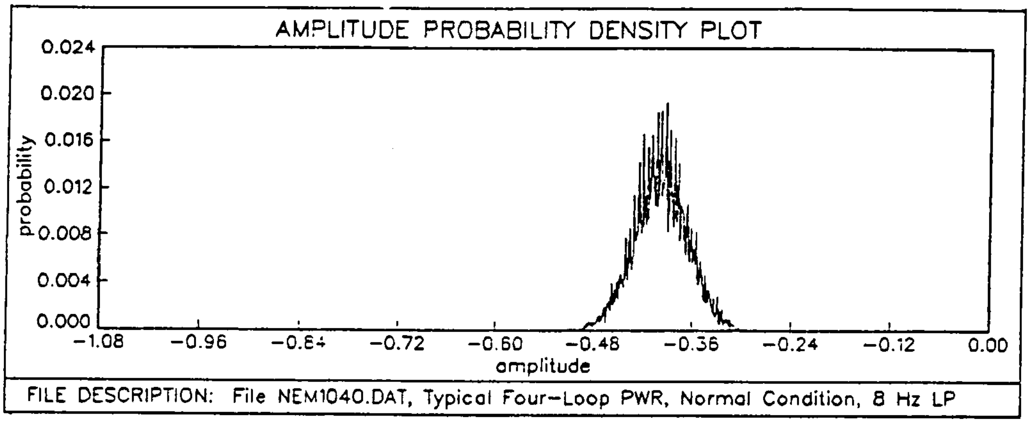

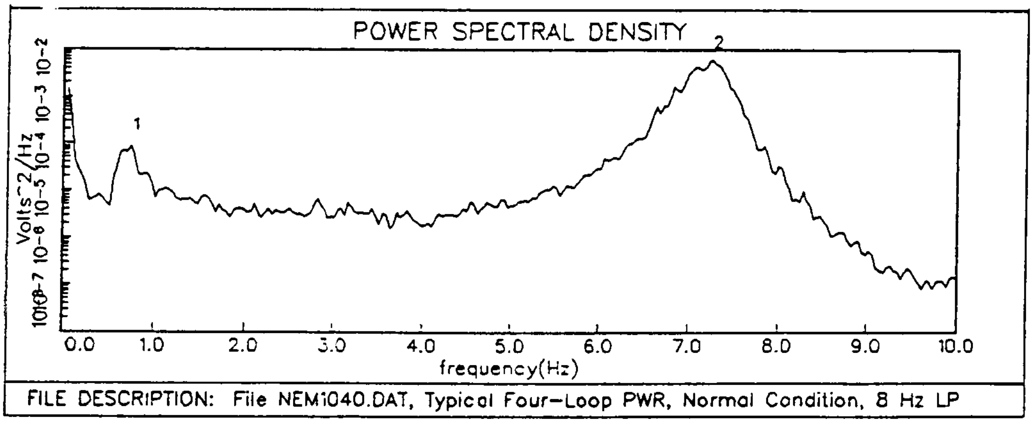

Figure 6.21 : Pressure noise amplitude probability density and power spectral density of typical four-loop PWR primary coolant loop-C at 97.8% power level.

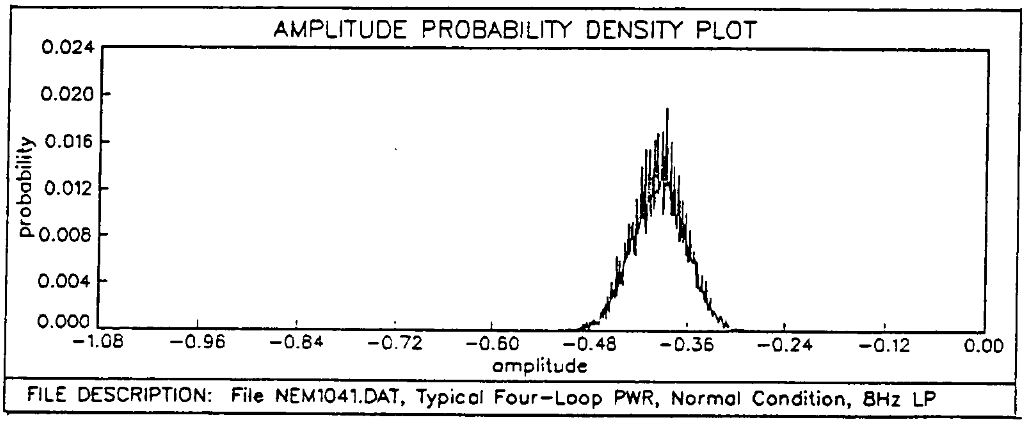

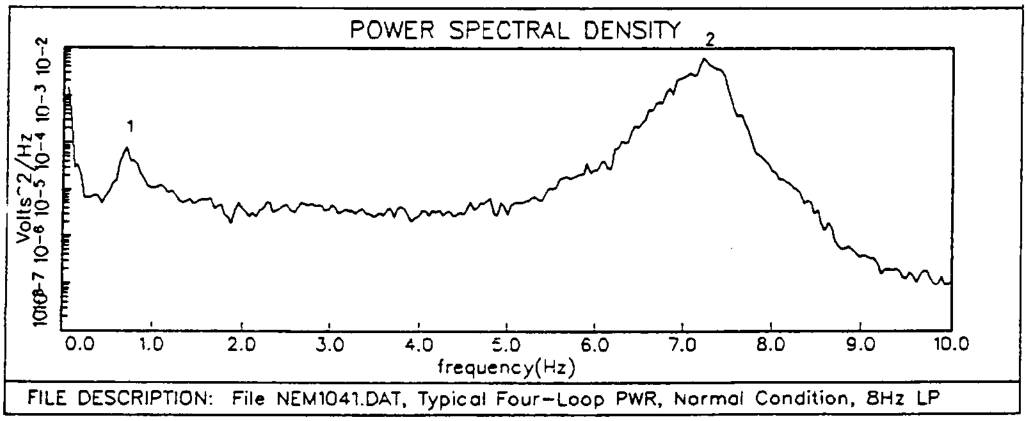

Figure 6.22 : Pressure noise amplitude probability density and power spectral density of typical four-loop PWR primary coolant loop-C at 98.3% power level.

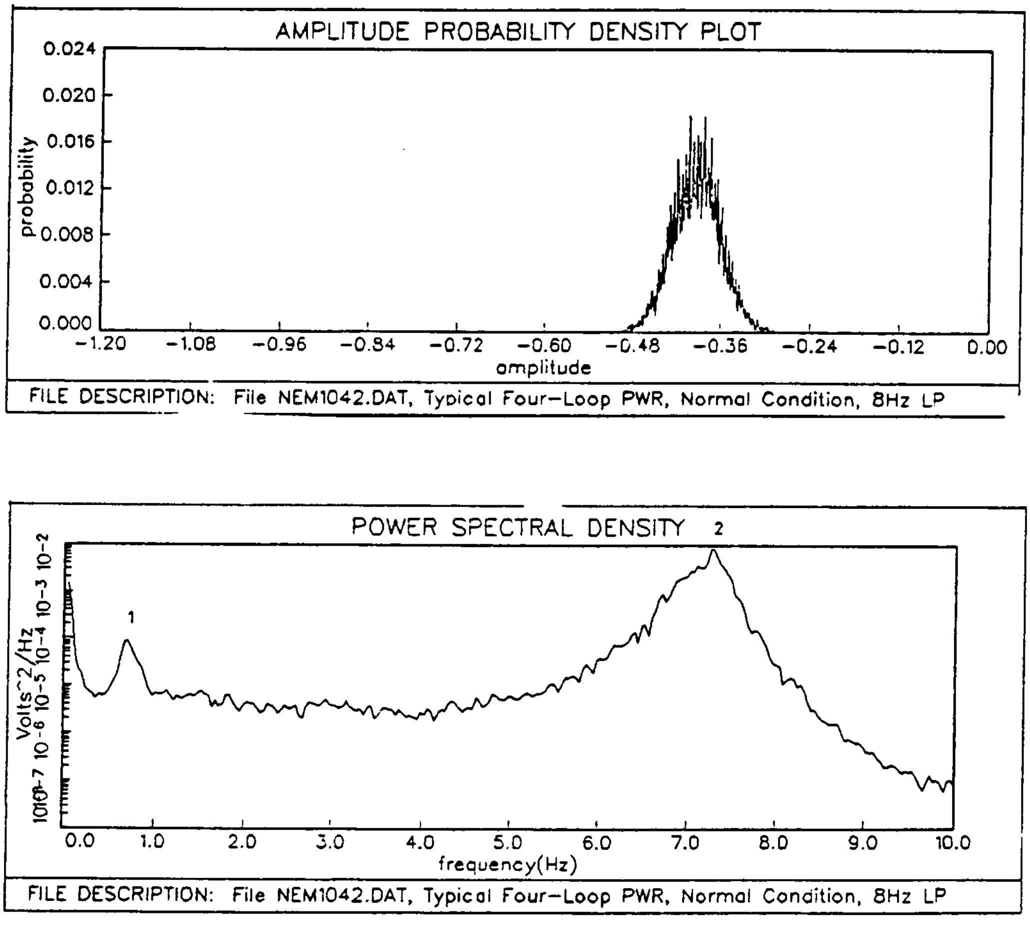

Figure 6.23 : Pressure noise amplitude probability density and power spectral density of typical four-loop PWR primary coolant loop-C at 98.2% power level.

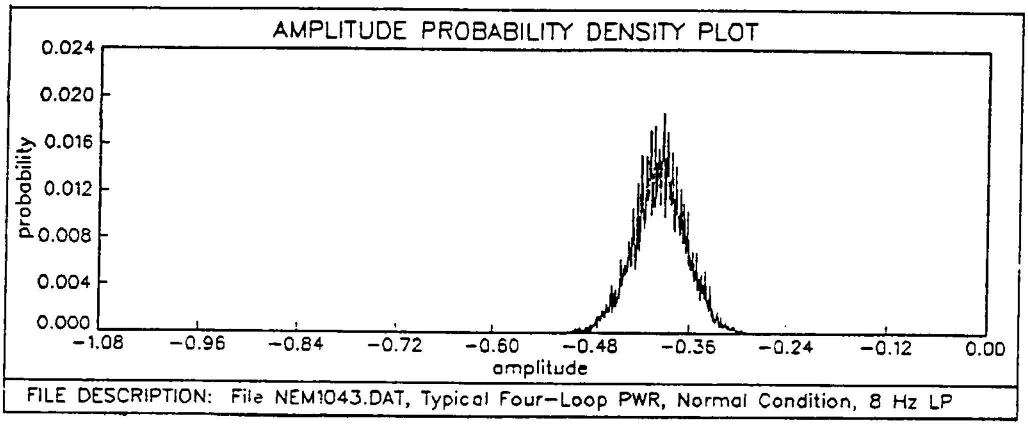

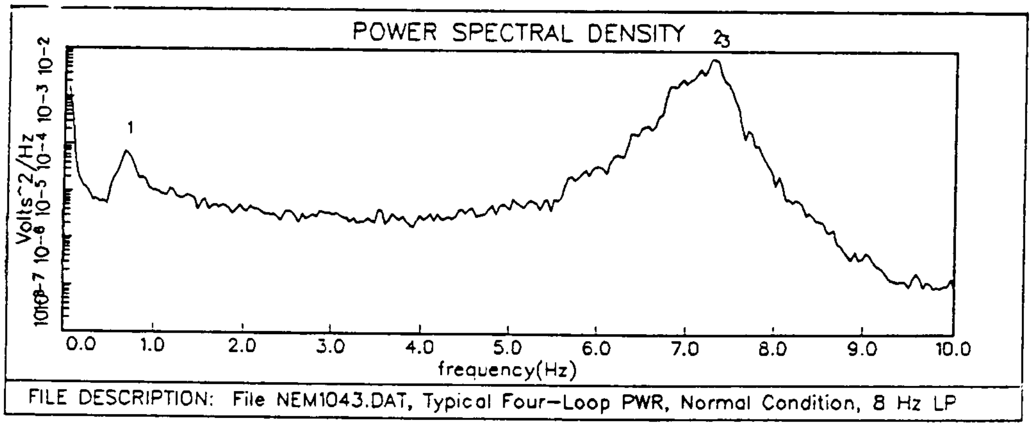

Figure 6.24 : Pressure noise amplitude probability density and power spectral density of typical four-loop PWR primary coolant loop-C at 98.9% power level.

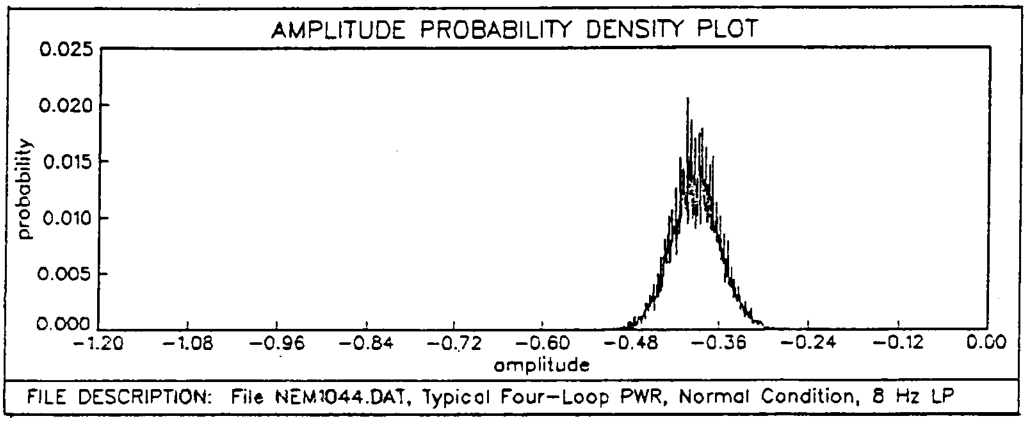

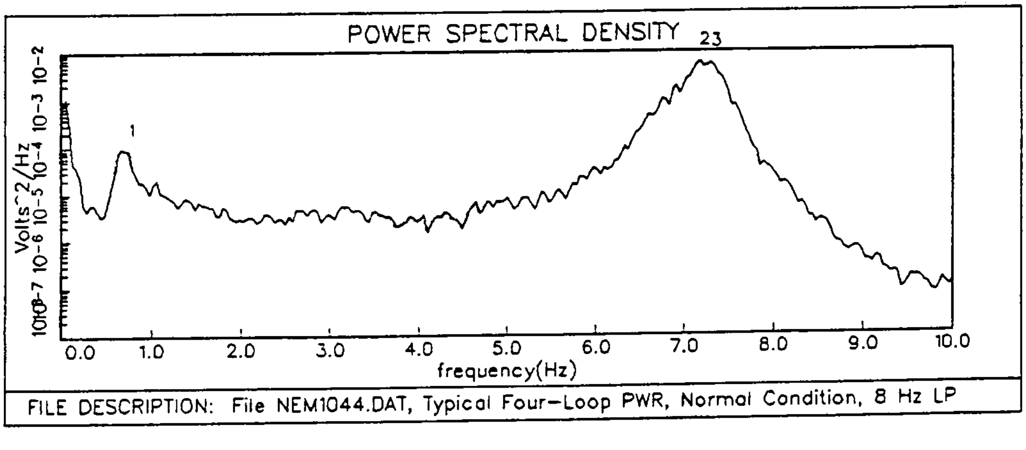

Figure 6.25 : Pressure noise amplitude probability density and power spectral density of typical four-loop PWR primary coolant loop-C at 99.2% power level.

CHAPTER 7

DISCUSSION OF RESULTS OF APPLICATION TO PRESSURIZED WATER REACTORS

7.1 Borssele Nuclear Power Plant

Table 7.1 summarizes the theoretical and experimental results indicating the natural frequency (standing wave frequency) of the primary coolant system of the Borssele Reactor. Figure 7.1 shows theoretical and experimental values of this frequency at various coolant temperatures. In all the plots, the temperature of coolant is represented by the temperature of coolant in the hot leg.

Model calculation showed that several frequencies fulfill the condition of Equations (3.18). Based on the observation in the Borssele PWR [3], the frequencies in the range of 6-8 Hz were related to the temperature of coolant in the hot leg, and the analytical study of pressure noise in the WWER-440 reactor proved that a frequency of 6.3 Hz was influenced by the compressibility behavior in the upper plenum of the reactor vessel. The coolant temperature in the upper plenum is approximately equal to the temperature of coolant in the hot leg piping. Therefore, this study considers only the frequencies in the range of 6-8 Hz. Since the source of temperature changes in the primary coolant is the pressure vessel, this suggests the logic of measuring pressure noise in the hot leg.

The theoretical calculation results show that the natural frequency of the pressure noise shifts from 7.73 Hz to 7.02 Hz as the average hot leg temperature changes from 269.5°C to 315°C. The changes in the pressure noise frequency corresponding to the

Table 7.1: Summary of theoretical and experimental results indicating the natural frequency of primary coolant pressure noise at Borssele PWR

File name	Pressure (psia)	Hot leg temperature (°C)	Natural frequency from measurement (Hz)	Natural frequency from theory (Hz)
B17001A9	2190.11	269.5	7.07	7.73
			7.07	
B17003F2	2219.11	290.0	6.59	7.37
			6.59	
B17003F3	2240.87	297.5	6.41	7.26
			6.41	
B17012	2303.23	315.0	6.53	7.02
			6.57	

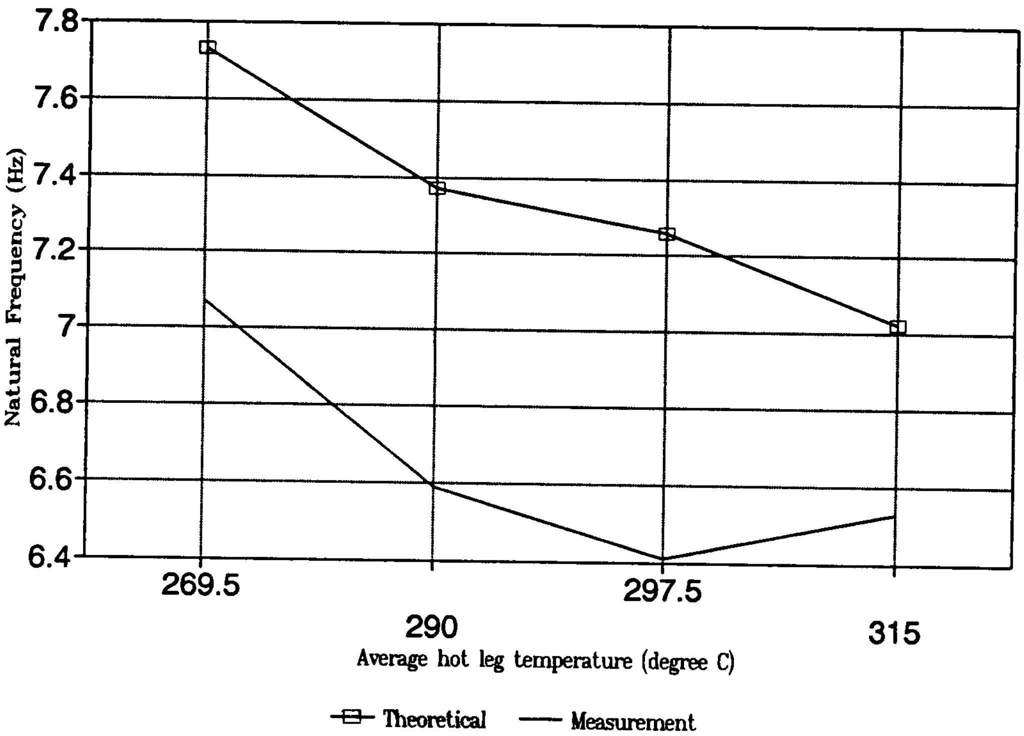

Figure 7.1 : Theoretical and experimental values of pressure noise frequency at various hot leg temperatures.

standing wave are not necessarily linear as a function of the hot leg temperature. The theoretical analysis assumed a uniform change in the temperature in all segments of the loop. This is not true in real operation.

The absolute pressure was assumed to be constant at 2245 psia (15.4 MPa) since the temperatures of the coolant were above 200°C. This assumption was proven acceptable since the theoretical calculation shows that the natural frequencies of pressure noise did not change significantly even though there was a small change in the absolute pressure, as shown in Table 7.2. This table shows the comparison between natural frequencies calculated at their original pressure and at the constant pressure equal to 2245 psia. Small changes in the primary pressure at different power levels did not affect the experimental calculations.

The first three pressure noise file data, corresponding to 0%, 10%, and 30% reactor power, showed that the peak frequency decreased from 7.07 Hz to 6.41 Hz as the temperature changed from 269.5 °C to 297.5 °C. This behavior matches the theoretical analysis of pressure noise for the Borssele PWR. With increasing temperature, the rate of frequency decrease is about 0.024 Hz/°C. Therefore, it is expected that the frequency at 100% power (315 °C) should be approximately 5.91 Hz. The actual frequency value is 6.53 Hz at 100% power.

The overall pattern matches the expected behavior of pressure noise. The explanation for the deviation in the peak frequency at 100% power level for the Borssele PWR requires further information about plant data.

For cycle 18, the power spectral density of three pressure noise data files at full power showed that the natural frequency is in the range of 6.50 - 6.6 Hz.

Table 7.2: Theoretical natural frequency calculation at constant pressure

File name	Pressure (psia)	Hot leg temperature (°C)	Natural frequency at original pressure (Hz)	Natural frequency at a pressure of 2245 psia (Hz)
B17001A9	2190.11	269.5	7.73	7.75
B17003F2	2219.11	290.0	7.37	7.41
B17003F3	2240.87	297.5	7.26	7.26
B17012	2303.23	315.0	7.02	7.01

7.2 A Four-Loop Westinghouse PWR

Table 7.3 summarizes the theoretical and experimental results indicating the natural frequency of the primary coolant system pressure for a typical four-loop PWR. Because of the small uncertainty in finding the exact values of parameters for the four-loop PWR, the primary piping length was varied in a small range. The natural frequencies were calculated for a few different lengths. The theoretical value of the peak frequency (7.34 Hz) at the operating temperature of 618 °F agrees very well with the peak in the experimental spectrum with an average peak frequency of 7.27 Hz at 100% power. This frequency component is not related to the effect of pressure sensing line.

This fact implies that wide-range pressure sensors in a four-loop PWR may be used to monitor the behavior of the pressure noise spectrum in the primary coolant system. Since the wide-range transmitter is not very sensitive to small changes in the pressure noise behavior, it is suggested that at least one narrow-range transmitter be installed for this implementation. These results were obtained for the first time (calculation and comparison) in this research effort.

For the Borssele reactor, the power spectral density was calculated with a data block size of N=1,024 points. This represents a frequency resolution of 0.06 Hz. In order to be able to distinguish the changes in pressure noise frequency as a function of temperature, it is necessary to have an improved frequency resolution of the power spectral density. The resolution must be at least as small as the frequency shift rate per °C. For example, the shift rate of the measured pressure noise signal for the first three data set is about 0.024 Hz/°C. In order to increase the resolution, the data block size must be at least three times 1,024. However, with fast Fourier transformation, the

Table 7.3 : Summary of theoretical and experimental results indicating natural frequency of primary colant pressure noise for a typical four-loop PWR

File name	Hot leg temperature (°F)	Natural frequency from measurement (Hz)
NEM1031	618.3	7.19
NEM1033	618.5	7.21
NEM1034	618.4	7.22
NEM1035	618.5	7.29
NEM1036	618.3	7.26
NEM1037	618.2	7.33
NEM1038	618.2	7.31
NEM1039	618.2	7.26
NEM1040	618.3	7.26
NEM1041	618.4	7.23
NEM1042	618.3	7.28
NEM1043	618.3	7.31
NEM1044	618.3	7.25
Average	618.30	7.27

Theoretical natural frequency at 618.3 °F or 325.7 °C = 7.34 Hz.

number of points per block $N = 2^n$. Therefore, the desired data block size must be 4 x 1,024 = 4,096.

The limited amount of data available for this work from Borssele was not sufficient to make a good comparison of the theory and the experiment. The theoretical study was able to predict correctly both nominal value of the standing wave frequency and its change as a function of temperature.

For a typical four-loop PWR, the power spectral density was calculated with a data block size of N = 512 that represents a spectral resolution of 0.04 Hz/°C.
The peak frequencies listed in Table 7.3 are averages of two frequencies that are close to each other. Therefore, it is difficult to see the changes in peaks due to small temperature changes in the primary coolant.

Since analytical and measurement results have shown the relationship between pressure noise and coolant temperature, it is possible to implement a method for estimating coolant temperature by measuring the pressure noise frequency. However, due to lack of a complete pressure noise database, the present study cannot provide a calibration-type curve of pressure noise frequency. The guidelines to establish a calibration curve are given.

(a) The pressure noise data must be acquired at different power levels and under normal operating conditions. The plant must be in steady-state conditions during data acquisition. It is suggested that at least one of the pressure transmitters be a narrow-range transmitter in order to provide quality signals.

(b) The frequency resolution should be small enough to provide high accuracy in detecting frequency shifts as a function of temperature.

(c) A plot of the measured coolant temperature versus the pressure noise frequency should be made using data from different power levels.

When the primary coolant temperature and pressure are measured accurately in a PWR, this calibration curve can be used for estimation of coolant temperature in PWRs.

CHAPTER 8

CONCLUSIONS AND RECOMMENDATIONS FOR FUTURE RESEARCH

8.1 Summary

Several parameters influence the characteristics of pressure noise in the primary coolant system of a PWR. These are pressurizer water level, water flow oscillations in surge line piping, water flow oscillations in the primary loop, vibration, pump rotation, and others. One of the oscillations involves a hydraulic displacement as a consequence of the compressible behavior of the water in the primary closed-loop of the PWRs. As a compressible medium, the coolant can give rise to pressure waves that propagate with the velocity of sound.

This fact allows us to use the properties of sound waves in water to study the pressure noise behavior of the primary coolant system. The governing equations of this study involve the acoustic wave field equations in fluid flow. After linearization, these equations become analogous to the properties of a two-port network. Therefore, the final model was developed through the properties of two-port networks.

This model was used to calculate the natural frequency of the primary coolant system pressure signal in the Borssele PWR and in a four-loop PWR. This frequency is 7.02 Hz at 100% power level for the Borssele system. In order to see the effect of temperature on frequency shift, calculations were made for the Borssele PWR at operating conditions corresponding to 0%, 10%, and 30% power levels. These calculations showed that the frequency decreased with increasing temperature.

Analysis of the measured pressure noise data was performed by calculating the statistical characteristics (rms value, skewness, flatness, and APD function) and power spectral density of pressure noise. From 16 data files taken from the Borssele PWR, only 6 data files fulfill the criterion of the stationarity. The analysis of these stationary pressure signals shows that the frequency peak of interest of the power spectral density (in the 6-8 Hz range) decreases with increasing temperature. These data were analyzed using the software program SAMS (available in the Nuclear Engineering Department).

Model calculations were also performed for a typical four-loop Westinghouse PWR. The detailed analysis showed that the natural frequency of pressure dynamics is 7.34 Hz. This agrees very well with the experimentally determined spectral frequency of 7.27 Hz at 100% power level. This calculation and comparison was performed for the first time as part of this research.

8.2. Conclusions

Both the theoretical and reactor operational data analysis show that the standing wave frequency is a characteristic of the pressure noise signal and is dependent on the coolant temperature. This supports the hypothesis that the frequency is related to the compressibility behavior of the medium in which the temperature plays a significant influence. In other words, this pressure noise characteristic represents the temperature behavior of the coolant. Therefore, it is possible to implement a method for estimating hot leg temperature by measuring the pressure noise frequency and a calibration curve of average temperature versus frequency peaks may be generated.

Theoretical calculations and spectral analyses of pressure noise signals from a four-loop PWR showed that the standing wave frequency is around 7.3 Hz at 100% power level. This is a very encouraging result in spite of the fact that wide-range pressure transmitters are used in this PWR. These results also indicate that this frequency component is not due to the dynamics of sensing line.

8.3 Recommendations for Future Research

In order to establish a reliable calibration of hot leg temperature versus pressure noise frequency, it is necessary to process data acquired at different power level (or temperature) conditions and for a short period during the fuel cycle. The resolution of the frequency spectrum must be improved in order to detect small changes in temperature by using zoom FFT or time-series modeling of band-limited signals.

The spectral features seen in the wide-range pressure transmitters in a typical four-loop U.S. PWR indicate the presence of a standing wave whose behavior changes as a function of temperature. In order to use this information for estimating the hot leg temperature accurately, it is suggested that at least one narrow-range transmitter be installed in the hot leg piping.

In order to prove that the frequency in the 6-8 Hz range in the pressure signal spectrum represents the temperature of the hot leg, pressure noise data should be aquired both from hot leg and cold leg piping. This would provide information about standing wave behavior in the hot and cold legs. The pressure noise data should be acquired from an operating PWR at different power levels (either during power ascension or shut-down phase) and processed to establish the clear behavior of hot leg temperature as a function of standing wave frequency.

BIBLIOGRAPHY

BIBLIOGRAPHY

1. I. Nagy and T. Katona, "*Theoretical Investigation of The Low-Frequency Pressure Fluctuation in PWRs*," SMORN IV, Prog. in Nuc. Energy, pp 671-682, 1985.

2. E. Turkcan, "*Review of Borssele PWR Noise Experiments, Analysis and Instrumentation*," SMORN III, Prog. in Nuc. Energy, pp 437-451, 1982.

3. E. Turkcan et al, "*Operational Experiences on The Borssele Nuclear Power Plant Using Computer Based Surveillance and Diagnostic System On-line*," Proceeding of Symposium on Nuclear Reactor Surveillance and Diagnostics, May 19-24, pp 1-12, 1991.

4. J.A. Mullens and J.A. Thie, "*Understanding Pressure Dynamic Phenomena in PWRs for Surveillance and Diagnostics Applications*," Proceeding of Fifth Power Plant Dynamics, Control and Testing Symposium, pp 65-78, Vol.1, March 21-23,1983

5. J.A Mullens and J.A Thie, "*Modeling and Diagnostic Technique Applicable to the Analysis of Pressure Noise in Pressurized Water Reactors and Pressure-Sensing System*," SMORN IV, Prog. in Nuc. Energy, pp 217-224, 1985.

6. G. Grunwald, G. Hessel and W. Schmitt, "*Low Frequency Pressure Oscillations in a PWR*," SMORN III, Prog. in Nuc. Energy, pp 651-659, 1982.

7. G. Grunwald, K. Junghanss and P. Liewers, "*Investigation of Pressure Oscillation in a PWR Primary Circuit*," SMORN IV, Progress in Nuc. Energy, pp 569-579, 1985.

8. B.R. Upadhyaya, " *An Introduction to Dynamics and Control,* " Volumes I and II, Nuclear Engineering Department, University of Tennessee, 1991.

9. A. Wood, "*Acoustics*," Dover Publication, New York, pp 265-271, 1966.

10. J. Lighthill, "*Waves in Fluids*," Cambridge University Press, pp 89-120, 1978.

11. K.U. Ingard,"*Fundamental of Waves and Oscillations*," Cambridge University Press,pp 286-305, 1988

12. J. Goldstein,"*Fluid Mechanic Measurements*," Hemisphere Publishing Co., pp 50-95, 1981.

13. D.D. Reynolds, "*Engineering Principles of Acoustics: Noise and Vibration Control*," Allyn and Bacon, Inc., Boston, pp 333-354, 1981.

14. J.A. Kleppe, "*Engineering Application of Acoustics*," Artech House, pp 80-120, 1982.

15. H.J. Carlin, "*An Introduction to Reciprocal and Non-Reciprocal Circuit*," Prentice-Hall, pp 250-280, 1964.

16. R.W.P. King, "*Transmissions Line*," McGraw-Hill, New York, pp 83-104 and 190-235, 1955.

17. T. Gonen, "*Electric Power Transmission System Engineering*," John Willey & Sons, New York, pg 99 -137, 1980.

18. J. Wilson, "*Thermohydraulic Parameters Computer Program,*" 1991.

19. R.C. Weast, "*CRC Handbook of Chemistry and Physics*," 1st edition, CRC Press pp E18-E37, 1981.

20. E. Turkcan, Private corrrespondence, 1993.

21. J.A. Thie, Private correspondence, 1992.

22. A.D. Kraus, "*Matrices for Engineers*," Hemisphere Publishing Corporation, pp 159-229, 1987.

23. N.E. Todreas and M.S. Kazimi,"*Nuclear System I,II: Thermal Hydraulic Fundamentals*," Hemisphere Publishing Corp., New York, pp 356-400 and pp 67-114, 1989.

24. H. Lamb, "*Hydrodynamics,*" Dover Publication, New York, pp 276-476, 1932.

25. Westinghouse Document, "*Fundamentals Course Manual: Pressurized Water Reactor,* " Chapter 3, 1979.

APPENDICES

APPENDIX A

EXAMPLE CALCULATION OF A-PARAMETER EQUIVALENT OF CLOSED LOOP [1]

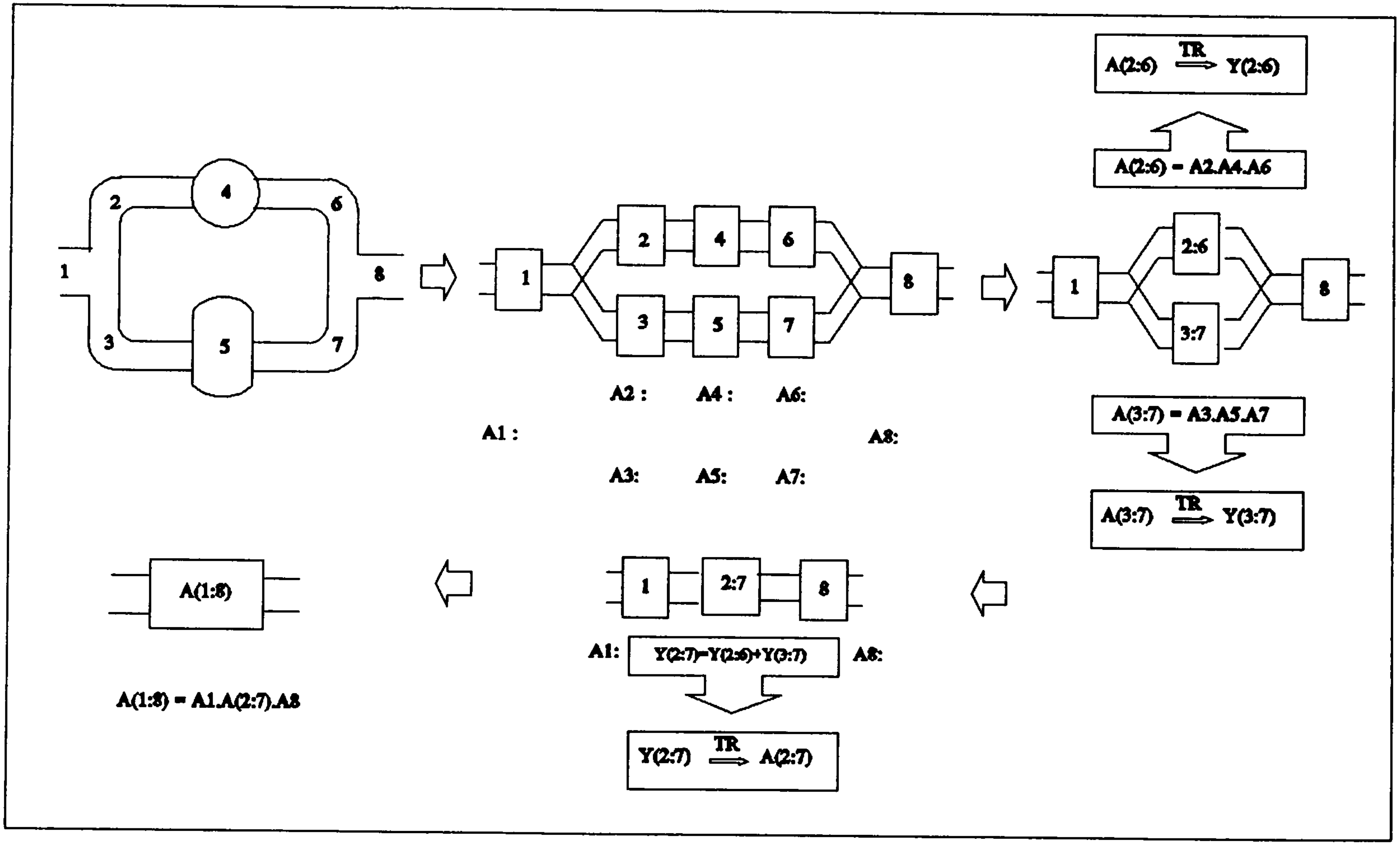

APPENDIX B

LISTING OF COMPUTER CODE PCSPRES

```
******************************************************************************
*      THIS PROGRAM IS TO CALCULATE THE EIGENFREQUENCY OF PRESSURE          *
*      NOISE IN THE COOLANT SYSTEM OF PRESSURIZED WATER REACTORS            *
*                                                                           *
*      RESEARCH TOPIC: ANALYSIS OF COOLANT PRESSURE DYNAMICS IN THE         *
*      PRIMARY SYSTEM OF PRESSURIZED WATER REACTORS                         *
*                                                                           *
*                                                                           *
******************************************************************************

      IMPLICIT   NONE
      INTRINSIC  COS,SIN,EXP,MIN
      INTEGER    MAXROW, NROW, NCOL, N,R,ROW, COL,ITER1,ITER2,ITER3
      INTEGER    I,J,K,L,M,NUM,NTEMP
      PARAMETER  (MAXROW=20)
      REAL       PI
      PARAMETER  (PI=3.141593)
      REAL     A(4),YY(35),XX(30),DTEMP(30)
      REAL     SV
      REAL     PRESS,SVEL,SNTEMP,SUMA,TEMP,TMIN,SLOPE,SOUNDVELSI,TEM
      REAL     TMINR, TMINI,TSAT,PSAT,RHOSAT,RHOX,PRESMPA
      REAL     DTMR,DTMI, DTRMIN,DTIMIN,P, PIVOT,X,Y
      REAL     PVLENG, PP1LENG, PP2LENG, PP3LENG, PPLENG, SGLENG
      REAL     PVAR, PP1AR, PP2AR, PP3AR, SLLENG,SLAR,PPAR,SGAR
      REAL     PVVOL,PPVOL, SGVOL, PUMPVOL,LIMITR,LIMITI, AREA
      REAL     TEMPPV,RHOPV,TEMPHL,RHOHL,TEMPSG,RHOSG,TEMPCL,RHOCL
      REAL     SOUNDVPV,SOUNDVHL,SOUNDVSG,SOUNDVCL,DELHLCL
      REAL     RHO,RHOSTD,TEMPSTD, SOUNDVSTD
      REAL     FRACT,ZA,DELFREQ,FREQ0, FREQI,FREQF, FRACTPP3
      REAL     FRACTPP1,FRACTPP2,FRACTSL,FRACTSG,FRACTPV,RNUM
      REAL     DELTAT,DELRHO,FREQ,ERROR,BULKM,LAMDA
      REAL     BDIAGR,CDIAGR,BDIAGI,CDIAGI,PHASE,DRHODT,DRHOD
      REAL     COSY,SINY,ETODX,ETODMX
      REAL     ZREAL,ZIMAG,SZREAL,SZIMAG,CZREAL,CZIMAG
      REAL     ZREALPP1,ZREALPP2,ZREALPP3,ZREALSL,ZREALPUMP
      REAL     ZIMAGPP1,SZREALPP1,SZIMAGPP1,CZREALPP1,CZIMAGPP1
      REAL     ZIMAGPP2,SZREALPP2,SZIMAGPP2,CZREALPP2,CZIMAGPP2
      REAL     ZIMAGPP3,SZREALPP3,SZIMAGPP3,CZREALPP3,CZIMAGPP3
      REAL     ZIMAGPP,SZREALPP,SZIMAGPP,CZREALPP,CZIMAGPP
      REAL     ZIMAGPV,SZREALPV,SZIMAGPV,CZREALPV,CZIMAGPV
      REAL     ZIMAGSL,SZREALSL,SZIMAGSL,CZREALSL,CZIMAGSL
      REAL     ZIMAGSG,SZREALSG,SZIMAGSG,CZREALSG,CZIMAGSG
      REAL     ZIMAGPUMP,SZREALPUMP,SZIMAGPUMP,CZREALPUMP,CZIMAGPUMP
```

```
      REAL      PVR(MAXROW, MAXROW), PVI(MAXROW,MAXROW)
      REAL      MIR(MAXROW, MAXROW), MII(MAXROW,MAXROW)
      REAL      PP1R(MAXROW,MAXROW), PP1I(MAXROW,MAXROW)
      REAL      PP2R(MAXROW,MAXROW), PP2I(MAXROW,MAXROW)
      REAL      PP3R(MAXROW,MAXROW), PP3I(MAXROW,MAXROW)
      REAL      SLR(MAXROW, MAXROW), SLI(MAXROW,MAXROW)
      REAL      PPR(MAXROW, MAXROW), PPI(MAXROW,MAXROW)
      REAL      SPR(MAXROW, MAXROW), SPI(MAXROW, MAXROW)
      REAL      SGR(MAXROW, MAXROW), SGI(MAXROW, MAXROW)
      REAL      PUMPR(MAXROW, MAXROW), PUMPI(MAXROW, MAXROW)
      REAL      PRESPR(MAXROW, MAXROW), PRESPI(MAXROW,MAXROW)
      REAL      PRESP2R(MAXROW, MAXROW), PRESP2I(MAXROW,MAXROW)
      REAL      PSG1R(MAXROW, MAXROW), PSG1I(MAXROW,MAXROW)
      REAL      PSG2R(MAXROW, MAXROW), PSG2I(MAXROW,MAXROW)
      REAL      PPUMP1R(MAXROW, MAXROW), PPUMP1I(MAXROW,MAXROW)
      REAL      PPUMP2R(MAXROW, MAXROW), PPUMP2I(MAXROW,MAXROW)
      REAL      PSPP1R(MAXROW, MAXROW), PSPP1I(MAXROW,MAXROW)
      REAL      PSPP2R(MAXROW, MAXROW), PSPP2I(MAXROW,MAXROW)
      REAL      LOOP1R(MAXROW, MAXROW), LOOP1I(MAXROW,MAXROW)
      REAL      LOOP2R(MAXROW, MAXROW), LOOP2I(MAXROW,MAXROW)
      REAL      CONDLOOP1R(MAXROW,MAXROW),CONDLOOP1I(MAXROW,MAXROW)
      REAL      CONDLOOP2R(MAXROW,MAXROW),CONDLOOP2I(MAXROW,MAXROW)
      REAL      CONDLOOPR(MAXROW, MAXROW),CONDLOOPI(MAXROW,MAXROW)
      REAL      LOOPR(MAXROW, MAXROW), LOOPI(MAXROW, MAXROW)
      REAL      SUMR(MAXROW, MAXROW), SUMI(MAXROW, MAXROW)
      REAL      SUM(MAXROW, MAXROW), DTR(499), DTI(499)
      REAL      EQUIVR(MAXROW, MAXROW), EQUIVI(MAXROW,MAXROW)
      REAL      EQUIVMIR(MAXROW, MAXROW), EQUIVMII(MAXROW,MAXROW)
      CHARACTER  OUT_F*100
      COMMON PRESS,FREQF
      OPEN (9,FILE ='PCSPRES.DAT',STATUS='UNKNOWN')
      OPEN (10,FILE='PCSPRES.OUT',STATUS='UNKNOWN')

      READ (9,1) PVLENG,PP1LENG,PP2LENG,PP3LENG,PPLENG,SGLENG,
     !         PVAR,PP1AR,PP2AR,PP3AR,PPAR,SGAR,
     !         RHOSTD,SOUNDVSTD,TEMPSTD,DELTAT,RNUM,DELFREQ,
     !         PVVOL,PPVOL,SGVOL,PUMPVOL,FREQI,FREQF,
     !         TEMPPV,DELHLCL,PRESS,LIMITR,LIMITI
      WRITE (10,1) PVLENG,PP1LENG,PP2LENG,PP3LENG,PPLENG,SGLENG,
     !         PVAR,PP1AR,PP2AR,PP3AR,PPAR,SGAR,
     !         RHOSTD,SOUNDVSTD,TEMPSTD,DELTAT,RNUM,DELFREQ,
     !         PVVOL,PPVOL,SGVOL,PUMPVOL,FREQI,FREQF,
     !         TEMPPV,DELHLCL,PRESS,LIMITR,LIMITI
      read (9,2) NTEMP

    1 FORMAT(6F10.4)
    2 FORMAT(I4)


      DATA NROW,NCOL/2,2/
```

```
 WRITE (10,*) 'THIS PROGRAM IS TO CALCULATE THE NATURAL FREQUENCY
! OF THE PRIMARY COOLING SYSTEM WITH DIFFERENT COOLANT TEMPERATURE'
 WRITE (10,4)
4 FORMAT (/,' THE PARAMETER OF THE COOLING SYSTEM ARE :',/)

 WRITE(10,5) PVLENG,PVAR,PVVOL,PP1LENG,PP1AR,PP2LENG,PP2AR
!        ,PPAR,PPVOL,SGLENG,SGAR,SGVOL,PUMPVOL
5 FORMAT (' PRESSURE VESSEL LENGTH =',X, F6.3,' METERS' ,/,
!      ' PRESSURE VESSEL AREA   =',X, F6.3,' METER-2',/,
!      ' PRESSURE VESSEL VOL    =',X, F8.3,' METER-3',/,
!      ' PIPE1 LENGTH           =',X, F6.3,' METERS' ,/,
!      ' PIPE1 AREA             =',X, F6.3,' METER-2',/,
!      ' PIPE2 LENGTH           =',X, F6.3,' METERS' ,/,
!      ' PIPE2 AREA             =',X, F6.3,' METER-2',/,
!      ' PRESSURIZER AREA       =',X, F6.3,' METERS ',/,
!      ' PRESSURIZER VOL        =',X, F6.3,' METER-2',/,
!      ' STEAM GENERATOR LENGTH =',X, F6.3,' METERS' ,/,
!      ' STEAM GENERATOR AREA   =',X, F6.3,' METER-2',/,
!      ' STEAM GENERATOR VOL    =',X, F6.3,' METER-3',/,
!      ' PUMP WATER VOLUME      =',X, F6.3,' METERS' ,/)


*****************************************************************************************
*   START TO CALCULATE                                                                  *
*****************************************************************************************

  DO ITER1=1,NTEMP

    TEMPHL = TEMPPV+0.5*DELHLCL
    TEMPCL = TEMPPV-0.5*DELHLCL
    TEMPSG = TEMPPV

    IF (RHOSTD.EQ.0.) THEN
      CALL DENSITY(TEMPPV,RHOPV)
      CALL DENSITY(TEMPHL,RHOHL)
      CALL DENSITY(TEMPCL,RHOCL)
      CALL DENSITY(TEMPSG,RHOSG)
    ELSE
      CALL DENSITY(TEMPPV,RHOX,DRHODT)
      RHOPV  = RHO(RHOSTD,DRHODT,TEMPSTD,TEMPPV)

      CALL DENSITY(TEMPHL,RHOX,DRHODT)
      RHOHL= RHO(RHOSTD,DRHODT,TEMPSTD,TEMPHL)

      CALL DENSITY(TEMPCL,RHOX,DRHODT)
      RHOCL  = RHO(RHOSTD,DRHODT, TEMPSTD,TEMPCL)

      CALL DENSITY(TEMPSG,RHOX,DRHODT)
      RHOSG  = RHO(RHOSTD,DRHODT, TEMPSTD,TEMPSG)

    END IF
```

```
      CALL VELOCITY (TEMPPV,SOUNDVPV)
      FRACTPV = FRACT(RNUM)

      CALL VELOCITY (TEMPHL,SOUNDVHL)
      FRACTPP1  = FRACT(RNUM)

      CALL VELOCITY (TEMPCL,SOUNDVCL)
      FRACTPP2 = FRACT(RNUM)

      CALL VELOCITY (TEMPSG,SOUNDVSG)
      FRACTSG = FRACT(RNUM)

      WRITE(10,*) ' ************************************************'
      WRITE(10,11) TEMPHL
 11   FORMAT (/,' HOTLEG TEMPERATURE = ',F6.2)
      WRITE(10,12) RHOHL,SOUNDVHL
 12   FORMAT (' HOTLEG DENSITY =',X,F8.3,2X,/,
  !   ' SOUND VELOCITY=',F10.4,/)

     DO ITER2=1,FREQF
      FREQ=FREQI+DELFREQ*ITER2

************************************************************************
*       ESTABLISHING THE MATRIX OF PRESSURE VESSEL, STEAM GENERATOR,      *
*       PRESSURIZER PRESSURE, PIPE FROM PRESSURE VESSEL TO STEAM GENERATOR*
*       AND FROM STEAM GENERATOR TO PV AND SURGE LINE                      *
************************************************************************

      DO ROW = 1,NROW
        DO COL = 1,NCOL
          IF (ROW.EQ.COL) THEN

            PVR(ROW,COL)=1.
            PVI(ROW,COL)=0

            ZREALPP1 = FRACTPP1*PP1LENG/SOUNDVHL
            ZIMAGPP1 = PHASE(FREQ,SOUNDVHL,PP1LENG)
            CALL HYP(ZREALPP1,ZIMAGPP1,SZREALPP1,SZIMAGPP1,
  !         CZREALPP1,CZIMAGPP1)
            PP1R(ROW,COL)=CZREALPP1
            PP1I(ROW,COL)=CZIMAGPP1



            PPR(ROW,COL)=1.
            PPI(ROW,COL)=0

            SGR(ROW,COL)=1.
            SGI(ROW,COL)=0
```

```
         PUMPR(ROW,COL)=1.
         PUMPI(ROW,COL)=0

         ZREALPP2 = FRACTPP2*PP2LENG/SOUNDVCL
         ZIMAGPP2 = PHASE(FREQ,SOUNDVCL,PP2LENG)
         CALL HYP(ZREALPP2,ZIMAGPP2,SZREALPP2,SZIMAGPP2,
!        CZREALPP2,CZIMAGPP2)
         PP2R(ROW,COL)=CZREALPP2
         PP2I(ROW,COL)=CZIMAGPP2

         ZREALPP3 = FRACTPP3*PP3LENG/SOUNDVCL
         ZIMAGPP3 = PHASE(FREQ,SOUNDVCL,PP3LENG)
         CALL HYP(ZREALPP3,ZIMAGPP3,SZREALPP3,SZIMAGPP3,
!        CZREALPP3,CZIMAGPP3)
         PP3R(ROW,COL)=CZREALPP3
         PP3I(ROW,COL)=CZIMAGPP3

      ELSEIF (COL.EQ.2) THEN


         PVR(ROW,COL)=0
         PVI(ROW,COL)=0

         PP1R(ROW,COL)=BDIAGR(RHOHL,SOUNDVHL,PP1AR,FREQ,
!                 FRACTPP1,SZREALPP1,SZIMAGPP1,PI)
         PP1I(ROW,COL)=BDIAGI(RHOHL,SOUNDVHL,PP1AR,FREQ,
!                 FRACTPP1,SZREALPP1,SZIMAGPP1,PI)


         PPR(ROW,COL)=0
         PPI(ROW,COL)=0

         SGR(ROW,COL)=0
         SGI(ROW,COL)=0

         PUMPR(ROW,COL)=0
         PUMPI(ROW,COL)=0

         PP2R(ROW,COL)=BDIAGR(RHOCL,SOUNDVCL,PP2AR,FREQ,
!                 FRACTPP2,SZREALPP2,SZIMAGPP2,PI)
         PP2I(ROW,COL)=BDIAGI(RHOCL,SOUNDVCL,PP2AR,FREQ,
!                 FRACTPP2,SZREALPP2,SZIMAGPP2,PI)

         PP3R(ROW,COL)=BDIAGR(RHOCL,SOUNDVCL,PP3AR,FREQ,
!                 FRACTPP3,SZREALPP3,SZIMAGPP3,PI)
         PP3I(ROW,COL)=BDIAGI(RHOCL,SOUNDVCL,PP3AR,FREQ,
!                 FRACTPP3,SZREALPP3,SZIMAGPP3,PI)


      ELSE
```

```
          PVR(ROW,COL)= 0
          PVI(ROW,COL)= 2*PI*FREQ*PVVOL/(RHOPV*SOUNDVPV**2)

          PP1R(ROW,COL)=CDIAGR(RHOHL,SOUNDVHL,PP1AR,FREQ,
     !           FRACTPP1,SZREALPP1,SZIMAGPP1,PI)
          PP1I(ROW,COL)=CDIAGI(RHOHL,SOUNDVHL,PP1AR,FREQ,
     !           FRACTPP1,SZREALPP1,SZIMAGPP1,PI)


          PPI(ROW,COL)= 2*PI*FREQ*PPVOL/(RHOHL*SOUNDVHL**2)

          SGI(ROW,COL)= 2*PI*FREQ*SGVOL/(RHOSG*SOUNDVSG**2)

          PUMPI(ROW,COL)= 2*PI*FREQ*PUMPVOL/(RHOCL*SOUNDVCL**2)

          PP2R(ROW,COL)=CDIAGR(RHOCL,SOUNDVCL,PP2AR,FREQ,
     !           FRACTPP2,SZREALPP2,SZIMAGPP2,PI)
          PP2I(ROW,COL)=CDIAGI(RHOCL,SOUNDVCL,PP2AR,FREQ,
     !           FRACTPP2,SZREALPP2,SZIMAGPP2,PI)

          PP3R(ROW,COL)=CDIAGR(RHOCL,SOUNDVCL,PP3AR,FREQ,
     !           FRACTPP3,SZREALPP3,SZIMAGPP3,PI)
          PP3I(ROW,COL)=CDIAGI(RHOCL,SOUNDVCL,PP3AR,FREQ,
     !           FRACTPP3,SZREALPP3,SZIMAGPP3,PI)

          ENDIF
        END DO
      END DO

!     CALL WRITEMATRIX(PVR,MAXROW,NROW,NCOL)
!     CALL WRITEMATRIX(PVI,MAXROW,NROW,NCOL)
!     CALL WRITEMATRIX(PP1R,MAXROW,NROW,NCOL)
!     CALL WRITEMATRIX(PP1I,MAXROW,NROW,NCOL)
!     CALL WRITEMATRIX(PP2R,MAXROW,NROW,NCOL)
!     CALL WRITEMATRIX(PP2I,MAXROW,NROW,NCOL)
!     CALL WRITEMATRIX(PPR,MAXROW,NROW,NCOL)
!     CALL WRITEMATRIX(PPI,MAXROW,NROW,NCOL)
!     CALL WRITEMATRIX(SLR,MAXROW,NROW,NCOL)
!     CALL WRITEMATRIX(SLI,MAXROW,NROW,NCOL)
!     CALL WRITEMATRIX(SGR,MAXROW,NROW,NCOL)
!     CALL WRITEMATRIX(SGI,MAXROW,NROW,NCOL)

************************************************************************
*    LOOP1 EQUIVALENT                                                  *
************************************************************************

!     CALL MATPROD(SLR,SLI,PPR,PPI,MAXROW,NROW,NCOL,SPR,SPI)
      CALL MATPROD(PP1R,PP1I,PPR,PPI,MAXROW,PRESPR,PRESPI)
      CALL MATPROD(PRESPR,PRESPI,SGR,SGI,MAXROW,PSG1R,PSG1I)
      CALL MATPROD(PSG1R,PSG1I,PP2R,PP2I,MAXROW,PSPP1R,PSPP1I)
      CALL MATPROD(PSPP1R,PSPP1I,PUMPR,PUMPI,MAXROW,PPUMP1R,PPUMP1I)
```

```
      CALL MATPROD(PPUMP1R,PPUMP1I,PP3R,PP3I,MAXROW,LOOP1R,LOOP1I)
      CALL MATCOND(LOOP1R,LOOP1I,MAXROW,CONDLOOP1R,CONDLOOP1I)

!      WRITE (10,*)' PSG1R'
!      CALL WRITEMATRIX(PSG1R,MAXROW,NROW,NCOL)
!      CALL WRITEMATRIX(PSG1I,MAXROW,NROW,NCOL)
!      CALL WRITEMATRIX(LOOP1R,MAXROW,NROW,NCOL)
!      CALL WRITEMATRIX(LOOP1I,MAXROW,NROW,NCOL)
!      WRITE (10,*)' CONDLOOP1R'

!      CALL WRITEMATRIX(CONDLOOP1R,MAXROW,NROW,NCOL)
!      CALL WRITEMATRIX(CONDLOOP1I,MAXROW,NROW,NCOL)


*****************************************************************************
*     LOOP2 EQUIVALENT                                                      *
*****************************************************************************

      CALL MATPROD(PP1R,PP1I,SGR,SGI,MAXROW,PSG2R,PSG2I)
      CALL MATPROD(PSG2R,PSG2I,PP2R,PP2I,MAXROW,PSPP2R,PSPP2I)
      CALL MATPROD(PSPP2R,PSPP2I,PUMPR,PUMPI,MAXROW,PPUMP2R,PPUMP2I)
      CALL MATPROD(PPUMP2R,PPUMP2I,PP3R,PP3I,MAXROW,LOOP2R,LOOP2I)
      CALL MATCOND(LOOP2R,LOOP2I,MAXROW,CONDLOOP2R,CONDLOOP2I)

!      CALL WRITEMATRIX(PSG2R,MAXROW,NROW,NCOL)
!      CALL WRITEMATRIX(PSG2I,MAXROW,NROW,NCOL)
!      CALL WRITEMATRIX(LOOP2R,MAXROW,NROW,NCOL)
!      CALL WRITEMATRIX(LOOP2I,MAXROW,NROW,NCOL)
!      CALL WRITEMATRIX(CONDLOOP2R,MAXROW,NROW,NCOL)
!      CALL WRITEMATRIX(CONDLOOP2I,MAXROW,NROW,NCOL)



*****************************************************************************
*     LOOP1 AND 2 EQUIVALENT                                                *
*****************************************************************************
!     WRITE (10,*)' CONDLOOPR'

      CALL MATADD(CONDLOOP1R,CONDLOOP2R,MAXROW,NROW,NCOL,CONDLOOPR)
      CALL MATADD(CONDLOOP1I,CONDLOOP2I,MAXROW,NROW,NCOL,CONDLOOPI)
      CALL MATINV(CONDLOOPR,CONDLOOPI,MAXROW,LOOPR,LOOPI)

!      CALL WRITEMATRIX(CONDLOOPR,MAXROW,NROW,NCOL)
!      CALL WRITEMATRIX(CONDLOOPI,MAXROW,NROW,NCOL)
!      CALL WRITEMATRIX(LOOPR,MAXROW,NROW,NCOL)
!      CALL WRITEMATRIX(LOOPI,MAXROW,NROW,NCOL)


*****************************************************************************
*    CALCULATE MATRIX EQUIVALENT FOR ALL SYSTEMS                            *
*****************************************************************************
```

```
      CALL MATPROD(PVR,PVI,LOOPR,LOOPI,MAXROW,EQUIVR,EQUIVI)
!     CALL WRITEMATRIX(EQUIV,MAXROW,NROW,NCOL)

**************************************************************************
*     TO CALCULATE DETERMINANT OF THE MATRIX EQUIVALENT AND FIND         *
*     THE VALUE OF FREQUENCY THAT MAKE THE DET(EQUIV-I)= 0               *
**************************************************************************

      DO ROW =1,NROW
        DO COL =1,NCOL
          IF (ROW.EQ.COL) THEN
            MIR(ROW,COL)=-1
            MII(ROW,COL)=0
          ELSE
            MIR(ROW,COL)=0
            MII(ROW,COL)=0
          END IF
        END DO
      END DO

!     CALL WRITEMATRIX(MI,MAXROW,NROW,NCOL)

      CALL MATADD(EQUIVR,MIR,MAXROW,NROW,NCOL,EQUIVMIR)
      CALL MATADD(EQUIVI,MII,MAXROW,NROW,NCOL,EQUIVMII)
!     CALL WRITEMATRIX(EQUIVMI,MAXROW,NROW,NCOL)
      CALL DETERM(EQUIVMIR,EQUIVMII,MAXROW,DTMR,DTMI)

!      WRITE(10,9) FREQ, DTMR,DTMI
!   9  FORMAT ('THE FREQUENCY=',F10.6,2X, 'THE DETR=',F10.6,'THE DETI
!    ! = ',F10.6)
!      DTR(ITER2)=DTMR
!      DTI(ITER2)=DTMI
!     END DO
!      PRINT *, DTR

!      CALL MINIM(DTR,DTI,TMINR,TMINI)

      IF (ABS(DTMR).LT.LIMITR.AND.ABS(DTMI).LT.LIMITI) THEN

      WRITE (10,13) DTMR,DTMI
   13 FORMAT (' THE REAL DETERMINANT = ', F10.6,2X,' THE IM. DETERMINANT
     ! = ',F10.6)
      WRITE (10,14) FREQ
   14 FORMAT (/,' THE NATURAL FREQUENCY  = ',x,f8.4,' HERTZ ')
      LAMDA = SOUNDVHL/FREQ
      WRITE (10,15) LAMDA
   15 FORMAT (/,' THE WAVE LENGTH         = ',x,f15.4,' METERS ',//)
      END IF
      END DO
```

```
*******************************************************************************

C     WE PUT DRHOD AS A FUNCTION BECAUSE LATER THE EQUATION WILL BE
C     USED TO DETERMINE THE LIQUID GRADIENT DENSITY OF LIQUID

*******************************************************************************
      PRINT *, DELTAT
      TEMPPV =TEMPPV + DELTAT
      END DO
      END

*******************************************************************************
*     END OF PROGRAM                                                          *
*******************************************************************************

      FUNCTION PHASE(FREQ0,SOUNDVEL,LENG)
      REAL PI0,FREQ0,LENG
      PHASE= (2*3.141593*FREQ0*LENG)/SOUNDVEL
      RETURN
      END

      FUNCTION BDIAGR(RHO1,SOUNDVEL1,AREA,FREQ1,FRACT1,SZREAL,SZIMAG,
     ! PI)
      REAL RHO1,SOUNDVEL1,AREA,FREQ1,FRACT1,SZREAL,SZIMAG
      BDIAGR=(RHO1*SOUNDVEL1/AREA)*SZREAL
     !     -RHO1*SOUNDVEL*FRACT1*SZIMAG/(AREA*6.283185*PI*FREQ1)
      RETURN
      END

      FUNCTION BDIAGI(RHO1,SOUNDVEL1,AREA,FREQ1,FRACT1,SZREAL,SZIMAG,
     ! PI)
      REAL RHO1,SOUNDVEL1,AREA,FREQ1,FRACT1,SZREAL,SZIMAG
      BDIAGI=(RHO1*SOUNDVEL1/AREA)*SZIMAG
     !     +RHO1*SOUNDVEL*FRACT1*SZREAL/(AREA*6.283185*PI*FREQ1)
      RETURN
      END

      FUNCTION CDIAGR(RHO1,SOUNDVEL1,AREA,FREQ1,FRACT1,SZREAL,SZIMAG,
     ! PI)
      REAL RHO1,SOUNDVEL1,AREA,FREQ1,FRACT1,SZREAL,SZIMAG
      CDIAGR=(AREA*(SZREAL-((FRACT1/(6.283185*PI*FREQ1))*SZIMAG)))/
     !     (RHO1*SOUNDVEL1*(1+(FRACT1**2/((6.283185*PI*FREQ1)**2))))
      RETURN

      END
      FUNCTION CDIAGI(RHO1,SOUNDVEL1,AREA,FREQ1,FRACT1,SZREAL,SZIMAG,
     ! PI)
      REAL RHO1,SOUNDVEL1,AREA,FREQ1,FRACT1,SZREAL,SZIMAG
      CDIAGR=(AREA*(SZIMAG+((FRACT1/(6.283185*PI*FREQ1))*SZREAL)))/
     !     (RHO1*SOUNDVEL1*(1+(FRACT1**2/((6.283185*PI*FREQ1)**2))))
      RETURN
```

```
END

FUNCTION RHO(RHOSTD,DRHODT,TEMPSTD,TEMPX)
RHO = RHOSTD*(1-DRHODT*(TEMPX-TEMPSTD))
END

FUNCTION SV(TEMP)
SV = 1072-5*(TEMP-270)
END

FUNCTION FRACT(RNUM)
IF (RNUM.EQ.0) THEN
  FRACT=0
ELSEIF (RNUM.LE.30000) THEN
  FRACT= 0.316*RNUM**(-0.25)
ELSE IF (RNUM.GT.30000.AND.RNUM.LT.1000000) THEN
  FRACT= 0.184*RNUM**(-0.2)
END IF
END

SUBROUTINE  DENSITY(TEMP,RHOX,DRHODT)
REAL TEMP,RHOX,PRESS,PSAT,PRESMPA
COMMON PRESS
PRESMPA = PRESS*0.0068947
IF (TEMP.GT.150 .AND. TEMP .LE. 160) THEN
DRHODT=0.00105
ELSEIF (TEMP.GT.160.AND. TEMP .LE. 170) THEN
DRHODT=0.00111
ELSEIF (TEMP.GT.170.AND. TEMP .LE. 180) THEN
DRHODT=0.00117
ELSEIF (TEMP.GT.180.AND. TEMP .LE. 190) THEN
DRHODT=0.00123
ELSEIF (TEMP.GT.190.AND. TEMP .LE. 200) THEN
DRHODT=0.00131
ELSEIF (TEMP.GT.200.AND. TEMP .LE. 210) THEN
RHOSAT=875.1809
DRHODT=0.001339
ELSEIF (TEMP.GT.210.AND. TEMP .LE. 220) THEN
RHOSAT=863.8172
TSAT=210
PSAT=1.9
DRHODT=0.001413
ELSEIF (TEMP.GT.220.AND. TEMP .LE. 230) THEN
TSAT=220
PSAT=2.32
RHOSAT=851.8594
DRHODT=0.001486
ELSEIF (TEMP.GT.230.AND. TEMP .LE. 240) THEN
TSAT=230
PSAT =2.798
RHOSAT=839.3660
```

```
DRHODT=0.001557
ELSEIF (TEMP.GT.240.AND. TEMP .LE. 250) THEN
TSAT=240
PSAT= 3.348
RHOSAT=826.1260
DRHODT=0.001767
ELSEIF (TEMP.GT.250.AND. TEMP .LE. 260) THEN
TSAT=250
PSAT= 3.978
RHOSAT=812.2159
DRHODT=0.001780
ELSEIF (TEMP.GT.260.AND. TEMP .LE. 270) THEN
TSAT=260
PSAT= 4.694
RHOSAT=797.3972
DRHODT=0.001989
ELSEIF (TEMP.GT.270.AND. TEMP .LE. 280) THEN
TSAT=270
PSAT=5.505
RHOSAT=781.5870
DRHODT=0.002212
ELSEIF (TEMP.GT.280.AND. TEMP .LE. 290) THEN
TSAT=280
PSAT= 6.419
RHOSAT=764.6037
DRHODT=0.002451
ELSEIF (TEMP.GT.290.AND. TEMP .LE. 300) THEN
TSAT=290
PSAT=7.445
RHOSAT=746.2377
DRHODT=0.002710
ELSEIF (TEMP.GT.300.AND. TEMP .LE. 310) THEN
TSAT=300
PSAT= 8.592
RHOSAT=726.0521
DRHODT=0.003086
ELSEIF (TEMP.GT.310.AND. TEMP .LE. 320) THEN
TSAT=310
PSAT=9.869
RHOSAT=703.6493
DRHODT=0.003672
ELSEIF (TEMP.GT.320.AND. TEMP .LE. 330) THEN
TSAT=320
PSAT=11.289
RHOSAT=678.2420
DRHODT=0.004473
ELSEIF (TEMP.GT.330.AND. TEMP .LE. 340) THEN
TSAT=330
PSAT= 12.864
RHOSTD=648.4553
DRHODT=0.005620
```

```
      ELSEIF (TEMP.GT.340.AND. TEMP .LE. 350) THEN
      TSAT=340
      PSAT=14.608
      RHOSAT=612.7453
      DRHODT=0.008184
      ELSE
      TSAT=350
      PSAT= 16.537
      RHOSAT=565.3603
      DRHODT = 0.00850
      END IF
      RHOX= RHOSAT + ((170/(375.-TEMP))-0.2)*(PRESMPA - PSAT)
      RETURN
      END

      SUBROUTINE WRITEMATRIX(X, MAXROW, NROW, NCOL)
      IMPLICIT   NONE
      INTEGER    MAXROW, NROW, NCOL, ROW, COL
      REAL       X(MAXROW, NCOL)
!      CHARACTER   OUT_F*100

      PRINT *
      DO ROW = 1, NROW
         PRINT 20, (X(ROW,COL), COL = 1, NCOL)
         WRITE (10,20) (X(ROW,COL), COL = 1, NCOL)
!         PRINT OUT_F, ( X(ROW,COL), COL = 1, NCOL)
   20 FORMAT (2F20.10,X)
      END DO
      PRINT *
      END

      Subroutine hyp(zreal,zimag,szreal,szimag,czreal,czimag)
      IMPLICIT NONE
      INTRINSIC EXP,COS,SIN
      REAL ZREAL,ZIMAG,SZREAL,SZIMAG,CZREAL,CZIMAG
      REAL COSY,SINY,ETODX,ETODMX

      ETODX=EXP(ZREAL)
      ETODMX=EXP(-ZREAL)
      COSY = COS(ZIMAG)
      SINY = SIN(ZIMAG)
      SZREAL= COSY*(ETODX-ETODMX)/2
      SZIMAG= SINY*(ETODX+ETODMX)/2
      CZREAL= COSY*(ETODX+ETODMX)/2
      CZIMAG= SINY*(ETODX-ETODMX)/2
      END

      SUBROUTINE MATPROD (XR,XI,YR,YI,MAXROW,PRODR,PRODI)
      IMPLICIT NONE
      INTEGER MAXROW
      REAL      XR(MAXROW,MAXROW), YR(MAXROW,MAXROW)
```

```
      REAL       XI(MAXROW,MAXROW), YI(MAXROW,MAXROW)
      REAL       PRODR(MAXROW,MAXROW), PRODI(MAXROW,MAXROW)
      CHARACTER*30 OUT_F

      PRODR(1,1)=XR(1,1)*YR(1,1)-XI(1,1)*YI(1,1)+XR(1,2)*YR(2,1)
     !-XI(1,2)*YI(2,1)
      PRODI(1,1)=XR(1,1)*YI(1,1)+XI(1,1)*YR(1,1)+XR(1,2)*YI(2,1)
     !+XI(1,2)*YR(2,1)

      PRODR(1,2)=XR(1,1)*YR(1,2)-XI(1,1)*YI(1,2)+XR(1,2)*YR(2,2)
     !-XI(1,2)*YI(2,2)
      PRODI(1,2)=XR(1,1)*YI(1,2)+XI(1,1)*YR(1,2)+XR(1,2)*YI(2,2)
     !+XI(1,2)*YR(2,2)

      PRODR(2,1)=XR(2,1)*YR(1,1)-XI(2,1)*YI(1,1)+XR(2,2)*YR(2,1)
     !-XI(2,2)*YI(2,1)
      PRODI(2,1)=XR(2,1)*YI(1,1)+XI(2,1)*YR(1,1)+XR(2,2)*YI(2,1)
     !+XI(2,2)*YR(2,1)

      PRODR(2,2)=XR(2,1)*YR(1,2)-XI(2,1)*YI(1,2)+XR(2,2)*YR(2,2)
     !-XI(2,2)*YI(2,2)
      PRODI(2,2)=XR(2,1)*YI(1,2)+XI(2,1)*YR(1,2)+XR(2,2)*YI(2,2)
     !+XI(2,2)*YR(2,2)
      END

      SUBROUTINE MATADD(X,Y,MAXROW,NROW,NCOL,SUM)

      IMPLICIT NONE
      INTEGER    MAXROW, ROW, COL, NROW, NCOL, K
      REAL       X(MAXROW,MAXROW), Y(MAXROW,MAXROW)
      REAL       SUM(MAXROW,MAXROW)
!      CHARACTER OUT_F*100

*     calculate elemens of sum........................................*

      DO ROW = 1, NROW
        DO COL = 1, NCOL
             SUM (ROW, COL) = X(ROW,COL)+Y(ROW,COL)
        END DO
      END DO

*      write SUM OF MATRIX...........................................*

       END

      SUBROUTINE MATCOND(XR,XI,MAXROW,CONDR,CONDI)

      IMPLICIT NONE
      INTEGER    MAXROW
      REAL       XR(MAXROW,MAXROW),  XI(MAXROW,MAXROW),DEN
      REAL       CONDR(MAXROW,MAXROW), CONDI(MAXROW,MAXROW)
```

```
      DEN = XR(1,2)**2+XI(1,2)**2

      CONDR(1,1) =-(XR(1,1)*XR(1,2) + XI(1,1)*XI(1,2))/DEN
      CONDI(1,1) =-(XI(1,1)*XR(1,2) - XR(1,1)*XI(1,2))/DEN

      CONDR(1,2) = XR(1,2)/DEN
      CONDI(1,2) = XI(1,2)/DEN

      CONDR(2,1) = XR(2,1)+CONDR(1,1)*XR(2,2)-CONDI(1,1)*XI(2,2)
      CONDI(2,1) = XI(2,1)+CONDR(1,1)*XI(2,2)+CONDI(1,1)*XR(2,2)


      CONDR(2,2) = (XR(2,2)*XR(1,2)+ XI(2,2)*XI(1,2))/DEN
      CONDI(2,2) = (XR(2,2)*XI(1,2)+ XI(2,2)*XR(1,2))/DEN

  END

 SUBROUTINE MATINV(XR,XI,MAXROW,LOOPR,LOOPI)

 IMPLICIT NONE
 INTEGER   MAXROW
 REAL      XR(MAXROW,MAXROW), XI(MAXROW,MAXROW),DEN
 REAL      LOOPR(MAXROW,MAXROW), LOOPI(MAXROW,MAXROW)

      DEN = XR(2,1)**2+XI(2,1)**2

      LOOPR(1,1) =-(XR(2,2)*XR(2,1) + XI(2,2)*XI(2,1))/DEN
      LOOPI(1,1) =-(XI(2,2)*XR(2,1) - XR(2,2)*XI(2,1))/DEN

      LOOPR(1,2) = XR(2,1)/DEN
      LOOPI(1,2) = XI(2,1)/DEN

      LOOPR(2,1) = XR(1,2)+LOOPR(1,1)*XR(1,1)-LOOPI(1,1)*XI(1,1)
      LOOPI(2,1) = XI(1,2)+LOOPR(1,1)*XI(1,1)+LOOPI(1,1)*XR(1,1)


      LOOPR(2,2) = (XR(1,1)*XR(2,1)+ XI(1,1)*XI(2,1))/DEN
      LOOPI(2,2) = (XR(1,1)*XI(2,1)- XI(1,1)*XR(2,1))/DEN

  END

 SUBROUTINE DETERM(XR,XI,MAXROW,DTMR,DTMI)

 IMPLICIT NONE
 INTEGER   MAXROW
 REAL      XR(MAXROW,MAXROW), XI(MAXROW,MAXROW)
 REAL      DTMR,DTMI

        DTMR = XR(1,1)*XR(2,2) - XI(1,1)*XI(2,2)-
!              (XR(1,2)*XR(2,1)-XI(1,2)*XI(2,1))
```

```
        DTMI = XR(1,1)*XI(2,2)+XI(1,1)*XR(2,2)-
   !            (XR(1,2)*XI(2,1)+XI(1,2)*XR(2,1))
      END


      SUBROUTINE VELOCITY(TEM,SOUNDVELSI)
      REAL*4  A(4),SV(35),YY(35),XX(30),DTEMP(30)
      REAL*4  PRESS,SVEL,SNTEMP,SUMA,TEMP,TMIN,SLOPE,TEM
     >SOUNDVEL,SOUNDVELSI
      INTEGER I,J,K,L,M,NUM
      COMMON PRESS
      DATA A/5381.86,-3.31547, 7.71407E-4, -6.26238E-8/
    5 FORMAT (2F8.2)
!      WRITE (10,15) tem

      TEMP= (9./5.)*(TEM)+32.
      SVEL=3000.0
      WRITE (10,*)
!      WRITE (10,15) PRESS
      WRITE (10,*)
      DO 99 I=1,30
        SV(I)=SVEL+.0404*(725.- PRESS)
        YY(I)=SVEL
        SVEL=SVEL+50.0
 99   CONTINUE
      DO J=1,30
      SUMA=0.
      DO K=1,4
        SUMA = SUMA + A(K)*SV(J)**(K-1)
      END DO
      SNTEMP=SUMA
      XX(J)=SNTEMP
      END DO
!      WRITE (10,15) (XX(I),I=1,30)
   15 FORMAT (F8.2)

      TMIN= ABS(TEMP - XX(1))
      DO I=1,30

        DTEMP(I)= TEMP - XX(I)

        IF(ABS(DTEMP(I)).LE.TMIN)THEN
          TMIN = ABS(DTEMP(I))
          NUM=I
        END IF
      END DO

      SLOPE = (YY(NUM)-YY(NUM-1))/(XX(NUM)-XX(NUM-1))
      SOUNDVEL = YY(NUM-1) + SLOPE*(TEMP - XX(NUM-1))
      SOUNDVELSI= 0.3048*SOUNDVEL
      END
```

```
Subroutine MINIM(DTR,DTI,TMINR,TMINI)
INTEGER MAXROW
REAL TMINR,TMINI, FREQF
REAL DTR(500),DTI(500)
COMMON FREQF
print *, dtr
TMINR= ABS(DTR(1))
DO I=1,FREQF-1
IF (ABS(DTR(I)).NE.0.AND.ABS(DTR(I)).LT.TMINR) THEN
  TMINR = ABS(DTR(I))
PRINT *, TMINR
END IF
END DO

TMINI= ABS(DTI(1))
DO I=1,FREQF-1
IF (ABS(DTI(I)).NE.0.AND.ABS(DTI(I)).LT.TMINI) THEN
  TMINI = ABS(DTI(I))
END IF
END DO
END
```

PCSPRES INPUT VARIABLES :

- PP1LENG = REACTOR OUTLET PIPING LENGTH
- PP2LENG = PUMP SUCTION PIPING LENGTH
- PP3LENG = PUMP OUTLET PIPING LENGTH
- PP1AR = REACTOR OUTLET PIPING SURFACE AREA
- PP2AR = PUMP SUCTION PIPING SURFACE AREA
- PP3AR = PUMP OUTLET PIPING SURFACE AREA
- PVVOL = PRESSURE VESSEL WATER VOLUME
- SGVOL = STEAM GENERATOR WATER VOLUME
- PUMPVOL = PUMP WATER VOLUME
- PPVOL = PRESSURIZER WATER VOLUME
- TEMPSTD = (HOT LEG + COLD LEG TEMPERATURE)/2.
- DELHLCL = HOT LEG - COLD LEG TEMPERATURE
- RHOSTD = WATER DENSITY AT TEMPSTD TEMPERATURE
- PRESS = REACTOR PRESSURE

VITA

Jupiter Sitorus Pane was born in Padang, Indonesia, on May 11, 1960. He graduated from elementary, junior high, and senior high schools in December 1973, December 1975, and July 1979, respectively. He entered The Institute Technology of Bandung in the following September without attending the selection test. He received his Bachelor of Science in Physics in October 1984. He worked for 5 years as a research staff at Multipurpose Research Reactor of Indonesian National Atomic Energy Agency. In 1989, he was promoted to head The Reactor Fuel Management Subdivision in this Research Reactor.

In March 1991 he received a fellowship from BAPPENAS as part of Indonesian national human resources development project. He came to the University of Tennessee, Knoxville in August 1991.

He received the Master of Science degree in Nuclear Engineering in May 1993.